

Model-based Assessment of Vehicle-to-grid: Implications for Vehicle Users and the Electricity System

Master's Thesis submitted by

Youmi Kim

Albert-Ludwigs-Universität Freiburg

Faculty of Engineering
Department of Sustainable Systems Engineering



INATECH
DEPARTMENT OF SUSTAINABLE
SYSTEMS ENGINEERING



Submitted master's thesis in accordance with the regulations of the examination regulations of the Albert-Ludwigs-Universität Freiburg for the graduation of the Master of Science (M. Sc.) Sustainable Systems Engineering course.

Submission date:

05. 05. 2021

Examiners

Prof. Dr. Anke Weidlich

Prof. Dr. Martin Wietschel

Declaration of Authorship

I, Youmi Kim, hereby declare that I am the sole author and composer of my thesis and that no other sources or learning aids, other than those listed, have been used. Furthermore, I declare that I have acknowledged the work of others by providing detailed references of said work.

I hereby also declare that my thesis has not been prepared for another examination or assignment, either wholly or excerpts thereof.

Freiburg im Breisgau, 05. 05. 2021

Youmi Kim

Abstract

The benefits and costs of electric vehicles (EVs) being utilized for vehicle-to-grid (V2G) are reviewed from the perspective of EV users, the electricity system, and the ecological domain. This thesis sets up a case study according to two different objectives: cost minimization for EV users and residual load minimization for the electricity system. These two objectives are formulated to explore the potential financial benefits to EV users and how much peak residual load reduction can be achieved using V2G. In addition, sensitivity analyses are conducted to validate the impact of the benefits on each stakeholder according to the V2G participation rate and the battery control setting. To determine the competitiveness of V2G in the electricity market, V2G is compared with the alternative charging strategies: demand response (DR) and uncontrolled charging.

The case study is analyzed with a model-based assessment for a simulation period of one week. This thesis provides a method to determine the optimal charging schedule of EVs on the national level and an evaluation method that considers the battery degradation in the benefit calculation. A mixed-integer linear programming (MILP) optimization model is created to determine the optimal charging and discharging schedule for EVs. The constraint-based approach is adopted to prevent extensive battery degradation by restricting the state-of-charge (SOC) of batteries. For the power price and residual load profile to use in both optimization and evaluation, the model includes a market simulation for the German wholesale electricity market of 2030. The battery degradation cost is derived from the calculated capacity loss of the EV battery depending on the cases.

The main findings in this thesis are as follows: In cost minimization, DR results in approximately a 20% reduction in operating costs compared to uncontrolled charging. The actual implementation of V2G occurs only if incentives are given, otherwise, only load shifting is performed even in the V2G cases to minimize the procurement cost. When the EVs are optimized for residual load minimization, positive peak residual load reduction of up to 7.9 GW (10.9%) for DR and up to 26.0 GW (36.1%) for V2G when compared with uncontrolled charging are observed during the simulation week. Moreover, V2G results in two times greater CO₂ emission reduction than DR. However, to achieve these benefits via V2G, the operating costs for the EV users increase by 65% compared to uncontrolled charging. This is mainly caused by the electricity cost for the additional charging. Overall, the electricity costs have the highest contribution to the total cost for EV users, and battery degradation has only a minor effect on the cost. As the V2G participation rate increases, competition for bi-directional charging activities between EV users increases. Additionally, battery degradation is found to be highly affected by the SOC restriction.

Even though DR gives positive economic benefits for EV users, to achieve a higher peak reduction and a higher CO₂ emission reduction, V2G would be an effective option to consider. To encourage the participation of V2G, however, an appropriate incentive for EV users needs to be introduced.

Contents

Abstract	I
Contents	II
List of Figures	IV
List of Tables	VI
List of Abbreviations	VII
1. Introduction	1
1.1. Motivation	1
1.2. Research gap	3
1.3. Approach	5
2. Related work	6
2.1. EV integration into the power system	6
2.2. Battery degradation	11
3. V2G optimization model and evaluation method	17
3.1. Study overview	17
3.2. Optimization module	21
3.3. Evaluation module	29
3.4. Model assumption, parameters, and input data	35
4. Results	44
4.1. Cost minimization based on pricing schemes (Part I)	44
4.2. Residual load minimization (Part II)	51
4.3. Sensitivity analyses (Part III)	58
5. Summary and discussion	63
5.1. Impacts on the cost for EV users based on pricing schemes	63
5.2. Impacts on the residual load of German electricity systems	64
5.3. Impacts of the participation rate and battery control	65
5.4. Limitation and outlooks	66
6. Conclusion	68

Bibliography	69
Appendix.....	75
A. Electricity market status of 2030	75
B. Detailed impact comparison of sensitivity analyses	77

List of Figures

Figure 1. Global EVs stock from 2010 to 2019 [1], Market share of EVs in Germany from 2014 to 2020 [2].....	1
Figure 2. Comparison of Li-ion battery used for EV [47].....	12
Figure 3. Battery degradation mechanism of a lithium-ion battery [47,48,50–57]	12
Figure 4. Frequency of SOC range depending on the charging strategy of SOC-optimized and cost-optimized [63].....	14
Figure 5. Conceptual diagram for different EV charging strategies	18
Figure 6. Overview of the simulation cases.....	18
Figure 7. The structure of the V2G assessment model	20
Figure 8. Flowchart of EV scheduling in the case of a single EV	22
Figure 9. Flowchart of EV scheduling in the case of a large number of EVs	23
Figure 10. EV driving and charging profile of a sample EV	38
Figure 11. EV driving and charging profile of accumulated six million EVs.....	38
Figure 12. Classification of EVs based on battery storage capacity.....	39
Figure 13. The SOC range of the EVs used for simulation	39
Figure 14. Simulated residual load of the German electricity system in 2030	41
Figure 15. Simulated wholesale price for electricity in 2030	41
Figure 16. Simulated electricity price and residual load	42
Figure 17. System demand and variable renewable energy source over the simulation week in 2030	43
Figure 18. Residual load and electricity price over the simulation week in 2030	43
Figure 19. Comparison of charging and discharging schedule of EVs depending on charging strategies and pricing schemes	45
Figure 20. Total cost comparison depending on the cases with cost minimization	46
Figure 21. Total cost for each EV batch and the correlation factors between cases.....	48
Figure 22. Battery status of EV batches that have the lowest and the highest total cost	48
Figure 23. Comparison of the cost components for the cases with cost minimization	49
Figure 24. Residual load comparison on cases with different pricing schemes	50
Figure 25. The comparison of positive and negative peak load	50
Figure 26. Comparison of charging and discharging schedule of EVs depending on EV charging strategies with residual load optimization.....	52
Figure 27. Residual load comparison based on cases with minimizing residual load	53
Figure 28. The residual load range between peak maximum and peak minimum of the cases with residual load minimization.....	53
Figure 29. Total cost comparison by EV scheduling strategies.....	55
Figure 30. Total cost ordered by highest values based on UC and the correlation factor between EV charging strategies	56

Figure 31. Comparison of the total cost of each EV batch according to the different objective functions	57
Figure 32. Cost comparison by cost elements for residual load minimization cases.	57
Figure 33. Final residual load variations depending on the participation rate of DR or V2G.....	59
Figure 34. Total cost variation depending on the participation rate of DR or V2G	59
Figure 35. The charging scheme of an example EV batch with the different SOC allowance range	61
Figure 36. Comparison in the final residual load by different SOC allowance range	61

List of Tables

Table 1. Summary of several prior studies that conducted EV schedule optimization	10
Table 2. Summary of battery degradation model [50].....	16
Table 3. Summary of the main variables, parameters, and abbreviations used in the equations..	24
Table 4. Main parameters applied for evaluation model of all simulation cases.....	35
Table 5. Power generation capacity configuration based on grid scenario NEP-B in 2030 [72] .	36
Table 6. The unit price of power generation based on energy type [73]	36
Table 7. The weighted average and weighted standard deviation of the total cost according to the pricing scheme	46
Table 8. Comparison of systemic impacts for the cases with cost minimization	50
Table 9. Comparison of ecological benefits by cases with different pricing scheme	51
Table 10. Comparison of systemic impacts for the cases with residual load minimization	53
Table 11. Comparison of ecological impacts depending on the cases with residual load optimization.	54
Table 12. The weighted average and weighted standard deviation of the total cost	55
Table 13. Overall compensation cost to be paid for the benefits of DR and V2G	58
Table 14. The compensation costs per benefit depending on the participation rate of DR or V2G program	60
Table 15. Cost comparison according to the SOC allowance ranges	62
Table 16. The specific compensation cost per benefit depending on the SOC allowance ranges	62

List of Abbreviations

DOD	Depth of discharge
DP	Dynamic programming
DR	Demand response
EV	Electric vehicles
FLP	Fuzzy linear programming
HES	Home energy storage system
LFP	Lithium iron phosphate
LMO	Lithium manganese oxide
LP	Linear programming
MILP	Mixed integer linear programming
NMC	Lithium manganese cobalt oxide
PLR	Peak load reduction rate
PSO	Particle swarm optimization
PSP	Peak shaving percentage
QP	Quadratic programming
RCC	Rain-flow cycle counting
RES	Renewable energy source
SOC	State of charge
SOH	State of health
TOU	Time of usage
UC	Uncontrolled charging
V2G	Vehicle-to-grid

1. Introduction

1.1. Motivation

Driven by national support policies and technological advances, the number of electric vehicles (EVs) worldwide has increased significantly over the past decade as shown in Figure 1 (left) [1,3]. Germany has also seen EVs rapidly gaining market share as shown in Figure 1 (right) due to policies, R&D support, and technological advances [4–6]. Along with the global movement in response to climate change, policies continue to support EV deployments. Therefore, it is expected that the market share of EVs will continue to grow over the next ten years [1].

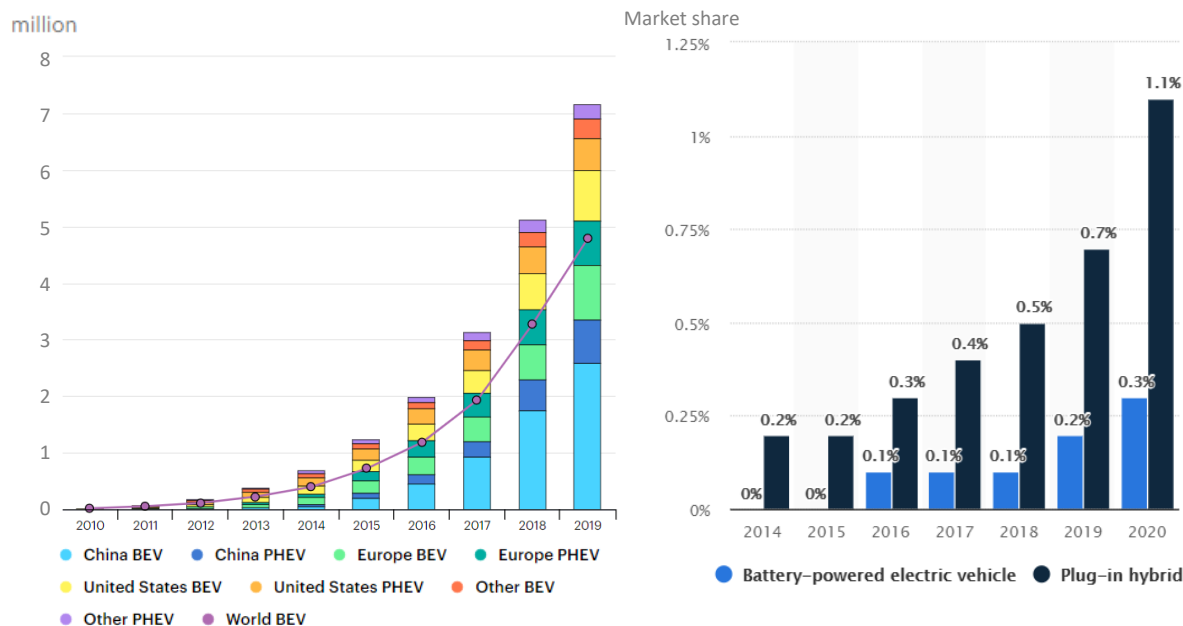


Figure 1. (left) Global EVs stock from 2010 to 2019 [1], (right) Market share of EVs in Germany from 2014 to 2020 [2]

The increasing market share of EVs can be expected to have positive effects on sustainability by providing solutions for the scarcity issues of fossil fuel [7]. One of the main advantages of EVs is that it reduces the amount of CO₂ released by vehicles through substituting conventional fossil fuel usage for greener electricity [8–10]. To be more precise, the ecological impact of EVs varies depending on the source of the electricity, but considering the current and forecasted growth in renewable energy source (RES) generation [11–13], the ecological impact of EVs is seen as highly positive [9,14,15].

Increasing penetration of EVs will decrease fossil fuel consumption, but on the other hand, this will increase electricity demand. According to a report from the International Energy Agency (IEA)

[1], the global EV demand in 2030 compared to 2019 is expected to increase by a factor between 6 to 11, depending on the scenario. There are concerns that the additional power demand for EVs can induce a large peak demand and system stress on the power grid, leading to the requirement for additional power generation capacity [16].

However, this problem can be solved by controlling the charging time [7,9,17]. Moreover, numerous studies have indicated positive impacts in power grid stabilization by utilizing EVs to cooperate with the power system [7,9,18–21]. Therefore, EVs are becoming more attractive in the electricity market as an alternative to energy storage systems (ESS). This point is even more prominent when considering the fact that personal vehicles are only utilized 4% of their lifetime for personal transportation [22]. This means that for 96% of their lifetime they could be used for this secondary use case.

To this end, the vehicle-to-grid (V2G) concept, also known as bi-directional charging of EVs, can be introduced. V2G is a method that allows idle EVs to be used as mobile electricity storage devices in a power system. [9,22]. With this concept, EVs can reduce the electricity peak as a flexibility option in power grids [1,9,14]. Through simple user programming and lower night time pricing, the contribution of EVs to peak demand could be reduced by more than half, and controlled charging on real-time price signals can further leverage synergies [1]. From the perspective of EV users, they can have a chance to earn a profit by using their EVs as a means of arbitrage trading in the electricity market [14,20]. Furthermore, since V2G systems can react very quickly with their quick ramp up and ramp down features, EVs can play a role of a frequency controller for grid stability by providing immediate capacity to the grid [9,18,22]. In this regard, a high number of EVs can mitigate the volatility of renewable energy-based power supplies by providing immediate spinning reserve [18,22] and by shifting the surplus RES generation to a time of high demand [19,23].

1.2. Research gap

The potential benefits from V2G described above can be achieved when a sufficient amount of EV users participate in a V2G program. To encourage voluntary involvement, economic benefits for EV users will be required.

The analysis of the impacts of V2G must consider not only the potential direct gains from V2G but also possible drawbacks from the participation, such as the additional usage of battery for V2G that would lead to faster battery degradation than the reference case. However, often this battery degradation cost is excluded in the V2G evaluation [14,24–36] or considered as a fixed rate regardless of battery status [20]. Moreover, to the best knowledge of the author, with respect to V2G, many studies until now have not considered the possible competition of economic benefits between EV users when there are substantial EVs in the market. However, when there is a high fraction of EVs in the market participating in V2G, not all EVs can profit as much compared to when there are only a small number of participating EVs. This is because the marginal benefit of reducing the residual load decreases. The approach to addressing this possible competition is well examined for demand response (DR) [37], but not for V2G.

An important element to encourage V2G for EV users is the electricity market price. Currently, in Germany, a fixed cost policy is typically applied to private electricity consumers. However, dynamic pricing is essential for promoting the participation in V2G to make profits from arbitrage [23] so that EV users can charge at a low price and resell at a higher price. Following this argument, most of the related studies have assumed dynamic pricing structures such as real-time-pricing (RTP) [7,14,25,27,29–31,38] or time-of-usage (TOU) tariffs [24,32,36] as a basic assumption.

Furthermore, the retail price for private consumers includes various surcharge fees such as network charges, concession fees, renewable surcharge, taxes [39], which is approximately three to four times higher than that of the wholesale price [40]. Therefore, since the power purchase cost is normally much higher than the selling price, the voluntary V2G participation of EV users who want to minimize their operating cost in this pricing scheme would be unexpected. Therefore, in such cases, the usage of incentives can be considered as a method of reducing the surcharge fees from the power purchase cost for EV users or compensating with their power selling price as the retail price. Assuming one of these incentives is applied, the question becomes: by how much would V2G participation increase and how would the potential benefits change?

On the other hand, V2G is expected to provide the public benefit of reducing the residual load peak, which eventually leads to reducing system costs and increasing the integration of renewable energy, as already suggested in many studies [9,14,24]. For the sake of those benefits, appropriate incentives are required to encourage the participation of EV users [19,41]. Loisel et al. [19] claimed that, due to the high battery cost, additional incentives are required to make the V2G business

model attractive enough to encourage EVs to become part of the power system. Guille et al. [41] suggested a business model including incentives for EV users and complementary battery exchange. At most, there is currently no specific price policy or incentive for V2G available in Germany. Taking this into consideration, the question arises: is it desirable to actively encourage V2G for the public benefit? If so, how much incentive should be provided? In order to clarify those questions, the quantity of the potential benefits and the corresponding cost should be investigated beforehand.

The research questions arising from the research gaps presented above can be summarized as follows:

- To what level can the economic and ecological benefits concerning EV users and society be expected from V2G between different pricing schemes? Such as:
 - A. Retail price for charging and the wholesale price for discharging
 - B. Wholesale price for both charging and discharging
 - C. Retail price for both charging and discharging
- Is V2G competitive compared to other charging strategies in the above pricing schemes?
- How much benefit can V2G bring to the electricity system when it is optimized to reduce the residual load and what would the associated compensation costs for EV users be?
- Would V2G be the better option for the above benefits compared to other charging strategies?
- How do the benefits or costs vary according to participation rate or the state-of-charge (SOC) restriction of EV batteries?

This study presents a model-based assessment to answer these research questions with a holistic perspective at a time of greater EV penetration: in this case, the year 2030. This will be conducted by quantifying and analyzing the potential effects of V2G on a national scale and considering battery degradation.

1.3. Approach

This study analyzes the competitiveness of V2G as a flexibility option from various perspectives compared to uncontrolled charging (UC) and DR. In order to conduct an accurate evaluation of V2G, it is crucial to conduct the optimal charging and discharging schedule of EVs. For this, a MILP (Mixed Integer Linear Problem) optimization model is created considering battery degradation. The simulated future representative EV profiles over a week are used by scaling up to the national scale.

For the first part of the study, the model schedules EVs based on an objective function that minimizes the operating cost for EV users. For the second part of the study, the model schedules EVs based on an objective function that minimizes the residual load of the electricity system. In addition to the objective function, a constraint-based approach was implemented to minimize the battery degradation of each EV. Lastly, sensitivity analyses are conducted to validate the impact of V2G participation rates and SOC restrictions for battery degradation.

To evaluate the quantitative benefit of V2G, the net cost of an individual EV is calculated combining both cost and revenue. Battery degradation cost is included by estimation of capacity fade for each EV's battery, which is calculated via a battery degradation model considering calendric and cyclic aging. Based on the additional load and supply derived from the accumulated EV profiles, the final electricity price and residual load of the electricity system will be defined and used for the evaluation.

This study is structured as follows: Chapter 2 introduces related studies; Chapter 3 describes the methods including study overview, detailed model explanation, model assumption, and input data; Chapter 4 presents the simulation results; Chapter 5 discusses the findings of the study, followed by concluding remarks in Chapter 6.

2. Related work

Research on methods to implement EV in the electricity system as a mobile storage device began in the 1990s [42], and extensive studies have been carried out in the last ten years after EVs began to appear in the consumer market. In particular, as the proportion of volatile RES such as solar and wind power systems has continued to increase, research on EV charging strategies that integrate with volatile RES has been conducted more actively [34,43].

In the first part of this chapter, relevant prior studies that focused on the interaction of EVs with power systems are introduced. Furthermore, the focus lies on papers that apply charging schedule optimization methods to effectively utilize EVs as storage devices.

In the second part, prior studies on battery degradation are presented. To include the economic effects of battery degradation in the charging schedule optimization model, fundamental battery degradation mechanisms are investigated. Next, studies of battery degradation evaluation methods are introduced to calculate the indirect cost of EV battery usage for additional purposes.

2.1. EV integration into the power system

Potential benefits using EV in power system

From the perspective of the EV user, White et al. [20] investigated the revenue potential when EVs apply a V2G strategy for peak reduction or frequency regulation in the grid. Since dynamic pricing was assumed, arbitrage profits were possible. Battery degradation was assumed to be fixed at 6.45-26.25 USD-cents/kWh of throughput depending on the battery cycle lifetime scenario. The authors concluded that there was a little financial incentive for EV users when EV is only used to reduce the peak load. But the authors stated that this benefit will be increased as RES increase in the electricity systems. Meanwhile, there is considerable revenue potential expected when EV is used for frequency regulation from the same paper. Therefore, the authors suggested a ‘dual-use’ program that operates EV for both peak reduction and frequency regulation: use for frequency regulation daily and use for peak reduction intermittently when arbitrage profit is expected to be high. In addition, the authors conducted sensitivity analyses on average driving distances and participation rates of around one million vehicles. The results were that the lower the driving mileage, the greater the revenue potential, and the greater the V2G participation rate, the lower the individual revenue potential.

Similarly, Kern et al. [14] also investigated the EV user’s revenue potential from V2G, which showed more beneficial results. The authors calculated the arbitrage profit from V2G based on an aggregated storage optimization model. An important assumption was the RTP pricing with no surcharge fees for the purchased electricity. Under this assumption, the potential revenue per individual EV per year resulted in 200-1,300 EUR. If the charging fees are considered as high as in the case of a pumped storage facility, the revenue decreased by 50-60%. In this regard, the

authors concluded that incentives should be presented to encourage arbitrage trading to increase the flexibility of future energy systems. In this paper, although the battery degradation cost was not quantified, the factors regarding battery degradation were calculated. When unlimited arbitrage proceeds, the full battery cycle increased by 200-600 full cycles per year, and the operating hours also increased by 2,000-6,000 hours per year. Therefore, the authors concluded that an appropriate regulatory framework and battery lifetime consideration are necessary for profitable V2G.

Pelzer et al. [44] presented arbitrage revenues considering battery degradation. The evaluation was made for four different energy markets from Ontario, New York, Singapore, and the eastern area of the US. Real-time prices were applied, and charging and discharging schedules for EVs were optimized through price forecasts. The model was designed to allow transactions only when the battery degradation cost was less than the expected arbitrage benefits. Assuming a battery price of 150 USD/kWh, the annual revenue was 30-100 USD with a capacity decrease of 2-3% depending on the city. Meanwhile, the battery price was assumed as 300 USD/kWh, the annual revenue decreased to 10-60 USD/kWh with a capacity decrease of 1-2%. This showed that when modeled with higher battery prices, the degradation cost is generally higher than the arbitrage profit, resulting in fewer transactions and a smaller capacity decrease as a tradeoff.

On the other hand, Hartmann et al. [17] presented the potential benefit of V2G from the aspect of the electricity system. The authors first looked at the effect on the grid for the uncontrolled charging (UC) case. When one million EVs were charged as UC, the peak load increased by only 1.5%. Meanwhile, assuming that all conventional German vehicles were replaced by EVs and performed UC, the maximum peak was shown to increase by about two times. When V2G was introduced and EVs are utilized as energy storage, it showed a maximum load reduction of 16% for one million EVs. Regarding the financial benefits for EV users, the authors concluded that trading energy in the electricity market can have a positive effect, but it would be at a low level, and the effect of battery performance degradation was not included.

The research on V2G concept is also actively conducted for integration with distributed power systems. As an example of EV integration with a photovoltaic (PV) system, Englberger et al. [45] carried out a techno-economic comparison according to the three charging strategies: simple charging (corresponding to UC), optimal charging (corresponding to DR), and V2B (vehicle-to-building, corresponding to V2G but building instead of the grid). The authors tried to minimize the operating expense (OPEX) of the prosumer by optimizing the interaction between electric load, EV, PV generation, and optional home energy storage systems (HES). The model targeted typical German households in the distributed grid level. As a result, optimal charging reduced OPEX by 15% over a ten-year simulation period, and when linked with V2B, it showed an additional reduction of 11%. However, this further reduction caused a 12% reduction in EV battery lifetime.

Regarding the EV battery lifetime, the EV battery lasted 19% longer on average when it operated with a stationary HES.

Huang et al. [32] proposed a method to integrate EVs into a building cluster so that the distribution network can be operated more efficiently. EVs are dispatched for optimizing the control of the distribution network. TOU pricing schemes with the reactive compensation of energy storage devices were considered together to effectively reduce system power loss and node voltage fluctuations. The introduction of this TOU not only increased the utilization of EVs but also reduced the power demand of distribution networks through load peak shaving and valley filling. With the proposed strategy, the results for a power distribution system showed a 13.41% reduction in the system peak load, with a 47.3% reduction in the total voltage excursion.

V2G schedule optimization

In order to utilize the EV with the power system as efficiently as possible and to model it, optimization of the charging and discharging schedules for EVs must be carried out. The goal of this sub-section is to provide an overview of the optimization models applied to determine the charging schedule. For the optimization models, there are wide differences depending on the objective functions, parameters, constraints, and solution methods even though they all cover the common basic problem as when and how much to charge and discharge the EV [46].

As an example of cost minimization with linear programming (LP), in Englberger et al. [45], LP based on the residential power flow model minimizes the OPEX by maximization of profits. The objective function is presented in Equation (1)

$$\text{Max} \sum_t (E_t^r \cdot p_t^r - E_t^P \cdot p_t^P) \quad (1)$$

At time step t , E is the amount of electricity, p is the electricity price, superscript r is remuneration and superscript P is purchase. As constraints, they considered SOC and C-rate for inequality constraints and power flow at each node for equality constraints.

For integrating a real-time charging and discharging schedule optimization, MILP can be considered. Yao et al. [35] proposed a system model adopting the MILP for an EV parking lot in which PV and ESS were integrated. This paper put two objectives into one objective function. The operation strategy is targeting a reduction of operational cost while satisfying the user's convenience as much as possible. The mathematical formulation is shown in the following Equation (2):

$$\begin{aligned} \max \sum_{t=k}^T & \left(\sum_{n=1}^N (s_n^{c,t} P_n^{c,\max} w_n^{c,t} \rho_n^{c,t} + s_n^{d,t} P_n^{d,\max} w_n^{d,t} \rho_n^{d,t}) \right. \\ & \left. + \rho^t (s_{\text{ESS}}^{d,t} P_{\text{ESS}}^{d,\max} - s_{\text{ESS}}^{c,t} P_{\text{ESS}}^{c,\max}) + \rho^t (P_{\text{grid}}^{s,t} - P_{\text{grid}}^{b,t}) \right) \end{aligned} \quad (2)$$

At timestep t , n is individual charging pole, superscripts c, d, s and b represent charging, discharging, selling, and buying. P is power, s is a continuous variable representing the charging and discharging rates in $[0,1]$, w is a weighting factor, and ρ is an auxiliary parameter.

One of the interesting parts of this method is the introduction of the last two factors w and ρ . The auxiliary parameter ρ quantifies the preference levels based on an electricity price. It is normalized into $[0,1]$. For the sake of this parameter, the objective function encourages charging behavior when the electricity price at j time step is high by granting a high preference level and vice versa. The weighting factor w grants priority to charging and discharging. It is calculated based on the remaining time until departure, the energy capacity, and the SOC of the attached EV. It is also normalized into $[0,1]$. Through this factor, this model is designed to charge as much as possible in the case of an EV that needs urgent charging, and to discharge the stored energy to the power grid in the case of an EV that has a lot of time remaining until departure. The main constraint considered is matching the quantity of demand and supply.

Similar to the two examples above, the optimization problem in many studies is cost-related as shown in Table 1. The minimization of charging cost (or maximization of revenue from electricity feeding back to the system) as an objective function for scheduling EVs associated with power systems was set in [14,24,31]. An objective function that minimizes charging cost in the context of a PV system connection was set in [29,30]. Some cases that integrate EV with a parking lot can be found in [25,26,38]. The total running cost of a parking lot is minimized in [26] while the profits of EV users are maximized [25] while maintaining the satisfaction of the parking system. Similarly, the profits of EV users were maximized in [38], but by setting an objective function that maximizes the charging and discharging rates of each EV. The EV schedule optimization coordinated with ESS was performed in [27] by setting the objective function to maximize the profits of intermediate aggregators. The dispatch of EVs that minimize the cost of DSO, which considers power loss cost and operation cost, was optimized in [28].

In addition to cost optimization, there are objective functions related to benefits for power systems or RES systems. Building integrated energy storage system (BIES) coordinated with EV was designed in [32] and an objective function to minimize active power loss and voltage excursion was set. In the case that EV is incorporated into a smart grid [33], overall load variance was minimized. Regarding RES related cases, an objective function to maximize the utilization of RES

was set [34] to ultimately reduce the cost and emission of the electricity industry. Likewise, maximization of the wind energy utilization was conducted in [36] together with minimization of system loss and cost.

For solving the optimization problem depending on the developed model, the optimization techniques utilized are mainly MILP [27,30,34,35] or particle swarm optimization (PSO) [26,34,35]. In addition, there are various techniques such as linear programming (LP) [45], dynamic programming (DP) [24], quadratic programming (QP) [31,33], fuzzy logic [29] or multi-objective optimization [32,36]. The optimization technique should be selected properly considering the set objective function and parameter as well as the resource used for computation.

One more point to note from Table 1 is that most of the EV optimization studies applied a dynamic pricing scheme. In many cases, RTP or TOU pricing scheme is applied. In the case of [45], a fixed price (FP) is applied as 0.123 EUR/kWh for remuneration and 0.437 EUR/kWh for electricity purchase.

Table 1. Summary of several prior studies that conducted EV schedule optimization

Reference	Objective function	Optimization technique	Integrated system	Pricing scheme
Englberger [45] (2020)	Max. profits (Min OPEX)	LP	PV, HES	FP
Kim [24] (2020)	Min. charging cost	DP	Power system	TOU
Kern [14] (2020)	Min. charging cost	MILP	Power system	RTP
Honarmand [38] (2014)	Max. charging and discharging rate for all EVs (Max. profits)	NLP	Parking lot	RTP
Hutson [25] (2008)	Max. profit of EV users	BPSO*	Parking lot	RTP
Saber [26] (2009)	Min. total operational cost	PSO	Parking lot	-
Jin [27] (2013)	Max. aggregator's revenue	MILP+LP	ESS	RTP
Zhang [28] (2018)	Min. cost	SOCP**	DSO	-
Mohamed [29] (2014)	Min. charging cost	Fuzzy logic	PV	RTP
Tushar [30] (2016)	Min. charging cost	MILP	PV	RTP
He [31] (2012)	Min. charging cost	QP	-	RTP
Huang [32] (2020)	Min. active power loss and min. voltage excursion	Multi-objective	BIES	TOU
Jian [33] (2014)	Min. overall load variance	QP	Regional Smart grids	-
Saber [34] (2011)	Max. utilization of RES	PSO	PV, Wind	RTP
Yao [35] (2017)	Max. satisfaction of EV users and min. cost	MILP	PV, ESS	RTP
Moeini-aghaie [36] (2014)	Max. wind energy utilization, min. system loss, and min. rescheduling cost	Multi-objective	Wind	TOU

*BPSO: Binary particle swarm optimization, ** SOCP: second-order cone program

Summary

In summary, from the previous studies, several findings can be gathered from the first part of this chapter: 1. The assumption of dynamic pricing is inevitable to implement V2G assessment especially for arbitrage profit for EV users. 2. When dynamic pricing is applied, most of the studies assumed the same price for both charging and discharging. In this assumption, the fluctuation of the electricity price easily turns into an arbitrage profit. Therefore, the active participation of V2G can be observed and many results show the economic benefits for the EV users. However, these economic benefits contain the assumption that the electricity price is the same for charging and discharging, which has a large gap from the reality where the surcharge fees exist. These excluded surcharge fees can be seen as a hidden cost in the system that has to be paid from third parties. To investigate the impact of the V2G in reality, a study needs to be carried out under the current pricing scheme. 3. The impacts of battery degradation can have a significant or minor impact on the user benefits depending on the examined works. Therefore, the battery degradation factor should be further investigated. 4. Most of the EV optimization relates to the direct economic benefits that demonstrate the main interest of program participants. There is a wide range of models used to investigate V2G. The techniques to solve them highly depend on the optimization model.

2.2. Battery degradation

Status quo of battery in EV

The batteries used in EVs have gone through several iterations and technological developments, starting with rechargeable lead-acid batteries and nickel-cadmium batteries [9]. Currently, lithium-ion batteries are used in most EVs due to their high specific energy (Wh/kg), cycle life, and efficiency [9,47]. Lithium-ion batteries are divided into various types according to chemical substances used to build the electrolytes and separators. Miao et al. [47] made a comparison of representative types as shown in Figure 2 according to several characteristics. The larger the colored area, the more promising for EV usage. The authors highlighted lithium iron phosphate (LFP), lithium manganese cobalt oxide (NMC), and lithium manganese oxide (LMO) are the most prominent for the EV. Therefore, the following related works are focused on these battery types.

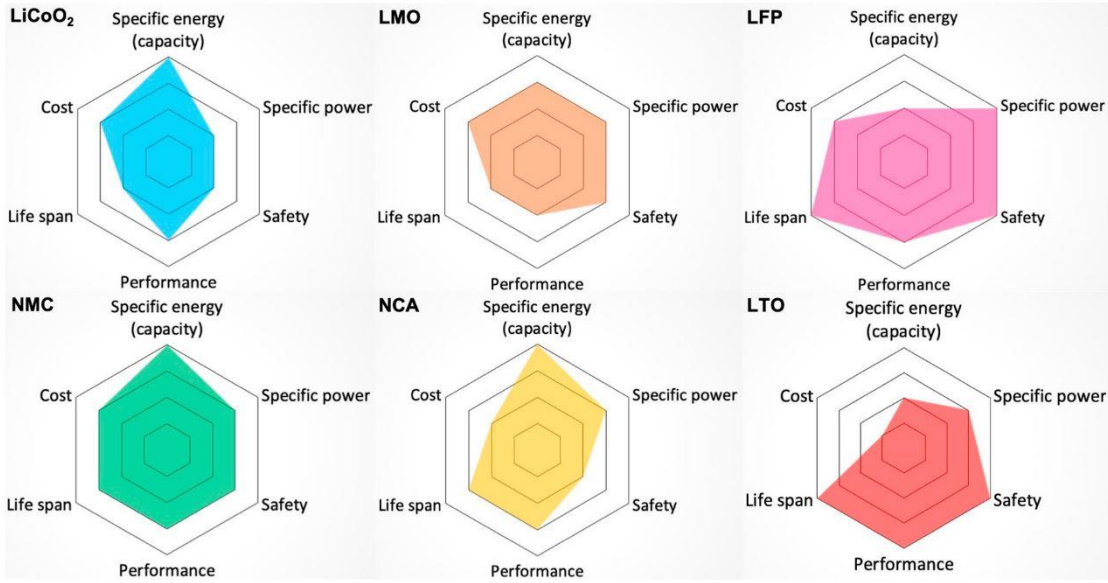


Figure 2. Comparison of Li-ion battery used for EV. The more competent, the bigger the colored area. [47].

Battery degradation mechanisms

An important aspect of energy storage planning and operation is the accurate modeling of battery degradation, especially in irregular cycling operations [48]. Furthermore, the accurate estimation of battery degradation is essential since it is one of the primary factors that prevents EV users from participating in the DR or V2G program [49]. To this end, it is necessary to know how battery degradation progresses.

The main mechanisms of degradation of a lithium-ion battery are visualized in Figure 3.

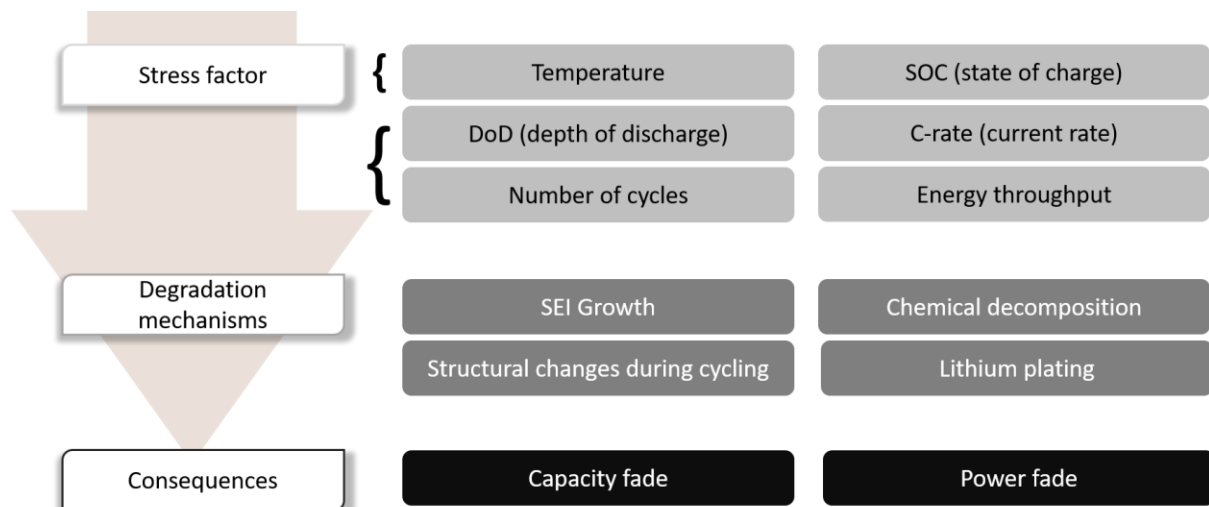


Figure 3. Battery degradation mechanism of a lithium-ion battery [47,48,50–57]

Battery degradation can be separated into calendar aging and cycle aging [51,58]. The former is mainly related to the temperature and SOC of the battery, and the latter is mainly influenced by depth of discharge (DOD), SOC, and cell temperature which are related to charge and discharge cycles [48]. These stress factors cause degradation mechanisms such as the formation of solid electrolyte interphase (SEI), chemical decomposition, structural changes during cycling, and lithium plating. These degradation mechanisms result in the loss of lithium-ion inventory and active material, eventually inducing capacity fade and power fade [50].

Temperature is one of the most primary impacts on battery degradation. Cui et al [52] conducted experiments on lithium-ion batteries cycled in shallow-depth discharge. The results show that the stress factors in the capacity loss were found to be the largest in the order of temperature, discharge rate, and discharge depth. According to Zhao et al. [53], the performance of Li-ion batteries is closely related to operating temperature. Exceeding the normal temperature can lead to a safety risk as well as accelerated battery degradation and performance degradation. The authors proposed a battery temperature control strategy in terms of internal electrode modification and external thermal management. This can be further overhauled by the battery cell technology and battery management system.

The other factor that influences battery degradation is the charging and discharging rate. Zhao et al. [54] indicated that when the charging rate is high, the lithium distribution in the particles is uneven, and the stress in the particles is high, which can lead to fracture and cavitation. Fast charging is one of the essential requirements that must be considered when it comes to the convenience of EV users. Therefore, studies to overcome this issue are in progress. For example, Sieg et al [55] investigated a method of reducing charging current to prevent the acceleration of degradation, and a charging method such as preventing local lithium plating at the edge of the cell and reducing charging current was proposed. Abdullah et al. [59] suggested adding resting periods during the charging process is to extend the battery lifetime by reducing temperature fluctuations and stress.

Another battery degradation factor is charging and discharging depth, which is mainly attributed to the user behaviors or vehicle profiles. The deeper the discharging depth, the worse the degradation [47,51]. An example can be seen in a Winston battery 100 Ah LFP cell [60]. According to the specification sheet, this battery has a guaranteed cycle life of more than or equal to 5,000 times with 80% DOD and more than or equal to 7,000 times with 70% DOD. This means a 10% reduction in DOD will bring an additional 90,000 Ah available over the lifetime. Mathews et al. [57] showed that battery life and final economic benefits differ depending on the control policy that sets the SOC limit. It is described that systems with a second life battery (that have reached 80% of their original capacity and became obsolete from EV) of 15-65% SOC limit extend the project life to more than 16 years. This showed that it is economically beneficial over the case

of new batteries with 20–85% SOC limit. In addition, the use of 15–95% SOC limit indicates a high profit initially, but further accelerates battery degradation and consequently shortens project life.

The influence of the SOC was pointed out in [61–63]. Each concluded that maintaining a high SOC for a long time accelerates degradation. Schmalstieg et al. [64] simulating a holistic degradation model concluded that lower SOC is beneficial in terms of calendric degradation but this may change to a SOC level of around 50% in terms of cyclic degradation.

Implementation of battery degradation in studies

The battery degradation can be considered in two domains for modeling EVs. First, when optimizing the schedule of EVs, it can be considered to minimize battery degradation cost. Secondly, it can be considered when evaluating the final optimized schedule.

Regarding the battery degradation during the optimization, a constraint-based approach or an objective function approach can be considered. Lunz et al [63] analyzed various charging strategies focusing on the fact that high SOC reduces the battery lifetime. With the options of DR and V2G, they further divided the charging strategy into SOC-optimized or cost-optimized. They simulated 40 households in the distribution grid with PHEV. As shown in Figure 4, depending on these further detailed strategies, the frequency of SOC differs. The battery stays mostly in higher SOC status with the cost-optimized strategy, which accelerates battery degradation. Meanwhile, the SOC-optimized option spreads more evenly throughout the SOC range, which reduces battery degradation. The results of [63] demonstrate the importance of considering battery degradation when formulating a charging strategy. Based on the simulation conditions, the intelligent charging algorithm shows that the extended battery life is twice as high as the economic savings from energy transactions, and the percentage of the battery's depreciation cost is about 70%.

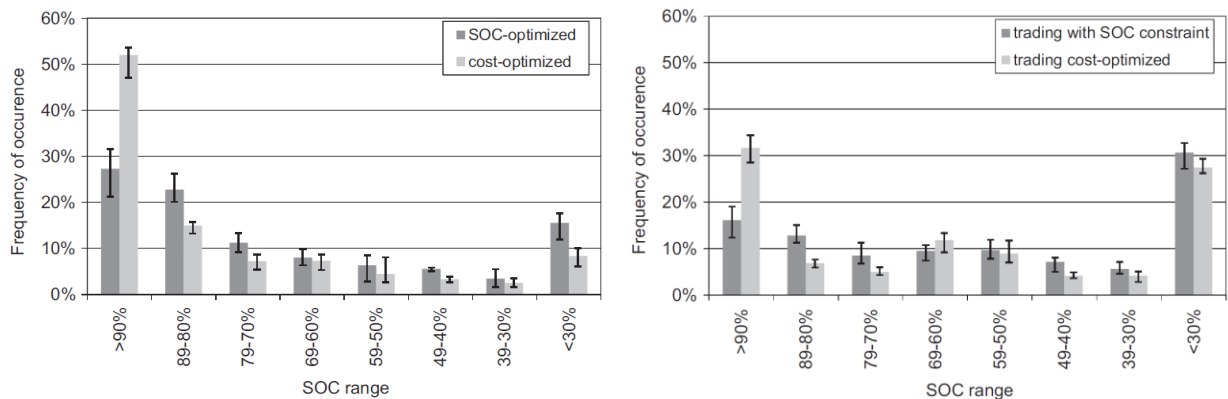


Figure 4. Frequency of SOC range depending on the charging strategy of SOC-optimized and cost-optimized. The left graph is for the DR case and the right one is for the V2G case. [63]

Likewise, a constraint-based approach has been often considered in the optimization of the EV charging schedule. For example, a SOC boundary of 8-95% for inequality constraints during the optimization was considered in [45]. Large-scale deployment of EV was conducted in [17,19] and they both applied DOD of 80% as a means of avoiding the battery degradation as much as possible.

In addition to the constraint-based approach, battery degradation can be considered in the objective function to actively consider the effect when arranging V2G scheduling. Li et al. [49] scheduled V2G through a multi-objective optimization problem for 47 vehicles with 40 households and 15 minutes of controlling interval. The optimization problem was solved using the PSO algorithm. They used the rain-flow cycle counting (RCC) method to count the number of cycles so that they can quantify battery degradation phenomena and apply it to optimization. RCC has been a popular counting method for fatigue models where random stress is applied rather than regular full cycles. Although the consideration of random cycles for EVs is a step forward the shortcoming of this approach is that it does not account for the SOC state. Since they faced obstacles derived from the weak features of PSO as a typical heuristic algorithm, they proposed a method called 'multi population collaborative mechanism' to overcome these chronic problems. The method is promising but since it is for real-time operation, high computational power is required.

When considering the battery degradation in evaluation, which is when the EV schedules are already set, model-based approaches allow to consider more factors. Besides the major factors listed earlier, there are numerous physical and chemical mechanisms during actual operation [65], which lead to the actual mechanism of battery degradation are much more complex. There are more detailed studies that proposed models that incorporate or deduce these factors [48]. Adoption of a proper model depending on purpose would be vital to get a more accurate evaluation of EV usage in the electricity system. Jingli et al. [50] presented a well-organized key summary in this regard as shown in Table 2.

A model can be selected according to the final indicators, characteristics of the model, and purpose of use. While capacity and resistance are mainly presented for theoretical models and semi-empirical models, remaining useful life (RUL) or state of health (SOH) can also be presented for empirical models. Theoretical models seem ideal in terms of high accuracy and low data dependency, but they contain high complexity and present implementation difficulties. Meanwhile, empirical models have low complexity but low accuracy and medium to high data dependency. Likewise, each model has its strengths and weaknesses. Unless high accuracy or a low complexity of model implementation are required, semi-empirical models appear to be a valid compromise.

As an example of the semi-empirical model, Schmalstieg et al. [64] carried out battery degradation tests for $\text{Li}(\text{NiMnCo})\text{O}_2$ (NMC) battery cell. The authors showed how accelerated aging experiments can be used to parameterize a holistic aging model. To investigate various impact

factors, more than 60 cells are tested. Temperature and various SOC statuses are considered for the calendric aging test and different cycle depths and mean SOC are considered for cyclic aging. A solid basis is given by validation based on various practical driving profiles and temperatures. Physically dependent functions are derived from these data, resulting in mathematical modeling of aging. An impedance-based electric-thermal model is coupled to the aging model to quantify stress variables including temperature or voltage. The model evaluates the final battery degradation resulting in a capacity loss by combining calendric and cyclic factors.

Table 2. Summary of battery degradation model [50]

Models	Indicators	Degradation Origins Captured	Accuracy	Complexity of Model Implementation	Data Dependency	Suitable Applications
Theoretical models	Capacity, Resistance	Calendric, Cyclic	High	High	Low	Mechanism analysis
Arrhenius-based	Capacity, Resistance	Calendric, Cyclic	Low	Low	Medium	
Cycle counting	RUL	Cyclic	Low	Low	Medium	
Empirical models	Ah/Wh-throughput	RUL	Cyclic	Low	Low	System planning and operation analysis; On-board estimation
	Other regression	Capacity, Resistance	Calendric, Cyclic	Low	Low	
	ANN-based	SOH	Calendric, Cyclic	Medium	Low	High
Semi-empirical models	Capacity, Resistance	Calendric, Cyclic	Medium	Medium	Medium	System planning, operation analysis

Summary

From the second part of this chapter, there are some insights for considering battery degradation into an assessment model: 1. There are extensive factors influencing battery degradation. In the domain of V2G, where increased battery usage is presumed, cyclic aging must be considered. In this regard, 2. SOC constraint-based methods can be well integrated into the optimization model for the charging schedule of EVs. 3. For the assessment of V2G, a dynamic battery degradation model is better to be considered to verify the potential difference in EV charging behavior. 3. There are a number of battery degradation models presented. It is required to choose a proper model compromising between accuracy, the complexity of model implementation, and data dependency.

3. V2G optimization model and evaluation method

The goal of this study is to quantify the systemic, economic, and ecological benefits or costs expected when EVs are coordinating with the electricity system by V2G. These benefits and costs will vary depending on the purpose of V2G. In this study, simulation cases are defined based on two purposes from different perspectives: 1. minimizing the total operating cost for the EV users¹, 2. minimizing the residual load² for the electricity system.

The entire assessment model developed in this study consists of an optimization module and an evaluation module. In the optimization module, the simulation of EV schedule optimization takes place. In the evaluation module, the benefits and the costs are quantified.

3.1. Study overview

Definition of the charging strategies

In order to determine the competitiveness of V2G, it is essential to compare it with comparable alternative strategies. In this study, UC and DR are used for these comparisons. The EV charging strategies considered in this study are defined as follows:

- UC : Uncontrolled charging. Also known as simple charging. EV is charged at EV users' will. As shown in the conceptual diagram in Figure 5, EV users tend to recharge immediately after EV operation, which has a high probability to overlap with high system loads of the grid [9].
- DR : Demand response. Also known as controlled charging or smart charging or V1G [1]. EV is charged considering the electricity system by shifting its charging schedule depending on the object given, e.g., it charges when the electricity price is low or the residual load is low as shown in Figure 5.
- V2G: Vehicle-to-grid. Also known as bi-directional charging. EV is more actively involved in grid stability. EV battery is used as a mobile ESS by communicating with the electricity system, e.g., EV stores electricity when the residual load is low and discharges the electricity back to the grid when the residual load is high as depicted in Figure 5.

¹ Total operating cost of EV users = cost for electricity purchase – revenue from electricity sales + cost for battery degradation

² Residual load = system demand - variable RES generation (here, the variable RES generation includes wind onshore, wind offshore and PV)

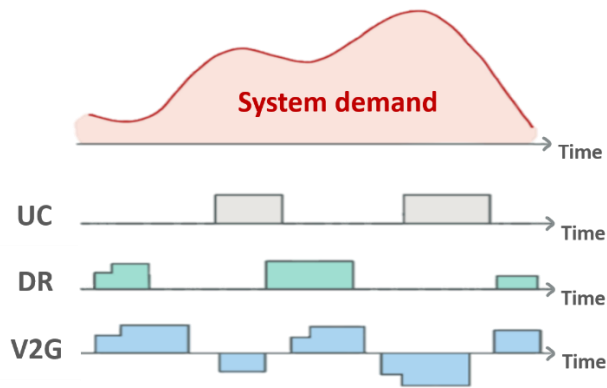


Figure 5. Conceptual diagram for different EV charging strategies. The square area represents the charging or discharging energy. UC is charging regardless of the status of system demand, DR shifts the load to where the system demand is low, and V2G actively reacts to the status of system demand by feeding back the electricity as well as shifting the load.

Case descriptions

Simulation cases are divided into the following three parts according to the research questions presented in Section 1.2. Figure 6 briefly shows all cases. V2G and the alternative charging strategies DR and UC, with different simulation parameters and conditions are compared on a national scale and with the presence of battery degradation effects.

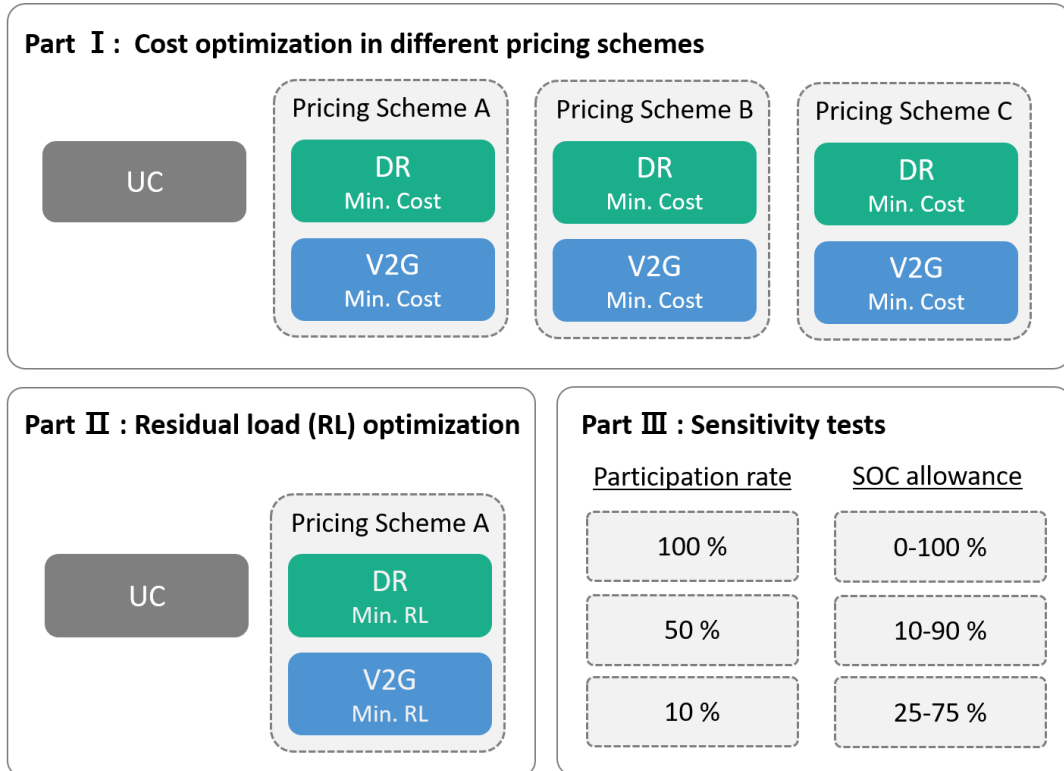


Figure 6. Overview of the simulation cases. All cases are divided into three parts according to the objectives of V2G.

In Part I, to determine the economic benefits for EV users, cost optimization is conducted. The optimal V2G and DR schedules minimize EV operating cost. The operating cost consists of the electricity cost for purchase and remuneration from selling the electricity back to the grid. The economic and ecologic benefits of V2G are examined according to the different pricing schemes:

- Pricing Scheme A: Retail price for charging; wholesale price for discharging
- Pricing Scheme B: Wholesale price for both charging and discharging
- Pricing Scheme C: Retail price for both charging and discharging

The wholesale price is the hourly electricity price derived directly from the electricity bidding market, while the retail price includes various surcharge fees such as network charges and taxes for private consumers [39].

In Part II, to determine the systemic benefits for electricity grids, the EVs are scheduled to minimize the residual load. The final cost will be evaluated using Pricing Scheme A, which corresponds to the current German pricing scheme for EVs. Furthermore, specific compensation costs for the benefits will be normalized and presented, e.g., specific cost for 1 MW of residual load reduction or specific cost for 1 ton of CO₂ emission reduction.

In Part III, sensitivity analyses are conducted by varying two parameters: the participation rate of V2G and the SOC allowance range of EV batteries. The reason for sensitivity analyses with different participation rates is to validate whether competition between EVs occurs when a substantial number of EVs apply DR or V2G. If the competition occurs, how it affects the interests of the final stakeholders. Furthermore, the reason for the SOC allowance range is to validate the impact of the constraints-based approach on battery degradation.

Model structure

The structure of the entire assessment model is as shown in Figure 7. It consists of a database, optimization modules, and evaluation modules.

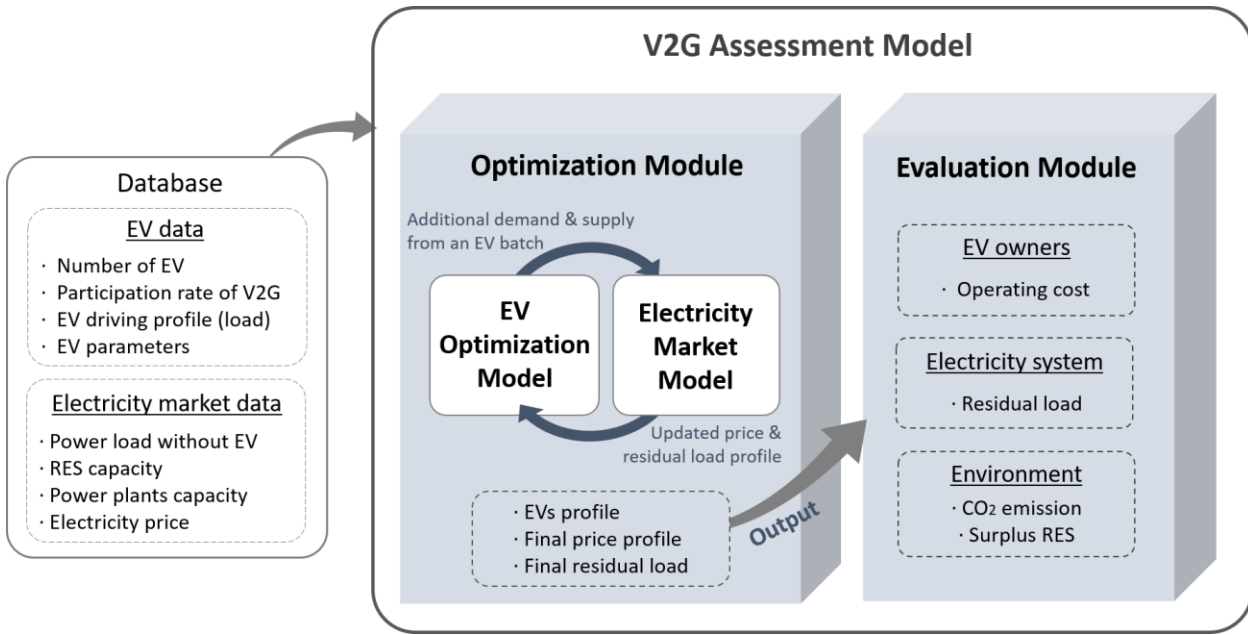


Figure 7. The structure of the V2G assessment model was created in this study. The model consists of an optimization module and an evaluation module. In the optimization module, two sub-models – an EV optimization model and an electricity market model - interact with each other.

As a first step, all the parameters are defined, and input data is collected and pretreated. The details regarding input data are described in the following Section 3.4. The representative EV profiles are selected and scaled up to a national scale. These scaled-up individual EVs are then grouped into batches with the same profiles, and the EV schedules are optimized. For the electricity market simulation, market basic input data such as power load of the electricity system, power generation configuration, and basic data for renewable generations are prepared.

In the optimization module, which is again composed of an EV optimization model and an electricity market model, the main optimization of EV scheduling takes place. Every EV batch is optimized in sequence. Every time an EV batch optimized its schedule, the corresponding load or supply is added to the electricity market model resulting in a newly updated price and residual load for the next batch. After optimizing the schedule of the last EV batches, the final output enters into the evaluation module. The detailed model description will be followed in the next sub-section.

Finally, in the evaluation module, potential benefits for each simulation case are analyzed from the perspective of EV users, the electricity system, and the ecological domain. The operating costs of EV, the residual load reduction, CO₂ emission, and surplus RES are evaluated as main indicators.

Each step is described in further detail in Sections 3.2 to 3.4.

3.2. Optimization module

In this module, the optimal EV schedule for charging and discharging is conducted according to the objective function. The optimization module is composed of an optimization model and a market model. The scheduling is simulated on an hourly basis for a representative week³ in 2030.

3.2.1. Simulation structure

For the sake of a quick grasp of the entire simulation structure, a schematic charging schedule optimization for a single EV is described in Figure 8.

First, the driving profile and EV parameters of a single EV are entered into the optimization model. The model is optimizing the EV schedule, either to minimize the cost of the EV derived from the initial electricity price or to minimize the initial residual load depending on the simulation cases. The initial price and residual load here are simulated values from the electricity market model excluding the corresponding EV load or supply.

The driving profile constraints the charging strategy as it determines time frames in which the EV is not connected to the grid or has to charge to meet the required driving distances. For example, EV must be able to conduct its driving schedule as a first priority. In other words, it must store enough energy for driving by the time to start driving. When the EV is driving, charging or discharging back to the grid is impossible.

After deriving the optimized charging and discharging schedule, this newly generated load or supply profile from the EV is additionally entered into the electricity market model resulting in a new price and residual load profiles. These new values together with the scheduled EV profiles become the input of the next step, the evaluation module.

³ The simulation period of this study was set to one week due to the available computational resources. Since the entire model simulates both the optimization model and the market model interacting with each other, the run time for one week was three to four hours per each case. Therefore, one representative week was selected and simulated. The method to select the representative week is described in Section 3.4.

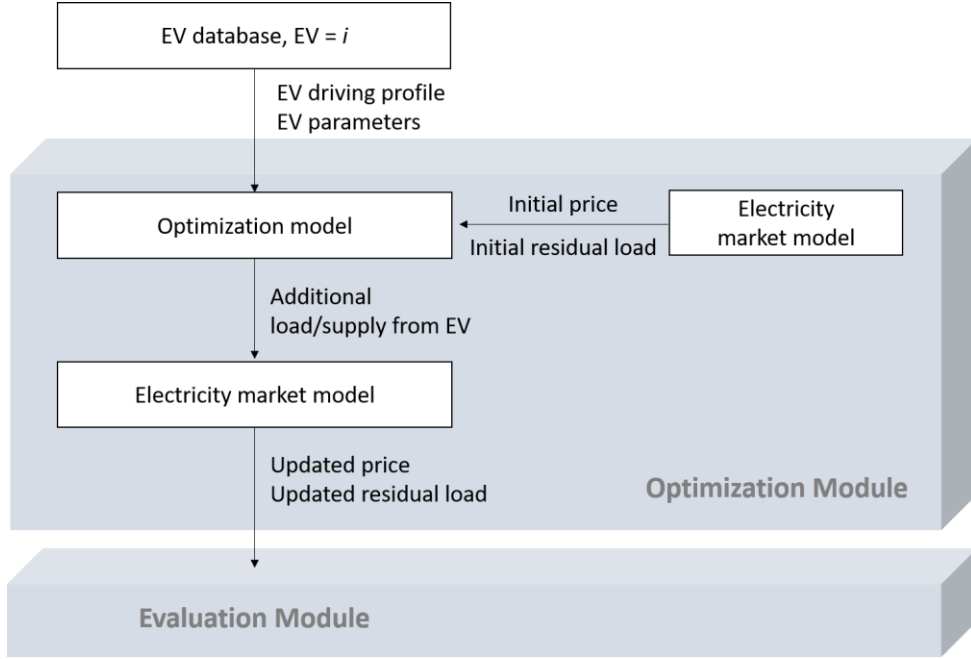


Figure 8. Flowchart of EV scheduling in the case of a single EV. The charging and discharging schedule is optimized in the optimization model with input data of driving profile, parameters, initial price, and initial residual load profiles. The market model then calculates the new price and residual load including the additional load and supply from the optimized EV schedule.

Based on the method to schedule a single EV, an approach to schedule six million EVs is as follows. If six million EVs are simulated at once and the price is not dynamically adjusted, all EVs will try to charge at the time slots with the lowest price. This would cause electricity prices to dramatically increase, and the electricity system would become severely unstable. This simulation setup problem is called the avalanche effect in [37]. Kühnbach et al. [37] mitigated this effect by dividing the EV pool into smaller batches which are sequentially simulated and the price is adjusted after each batch. In reality, a real-time electricity price increase would prevent large agglomerations of charging EVs. However, in this thesis, the individual EVs are grouped into batches with the same profile. The optimized charging schemes for each EV batch are sequentially calculated and applied to the electricity market model.

The flowchart of the EV scheduling in the case of a large number of EVs is visualized in Figure 9. In this thesis, the selected profiles of 1355 EVs are scaled up to create a set of six million EVs. The scale factor is applied by the representativeness of the corresponding individual EV over all EVs in the pool. Afterward, The EVs with the same profile are grouped into batches (i). Thus, there are initially 1355 EV batches. The batch size (s) depends on its scale factor. Similar to the previously described optimization method for a single EV, the hourly charging and discharging schedule for each EV batch is derived. In other words, all EVs in the same batch will have the same charging and discharging schedule.

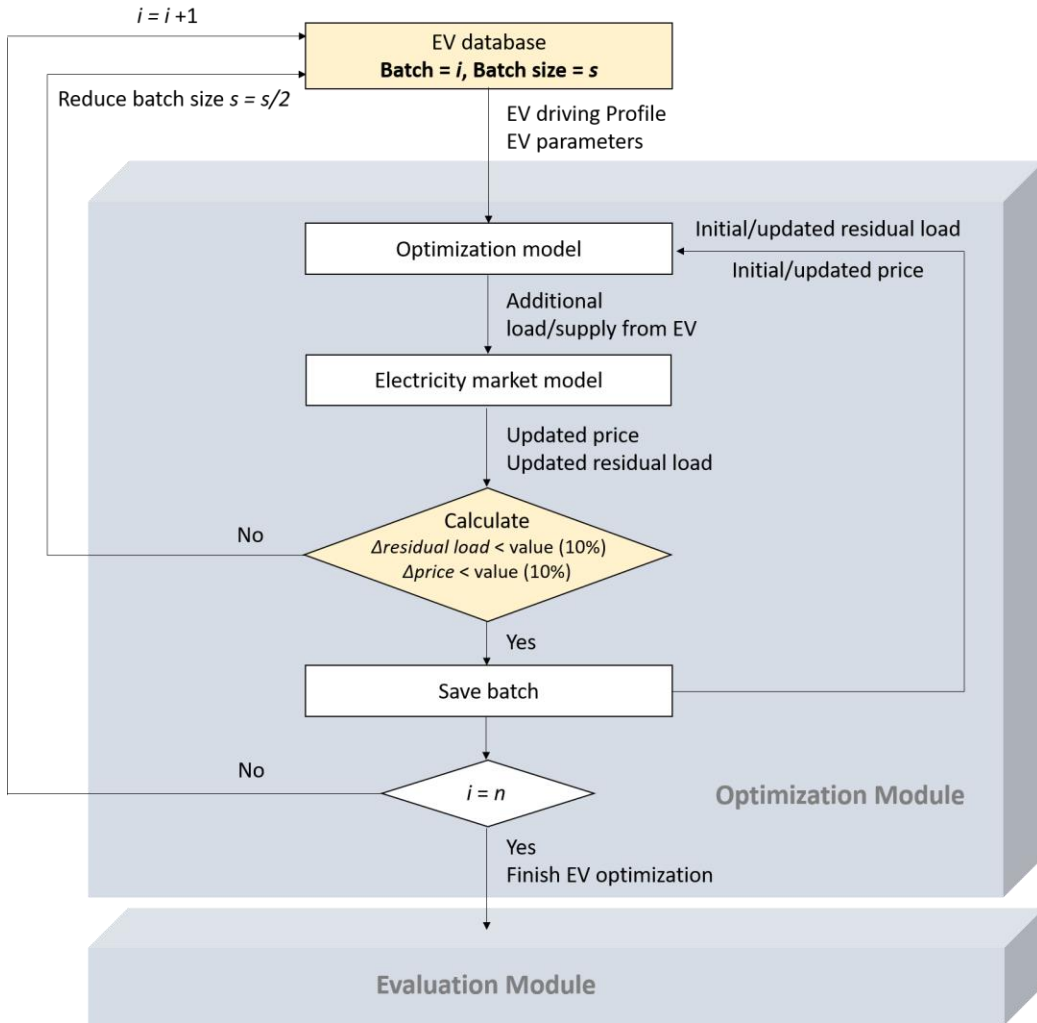


Figure 9. Flowchart of EV scheduling in the case of a large number of EVs. Compared to the individual flowchart, A loop that judges the suitability of the batch size and a loop that iterates the EV batches to the end are added.

Instead of a single EV, the EV driving profile and parameters of the EV batch $i = 1$ with a batch size of s are entered into the optimization model. The charging and discharging schedule of the EV batch $i = 1$ is calculated to minimize the operating cost or residual load of the electricity system. The initial price and residual load derived from the electricity market model are used as constant inputs to the objective function. The resulting optimized charging and discharging schedule, which is an additional load and supply to be added to the grid, enters into the electricity market model again as input values. Then the new electricity price and residual load are updated. When the optimization of the EV scheduling of the first batch is completed, the EV driving profile and parameters of the next batch are entered into the optimization model. This time, the updated electricity price and residual load from the optimization of the previous batch are used for the components of the objective function.

For the sensitivity analysis with a participation rate of 10% and 50%, the initial electricity price and residual load for the first batch are calculated including the portion of the uncontrolled EV load.

One of the considerations to note in this model is the suitability of the batch size. To mitigate discretization errors caused by oversized batches and to model real-time price adjustments, an additional loop is introduced. This corresponds to the rhombic box in the middle of Figure 9. In other words, the six million EVs have been grouped into batches, but this does not guarantee whether they avoid avalanche effects. Thus, it is crucial to determine the appropriate EV group size. Otherwise, it can result in unfavorable incidental demand or supply peak in the electricity market when the group size is too big. Therefore, the price and residual load simulated based on the optimization of each batch are compared with the previous values. When the difference of an EV batch is more than 10%, the batch size is bisected. When the discretization is fine enough to pass the aforementioned criteria, the current batch and the optimized schedule are saved. This process is applied iteratively until all batches have been appropriately sized. By applying this loop, the simulation is independent of batch size, and the avalanche effect is avoided.

The model ends the iteration at the end of the last batch n , and the aggregated demand and supply profiles of all EV batches enter the evaluation module along with the final price and residual load.

3.2.2. Optimization model

As discussed above, the charging and discharging schedule of each EV batch is sequentially optimized in the optimization model. The model is designed as a MILP since the status of the EV can only be in one status, either charging, discharging (back to the grid), driving or parking. The model has perfect foresight, which means that the EV driving profile, RES generation, and the power demand in the electricity market for the considered period are already known. The detailed input parameters and assumptions are described in the following Section 3.4. The main variables, parameters, and abbreviations used in the equations are shown in Table 3.

Table 3. Summary of the main variables, parameters, and abbreviations used in the equations.

E	electricity energy [MWh]	Bi	binary variable
P	power [MW]	η	efficiency
RL	residual load [MW]	V2G	vehicle to grid
SD	system demand [MW]	G2V	grid to vehicle
RES	RES supply [MW]	ch	charging
t	time [hour]	dch	discharging
SOC	SOC of battery [-]	drv	driving
p	electricity price [EUR/MWh]	m	a big number constant

Objective function

There are possibly two objective functions in the model depending on the simulation cases. The objective function for the cases aiming at cost minimization is described in Equation (3):

$$\text{Min. Cost} = \text{Min.} \left(\sum_t E^{G2V}_t \cdot p_t^{\text{ch}} - \sum_t E^{V2G}_t \cdot p_t^{\text{dch}} \right) \quad (3)$$

E^{G2V}_t is the electricity energy charged from grid to EV at time t , E^{V2G}_t is the electricity energy discharged from EV to grid at time t , and p_t is the electricity price at time t . In this model, an RTP pricing scheme is assumed, therefore, the hourly electricity price for charging and discharging are applied depending on the pricing scheme option defined for each case. The equation is minimizing the cost to EV users obtained by subtracting the remuneration benefits from the charging cost. The model allows negative values if the remuneration benefits are greater than the charging costs.

Secondly, the objective function for the cases aiming at minimization of the residual load is as shown in Equation (4):

$$\text{Min. } (RL_t)^2 = \text{Min.} \sum_t (SD_t - RES_t + P^{G2V}_t - P^{V2G}_t)^2 \quad (4)$$

SD_t is the system demand without EV addition at time t , and RES_t is the variable RES generation at time t , P^{G2V}_t is the electricity load charged from the grid to EV at time t , and P^{V2G}_t is the electricity load discharged from EV to the grid at time t . Here, the residual load value was set to obtain the minimum value after squaring in order to consider the situation when the residual load is negative. The reason for using the squared value as the objective function instead of the absolute value is to give greater weight to times with a larger residual load. This is because even if the same amount of residual load is reduced, it is more beneficial for the grid to reduce the case where the residual load is larger.

Constraints

In order to optimize the EV schedule, conditions for achieving the objective function must be satisfied. The following Equations (5) – (14) represent the constraints considered in this model.

- a. Stored energy of EV battery at time t

$$E^{EV}_t = E^{EV}_{t-1} + E^{G2V}_t \cdot \eta_{\text{ch}} - E^{V2G}_t / \eta_{\text{dch}} - E^{\text{drv}}_t / \eta_{\text{drv}}, \quad \forall t \quad (5)$$

The stored energy of the battery at time t is calculated by adding the charged energy to the battery status at the previous time step $t-1$ and subtracting the energy consumed for discharging or driving.

The actual charged energy to the battery is the value obtained by multiplying the energy purchased from the grid (E^{G2V}_t) by the charging efficiency (η_{ch}). Meanwhile, the actual discharged or driving amount is the value obtained by dividing the respective efficiency (η_{dch} , η_{drv}) from the amount of energy sold (E^{V2G}_t) or the amount of energy for driving (E^{drv}_t).

b. Initial SOC equals to final SOC

$$E_{\max}^{\text{EV}} \cdot SOC_{\text{initial}} = E_{\text{end}}^{\text{EV}} \quad (6)$$

The initial SOC for all EV batteries should be the same as the final SOC. This is written in stored energy in Equation (6). E_{\max}^{EV} is the storage capacity of the battery, and multiplying this by the initial SOC gives the initial stored energy. This constraint is applied to match the input EV profiles used in this study. This is also an essential condition when executing the model for a long-term period like one year, by repeatedly using EV profiles of one week.

c. Binary constraints: EVs can be only in one status: either charging, discharging, driving, or idle.

$$Bi^{G2V}_t + Bi^{V2G}_t + Bi^{drv}_t \leq 1, \forall t \quad (7)$$

$$Bi^{G2V}_t \geq E^{G2V}_t / m, \forall t \quad (8)$$

$$Bi^{V2G}_t \geq E^{V2G}_t / m, \forall t \quad (9)$$

$$Bi^{drv}_t \geq E^{drv}_t / m, \forall t \quad (10)$$

Each variable Bi is a binary variable of the corresponding superscript. That is, at each time t , the value of Bi^{G2V}_t is assigned as one when the EV is in the state of G2V (charging from the grid to the EV), which means E^{G2V}_t is more than zero. The value of Bi^{G2V}_t is zero when the EV is not in the state of G2V. The same applies to the variables Bi^{V2G}_t and Bi^{drv}_t .

Equation (7) means that during the entire simulation period, the sum of the binary variables of G2V, V2G, and driving status at each time t must be less than or equal to one. That is, only one variable of these three can be one, which means again, only one status is possible for each time step. If it is zero, it means none of the three statuses are active in the EV, so EV is in idle status. In the case of the following Equations (8), (9), and (10), these make each binary variable as one when the energy corresponding to each status is greater than zero at each time t . Here, a large number constant m is introduced. Thus, if energy is present for the corresponding timestep, its value is divided by m so that it becomes greater than zero and less than one. In this model, this constant m is set to ten times each battery storage capacity.

d. Maximum charging/discharging power per time

$$P_{G2V}^t \leq P_{\max} , \forall t \quad (11)$$

$$P_{V2G}^t \leq P_{\max} , \forall t \quad (12)$$

For all simulation periods, the power purchased from the grid and the power sold to the grid at time t is less than or equal to the maximum power of the battery. For the DR cases, P_{V2G}^t in Equation (12) will be set to be less than or equal to zero because there is no energy feeding back to the grid.

e. Minimum/maximum SOC

$$E_{\max}^{\text{EV}} \cdot SOC_{\min} \leq E_{\text{EV}}^t , \forall t \quad (13)$$

$$E_{\text{EV}}^t \leq E_{\max}^{\text{EV}} \cdot SOC_{\max} , \forall t \quad (14)$$

During all simulation periods, the battery status of EVs is designed to stay in a specific SOC range. This is due to the SOC constraint-based approach to prevent extensive battery degradation in the model, as described in the previous Section 2. Related Work. The deep DOD causes battery degradation rapidly [47,51] while keeping the SOC range at the middle is beneficial in terms of cyclic degradation [64]. Therefore, the SOC allowance range is restricted to avoid battery degradation as much as possible during the simulation. Exceptionally, the SOC allowance range can be expanded for several EVs when the extended range is inevitable to satisfy a specific EV driving profile. Nonetheless, the maximum expansion cannot exceed above SOC 1.0 or below SOC 0.0. For example, the default SOC range is set by 0.25 to 0.75 for most of the cases. This means that when scheduling EVs, it is desired to use only half of the possible capacity. However, half of the capacity may not be sufficient depending on the driving profile of the EVs such as a long-term driving of more than half of the capacity required. This is solved through model iteration by increasing the SOC range gradually.

Computation

The optimization model was developed and executed in Python environment. The optimization is designed in PYOMO, “an extensible Python-based open-source optimization modeling language” [66]. The commercial program GUROBI [67] was used as the solver.

3.2.3. Electricity market model

In the optimization module, the electricity market model provides price and residual load, which are important inputs to the objective function when the optimization model is optimized with a given EV driving profile. In addition, when all EVs are optimized, the market model provides the final prices and residual loads that include the additional EVs' load and supply. In this study, the electricity market model MiPU (Minimal Cost Allocation of Power Units), which was already developed by other projects of Fraunhofer ISI [39,68], was adopted and implemented. In this subsection, a brief introduction regarding this model will be delivered.

The MiPU model simulates the German electricity market on an hourly basis. The basic input data are power demand, renewable energy generation, available conventional power plant generation, corresponding parameters, and fuel costs. It calculates the optimal configuration of the power supply, which is the minimum cost power plant dispatch, based on the merit order method. In other words, the marginal cost and usable power capacity of all available power plants are calculated and sorted by price. The generation of the power plants is summed starting with the lowest price and ending when the demand is matched by the sum of supply providing power plants. The price of the most expensive power plant that contributes generation is set as the market price and every power plant receives this price. “The power plant-specific marginal costs are calculated considering fuel costs, CO₂ allowances, the type and age of the power plant, ramp-up times, ramp-up costs and downtimes” as shown in Equation (15) [39].

$$C_{k,t}^{\text{var}} = \frac{1}{\eta_k} \cdot P_{k,t} (p_{k,t}^{\text{fuel}} + p_t^{\text{CO}_2} \cdot e_k^{\text{CO}_2}) + C_{k,t}^{\text{st}}, \quad \forall k, \forall t \quad (15)$$

$C_{k,t}^{\text{var}}$ is the power plant-specific marginal costs of power plant k at time t , η_k is the conversion efficiency of power plant k , $p_{k,t}^{\text{fuel}}$ is fuel cost, $p_t^{\text{CO}_2}$ is CO₂ cost, $e_k^{\text{CO}_2}$ is the CO₂ conversion factor for each power plant k , $C_{k,t}^{\text{st}}$ is the ramp-up costs.

As a result, the hourly market prices are attained within the system boundaries of Germany. These are wholesale prices and do not include other surcharge fees. The market model used in this thesis does not include external trading with neighboring countries and additional stationary electricity storage is not considered as well. Therefore, there might be some cases that the available power plant does not meet the power demand. In this case, the price is set as a default value. In this thesis, the highest value among all cases is substituted for this price and used for the comparison between cases in the evaluation step. One important point to note is that the model does not allow negative prices, and the minimum price is set at zero. This will be further discussed in Chapter 5. Discussion.

3.3. Evaluation module

In order to evaluate whether V2G is competitive, and to validate the impact of the parameters set for the sensitivity analyses, the following three aspects are mainly compared between simulation cases. First, the total operating cost is calculated from the perspective of EV users. This corresponds to the economic competitiveness of V2G. Next, from the perspective of the electricity system, residual loads of each case are compared. Finally, CO₂ emissions and surplus RES are compared to evaluate V2G from an ecological point of view.

3.3.1. Cost benefits to the EV users

The total operating cost for the EV users is calculated by taking into account the electricity cost for charging, revenue from electricity sold back to the grid, and the battery degradation cost. For the electricity price, three different pricing schemes are applied corresponding to the cases as defined in Section 3.1.

Electricity costs and remuneration

After the charging schedule of all EVs is optimized, the final electricity market price is determined. This final price is applied to the collected charging and discharging schedule of individual EV j participating in the DR or V2G. The electricity cost, $C_j^{\text{elect.}}$ and revenue, $R_j^{\text{elect.}}$ of individual EV j are calculated for the simulation period as shown in Equation (16), and (17) respectively. In this study, the simulation period is set to 168 hours.

$$C_j^{\text{elect.}} = \sum_t E^{\text{V2G}}_t \cdot p_t^{\text{ch}} \quad (16)$$

$$R_j^{\text{elect.}} = \sum_t E^{\text{G2V}}_t \cdot p_t^{\text{dch}} \quad (17)$$

For the comparison between the cases, the average and the standard deviation are weighted by the scale factor for both electricity costs and revenues of six million individual EVs. Therefore, $\bar{C}^{\text{elect.}}$ and $\bar{R}^{\text{elect.}}$ are the weighted average of electricity cost and electricity remuneration for total EVs, $\bar{\sigma}_C^{\text{elect.}}$ and $\bar{\sigma}_R^{\text{elect.}}$ are the weighted standard deviation of electricity cost and electricity remuneration for total EVs, w_j is the scale factor of individual EV j . These are shown in the following Equations (18) - (21).

$$\bar{C}^{\text{elect.}} = \frac{\sum_{j=1}^n C_j^{\text{elect.}} \cdot w_j}{\sum_{j=1}^n w_j} \quad (18)$$

$$\bar{R}^{\text{elect.}} = \frac{\sum_{j=1}^n R_j^{\text{elect.}} \cdot w_j}{\sum_{j=1}^n w_j} \quad (19)$$

$$\bar{\sigma}_C^{\text{elect.}} = \sqrt{\frac{\sum_{j=1}^n w_j \cdot (C_j^{\text{elect.}} - \bar{C}^{\text{elect.}})^2}{\sum_{j=1}^n w_j}} \quad (20)$$

$$\bar{\sigma}_R^{\text{elect.}} = \sqrt{\frac{\sum_{j=1}^n w_j \cdot (R_j^{\text{elect.}} - \bar{R}^{\text{elect.}})^2}{\sum_{j=1}^n w_j}} \quad (21)$$

Battery degradation cost

As aforementioned, the cost of battery degradation is one of the major points to be clarified. In this thesis, the cost of battery degradation is calculated by estimating the capacity loss of the battery. The capacity loss is calculated by applying a method by Schmalstieg et al. [64]. The battery aging-related calculation method presented below and the basic Equations (22), (23), (25), and (26) are derived from [64].

The reduction of battery capacity is calculated by combining the effects of calendric aging and cyclic aging on battery degradation. These are assumed to be independent of each other. The initial state-of-health (SOH) of all EV batteries is assumed to be at 95% of the ideal state which does not have any degradation.

The calendric aging is based on an Arrhenius equation. The fit function adopted for calendric aging is given in Equation (22) and the corresponding empirical factors are given in Equation (23):

$$CL_{\text{cal}} = \alpha_{\text{cap}} \cdot d^{0.75} \quad (22)$$

$$\alpha_{\text{cap}} = (7.543 \cdot V - 23.75) \cdot 10^6 \cdot e^{-\frac{6976}{T}} \quad (23)$$

CL_{cal} is the capacity loss ratio considering calendric degradation, α_{cap} is combined aging factors for capacity, d is duration time in day unit, V is voltage in volts, T is the absolute temperature in Kelvins which is assumed as 298.15 K in this thesis. Voltage is calculated from SOC as shown in Equation (24) based on the open-circuit voltage curve presented in Schmalstieg et al. [64]. and assuming linearity. The SOC is assumed to be ranging between 0 and 1. V_{max} of 4.1 V and V_{min} of 3.3 V are applied.

$$V[V] = SOC \cdot (V_{\max} - V_{\min}) + V_{\min} \quad (24)$$

The calendric aging is evaluated on an hourly basis based on the SOC of each time step instead of calculating at once assuming constant SOC for the entire simulation period. The reason for this is that the range of SOC level of battery differs according to the cases, and this will cause different degrees of battery aging. For instance, a too low or too high SOC accelerates battery aging. Therefore, in the cases where the SOC range is restricted to 25-75% and the case of the unrestricted SOC range of 0-100%, there is not only a DOD difference in cyclic aging but also a difference in calendric aging according to its SOC level.

The total capacity loss of calendric aging for the entire simulation period is calculated from the hourly capacity loss derived for each time step. This is implemented by introducing virtual time as shown in Equation (25). This calculation approach of total capacity loss from the hourly capacity loss is modified from a part of an open source modeling framework for simulating stationary energy storage systems (SimSES) [69] conducted by Technical University Munich.

$$t_{\text{virtual}, t} = \left(\frac{CL_{\text{cal},t-1}}{\alpha_{\text{cap},t}} \right)^{\frac{4}{3}} \quad (25)$$

$t_{\text{virtual}, t}$ is the virtual time at time step $= t$, $CL_{\text{cal},t-1}$ is capacity loss until time step $= t-1$, $\alpha_{\text{cap},t}$ is combined aging factor for capacity at time step $= t$. In other words, the virtual time is the time that it would take for the capacity loss up to time step at $t-1$ based on the aging factor at time step t . Therefore, the capacity loss for the calendric aging at time t is as shown in Equation (26)

$$CL_{\text{cal}, t} = \alpha_{\text{cap},t} \cdot (d + t_{\text{virtual}, t})^{0.75} \quad (26)$$

Here, the duration time d is in days, i.e., a time step corresponds to 1/24 day.

Likewise, the cyclic aging is calculated with the basic fit function of Equation (27) and the corresponding factors as Equations (28) and (29):

$$CL_{\text{cyc}} = \beta_{\text{cap}} \cdot \sqrt{Q} \quad (27)$$

$$\beta_{\text{cap}} = 7.348 \cdot 10^{-3} \cdot (\emptyset V - 3.667)^2 + 7.600 \cdot 10^{-4} + 4.081 \cdot 10^{-3} \cdot \Delta DOD \quad (28)$$

$$Q [\text{Ah}] = \frac{E_{\text{dch}}}{\emptyset V} \quad (29)$$

C_{cyc} is capacity loss ratio considering cyclic degradation, β_{cap} is combined aging factors for capacity from the cyclic aging tests, Q is the charge throughput in ampere-hours, $\emptyset V$ is the average voltage in volts, and ΔDOD is the depth of discharge in a range between 0 and 1. Since the equations and parameters suggested in Schmalstieg et al. [64]. are based on the battery cell, the charge throughput Q is calculated based on the cell level. The reference battery cell used in [64] is rated with 2.15 Ah typically.

The total capacity loss of cyclic aging is accumulated from each cycle, and in this thesis, the cycle is defined based on the period that the battery is constantly discharged. Similar to the total calendric loss calculation, virtual throughput is introduced as shown in Equation (30). This is to calculate the total capacity loss of cyclic aging from the discrete each cyclic aging. Again, this calculation approach is modified from a part of [69].

$$Q_{\text{virtual}, v} = \left(\frac{CL_{\text{cyc},v-1}}{\beta_{\text{cap},v}} \right)^2 \quad (30)$$

$Q_{\text{virtual}, v}$ is virtual throughput at the v -th cycle, $CL_{\text{cyc},v-1}$ is capacity loss until $v-1$ -th cycle, $\beta_{\text{cap},v}$ is combined aging factor of cyclic aging for capacity at the v -th cycle. In other words, the virtual throughput is the throughput that it would take for the capacity loss up to the v -th cycle based on the aging factor at the v -th cycle. Therefore, the capacity loss for the cyclic aging of the v -th cycle is shown in Equation (31)

$$CL_{\text{cyc},v} = \beta_{\text{cap},v} \cdot \sqrt{(Q_v + Q_{\text{virtual},v})} \quad (31)$$

The total battery degradation cost is then calculated as the combined capacity loss at the final simulation time step multiplied by the battery cost as shown in Equation (32):

$$C_j^{\text{bd}} = (\alpha_{\text{cap}} \cdot t^{0.75} + \beta_{\text{cap}} \cdot \sqrt{Q}) \cdot \text{Battery cost}_j \quad (32)$$

C_j^{bd} is the total battery degradation cost of an individual EV, Battery cost_j is estimated by multiplying the battery capacity of each individual EV j by the battery pack price per kWh. The expected battery pack price in 2030 assumed in this thesis is 62.05 EUR/kWh [70] (converted from 73 USD/kWh with an 0.85 EUR/USD exchange rate).

For each case, the weighted average battery degradation cost \bar{C}^{bd} , and the standard deviation $\bar{\sigma}_C^{\text{bd}}$ are calculated, again using the scale factor w_j of individual EV j (see Equation (33) and (34)).

$$\bar{C}^{\text{bd}} = \frac{\sum_{j=1}^n C_j^{\text{bd}} \cdot w_j}{\sum_{j=1}^n w_j} \quad (33)$$

$$\bar{\sigma}_C^{\text{bd}} = \sqrt{\frac{\sum_{j=1}^n w_j \cdot (C_j^{\text{bd}} - \bar{C}^{\text{bd}})^2}{\sum_{j=1}^n w_j}} \quad (34)$$

Total Cost

Finally, the total operational cost for an individual EV j is calculated as shown in Equation (35).

$$C_j^{\text{total}} = C_j^{\text{elect.}} - R_j^{\text{elect.}} + C_j^{\text{bd}} \quad (35)$$

The cases are compared using the weighted average total costs \bar{C}^{total} and the total costs' weighted standard deviation $\bar{\sigma}_C^{\text{total}}$ (see Equations (36) and (37)).

$$\bar{C}^{\text{total}} = \frac{\sum_{j=1}^n C_j^{\text{total}} \cdot w_j}{\sum_{j=1}^n w_j} \quad (36)$$

$$\bar{\sigma}_C^{\text{total}} = \sqrt{\frac{\sum_{j=1}^n w_j \cdot (C_j^{\text{total}} - \bar{C}^{\text{total}})^2}{\sum_{j=1}^n w_j}} \quad (37)$$

3.3.2. Benefits from the electricity system perspective

To evaluate the impacts for the electricity system, implications on the residual load are assessed using the following indicators provided by Erdogan et al. [71]

Peak residual load reduction

The calculation for the positive and negative peak load reduction rate compared to UC, PLR_{pos} and PLR_{neg} are shown in Equations (38) and (39), respectively. The peak load is indicated as PL .

$$PLR_{\text{pos}} [\%] = \frac{PL_{\text{pos}}^{\text{UC}} - PL_{\text{pos}}}{PL_{\text{pos}}^{\text{UC}}} \cdot 100 \quad (38)$$

$$PLR_{\text{neg}} [\%] = \frac{PL_{\text{neg}}^{\text{UC}} - PL_{\text{neg}}}{PL_{\text{neg}}^{\text{UC}}} \cdot 100 \quad (39)$$

Peak shaving performance

“The ratio of the total shaved energy to the total energy to be shaved” is also suggested by [71]. In this thesis, it is assumed that the state of the ideal residual load is zero. This is referred to as the peak shaving performance rate, PSP as shown in Equation (40). It is calculated with the absolute residual load of each case, $|RL|$, and the absolute residual load of UC, $|RL^{UC}|$.

$$PSP [\%] = \frac{\int (|RL^{UC}|_t - |RL|_t) dt}{\int |RL^{UC}|_t dt} \cdot 100 \quad (40)$$

3.3.3. Ecological benefits

The ecological evaluation is carried out in terms of CO₂ emission and surplus of the variable RES. Similar to the electricity system in the previous sub-section, the increase or decrease of CO₂ emissions and surplus RES are compared in percent according to simulation cases based on UC. This is shown in Equations (41) and (42).

$$CO_2 \text{ emission reduction } [\%] = \frac{\sum_t CO_2 \text{ emission}^{UC} - \sum_t CO_2 \text{ emission}}{\sum_t CO_2 \text{ emission}^{UC}} \cdot 100 \quad (41)$$

$$Surplus \text{ RES reduction } [\%] = \frac{\sum_t RES \text{ surplus}^{UC} - \sum_t RES \text{ surplus}}{\sum_t RES \text{ surplus}^{UC}} \cdot 100 \quad (42)$$

3.3.4. Specific cost: compensation costs per benefit

The specific compensation costs are calculated based on the expected benefits from V2G compared to UC and the additional costs incurred to EV users by it for each case. In this study, the specific cost for the positive peak residual load reduction, $Specific \text{ cost}_{RL}$, and the CO₂ emission reduction, $Specific \text{ cost}_{CO_2}$ are presented as shown in Equation (43), (44). In other words, these values represent the needed compensation costs for the EV users per reduced peak load of 1 MW and per reduced CO₂ emission of 1 ton.

$$Specific \text{ cost}_{RL} [\text{EUR/MW}] = \frac{C_{total} - C_{total}^{UC}}{PL_{pos}^{UC} - PL_{pos}} \quad (43)$$

$$Specific \text{ cost}_{CO_2} [\text{EUR/ton}] = \frac{C_{total} - C_{total}^{UC}}{CO_2 \text{ emission}^{UC} - CO_2 \text{ emission}} \quad (44)$$

3.4. Model assumption, parameters, and input data

3.4.1. Model assumption and parameters

The main model parameters of this study are provided in Table 4. Each simulation case is simulated on an hourly basis over a week in 2030. The conventional power generation capacity and renewable generation capacity in 2030 are assumed based on the NEP-B scenario of the network development plan (Netzentwicklungsplan) by the German transmission system operators [72]. The report presents scenarios NEP-A, NEP-B, and NEP-C according to innovations (sector-coupling, flexibility, and storage) and the share of renewable energy as of 2030, with NEP-C being the most progressive scenario, and NEP-B being an intermediate scenario. The configuration of power generation for NEP-B is shown in Table 5, and the unit price for both fuel and CO₂ used in the model derived from the World Energy Outlook [73] is shown in Table 6.

Table 4. Main parameters applied for evaluation model of all simulation cases.

Category	Description
Target year	2030
Power generation configuration scenario	NEP-B [72]
Simulation period	1 week
Time interval	1 hour
Modeling prediction	Perfect foresight
Number of EV	6,000,000 [74]
Electricity price	RTP
Surcharge	16.45 EURcents/kWh [39]
Charging power	1C (no fast charging)
Battery charging/driving efficiency	1.0
Battery discharging efficiency	0.95
Initial and final SOC	0.75
SOC allowance range	0.25-0.75 / 0.1-0.9 / 0.0-1.0 (possibly increase for exceptional EV profiles)
Initial battery SOH	0.95 (Calendric: 0.985, Cyclic: 0.965)

Table 5. Power generation capacity configuration based on grid scenario NEP-B in 2030 [72]

Conventional power plant	Capacity (GW)	Renewable generation	Capacity (GW)
Brown coal	9.3	Wind onshore	81.5
hard coal	9.8	Wind offshore	17.0
natural gas	35.2	Photovoltaic	91.3
Oil	1.2	Biomass	6.0
Pumped storage	11.6	Hydropower	5.6
Other conv. generation	4.1	Other RES	1.3
capacity reserve	2.0		
Sum	73.2	Sum	202.7

Table 6. The unit price of power generation based on energy type [73]

Generation	Price	Unit
Renewable	0	EUR/MWh
Oil	53.86	EUR/MWh _{th}
Gas	24.9	EUR/MWh _{th}
Coal	9.07	EUR/MWh _{th}
Lignite	6.4	EUR/MWh _{th}
Biomass	0	EUR/MWh _{th}
CO ₂	27.59	EUR/ton

The simulation week is selected as a week in which the contrast of residual loads over the simulation period is clearly shown, and the domestic power generation combined with conventional and renewable generation could meet the basic system power demand over the simulation period. The further details are described in the following Sub-section 3.4.3. The number of EVs is assumed as six million based on BMU (Federal Ministry for the Environment, Nature Conservation, and Nuclear Safety) in 2019 [74].

Depending on the simulation cases, surcharge fees apply (see Section 3.1). In this thesis, the surcharge fees are assumed as 16.45 EURcents/kWh. This is calculated by subtracting procurement cost and renewable surcharge from the retail electricity price, which is based on the household of the annual consumption of 3,500 kWh electricity in 2018 described in [39].

The charging power is considered to be constant, therefore fast charging is not considered. The battery efficiency for charging and driving are set to 1.0 for consistency with the EV profile database used for this thesis. Instead, the battery efficiency for discharging is applied as 0.95 in order to make the difference between the ones that constantly charge and discharge and the ones

that do not. The initial SOC of all EVs is set to 0.75, and the final SOC at the end of the simulation has to be equal to the initial SOC. The SOC allowance range, which is applied to minimize battery degradation, is set to 0.25-0.75 for most of the cases. Additionally, SOC allowance ranges of 0.1-0.9 and 0.0-1.0 are used in the sensitivity analysis. The initial battery SOH for all cars is assumed as 0.95. This value is used as the starting capacity fade when evaluating battery degradation.

Lastly, by 2030, under the assumption that the infrastructure for EVs will be well established, it was assumed that charging and recharging are possible at any time without restrictions on access to the grid as long as the EV is not driving.

3.4.2. Input data for EV data

In order to simulate six million EVs, the 1355 representative EV profiles for 2030 are scaled up by applying corresponding scale factors. Those representative EV data and scale factors are simulated data from a research project conducted by Fraunhofer ISI [75] based on historic vehicle usage data by [76]. The scale factor considers the representativeness of the corresponding individual EV over the entire EV in the simulation. There were 2677 EV profiles for one week available in the raw data, and in this thesis, 1355 were selected through the following pre-processing.

- Exclude EV profiles in the case of data omission.
- Exclude EV profiles in the case that the limit of SOC is exceeded ($SOC_t > 1.0$ or $SOC_t < 0.0$) during the simulation period when starting SOC is set to 0.75.
- Exclude EV profiles when the starting SOC and ending SOC do not match.

EV driving profile

The 1355 representative EV profiles include discharging and charging schedule over a week on an hourly basis. The charging schedule is divided into four areas: domestic, commercial, work, and public. In this thesis, those charging schedules are merged and used as uncontrolled charging.

Figure 10 shows an example of a sample EV profile named ‘199411’ during the simulation period. The accumulated EV driving profile for the whole data set, which is scaled up to six million EVs, is shown in Figure 11. The first 120 hours represent Monday till Friday and the rest corresponds to the weekend.

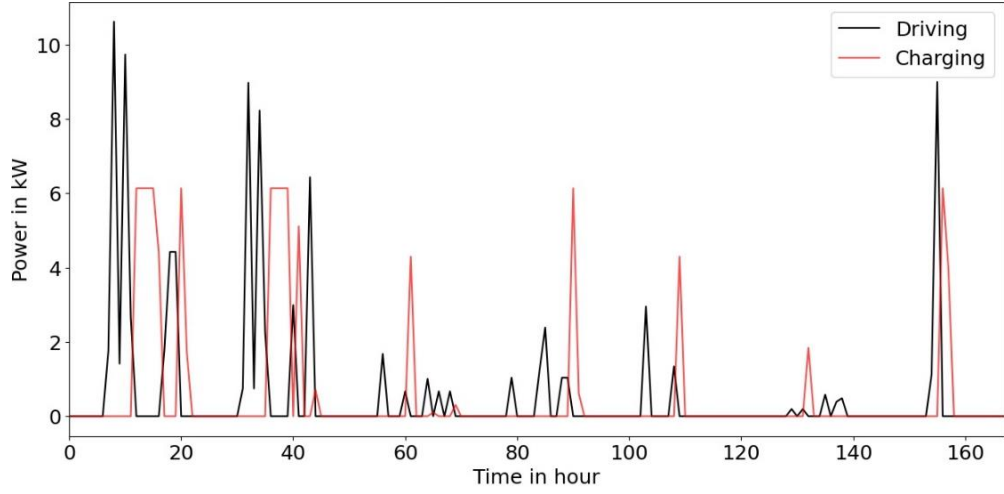


Figure 10. EV driving and charging profile of a sample EV named ‘199411’.

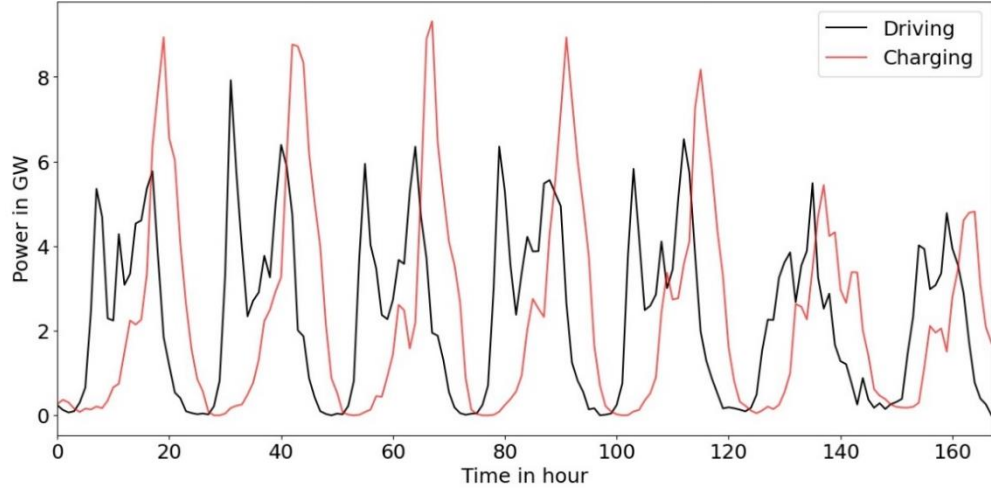


Figure 11. EV driving and charging profile of accumulated six million EVs.

In the case of the sample profile, driving and charging are prominent during the first two days, and it seems that relatively long-distance travels take place on Sunday. There are several points that can be clearly seen from the accumulated EV profile. First, driving in the morning hours and after work hours are prominent during weekdays, and the demand for operation and charging is relatively low on weekends. Also noteworthy, it can be seen that most of the charging occurs immediately after operation. The total electricity demand of six million EVs for one week is about 393.58 GWh, which is on average 2.34 GWh per hour.

EV parameters

In order to optimize the charging schedule of the selected EVs, corresponding parameters are required. The charging power for all individual 1355 EVs is assumed to be 6.1 kW. The EVs are agglomerated into three different storage capacity groups, respectively 34.2 kWh, 62.1 kWh, and 90 kWh. The classification of each is shown in Figure 12, where the scale factors are already applied. More than half of all EVs have a battery capacity of 62.1 kWh, 26% have a battery capacity of 34.2 kWh, and the remaining 20% have a large battery capacity of 90 kWh [75].

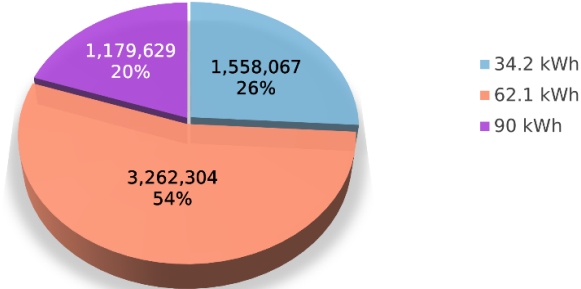


Figure 12. Classification of EVs based on battery storage capacity.

Figure 13 below shows the SOC range of the scaled up EV profiles during the simulation week. Each circle represents EV batches which are scaled up from the 1355 representative EVs. The size of the circle shows the number of each EV batch and the color of the circle shows the storage capacity. Many of the EV batches have minimum SOC between 0.3 to 0.7 and Maximum SOC of 0.75 to 0.85. Since there was no SOC restriction for the raw data, there are high numbers of EV batches that use SOC up to 0.0 and 1.0. In the case of an EV batch with a storage capacity of 90 kWh, when the scale factor is large, the SOC range usually stays in the range of 0.5 to 0.95, but overall, the effect on the SOC range according to the storage capacity does not seem to correlate.

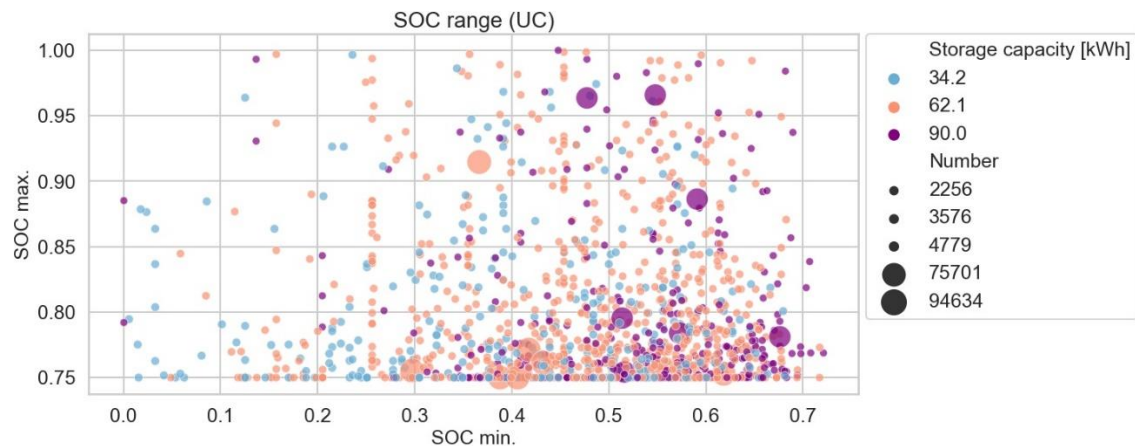


Figure 13. The SOC range of the EVs used for simulation. SOC max. and SOC min. are obtained based on charging and driving profile of raw data (Own calculation based on data from [75]). The initial SOC and final SOC of EVs are all set to 0.75. Each circle represents an EV batch. The color represents the storage capacity of each EV in kWh, and the size of the circle represents the number of EVs in the EV batch.

3.4.3. Input data for electricity market model

In this section, the primary elements of the electricity market model are introduced. First, the input data required for the model are outlined. Then the overall electricity market status of 2030 without EV is introduced, and finally, the electricity market status of the selected simulation week among the one-year period is introduced.

Market model input data

The electricity market model used in the optimization module provides the electricity price and residual load on an hourly basis as output. For this, system load, available power capacity, the corresponding parameters are required. Data of the conventional power capacity is derived from [72], and system load and RES profile are derived from [77] which is calculated based on the wind speed and solar radiation data as of 2015.

Electricity market status of 2030

Figure 14 to Figure 16 show the simulated electricity market status of 2030 without considering additional demand and supply from EV. The x-axis represents the day of the year and the y-axis represents the hour of each day. The starting point is the 1st of January. Additional heatmaps for the system load, the PV generation, and the wind generation are given in Appendix A.

Figure 14 shows the expected residual load as of 2030, which is defined as the system demand minus the variable renewable generation in this thesis. When the value is closer to zero, variable renewable generation matches well with the system demand. The dark blue color indicates that the residual load is high, that is the variable renewable generation is insufficient. Meanwhile, the dark red color indicates that there is excess supply from variable renewable generation. The color in the middle of the heatmap is pale, where the PV generation is prominent. The highest residual load sections (dark blue) are mostly in winter when the system demands are high and the PV generations are relatively low. Those generations are shown in Figure A-1 and Figure A-2 in Appendix A. On the other hand, the high negative residual loads are also mostly in winter, where the high wind generations occur. The time step with high wind generation and the time step with strong negative residual load are almost identical.

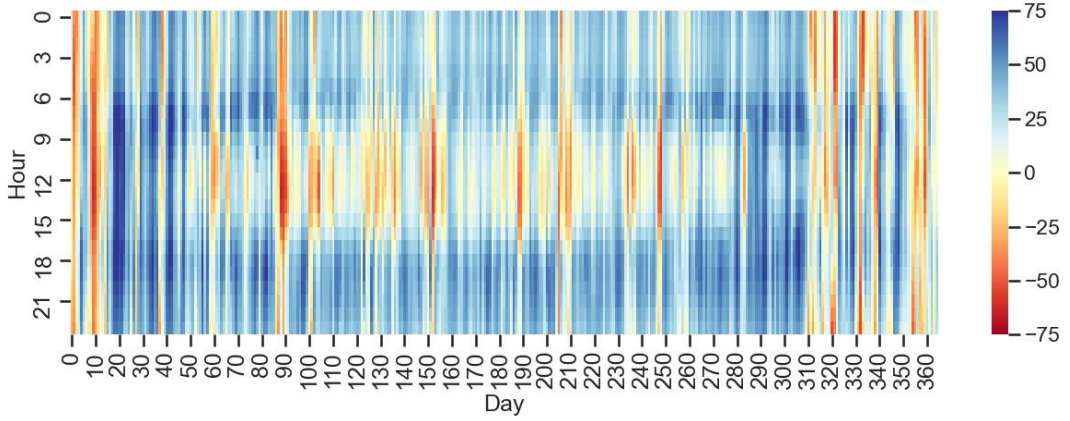


Figure 14. Simulated residual load of the German electricity system in 2030 [GW]

The simulated electricity price of 2030 is shown in Figure 15. Comparing with the residual load heat map, the highest prices appear when the residual loads are very high. There is a positive correlation with the residual load even though it is not identical throughout the entire extend. This relationship is illustrated in Figure 16. Electricity price is increasing according to the residual load. The color of each dot represents the power plant, that is determines the electricity price, locating at the end of the merit order at the corresponding timestep. When the residual load is negative or zero, it is sufficiently covered by variable renewable generation and the price is zero. As the residual load is positive, the electricity price is determined according to the marginal cost. As explained in Section 3.3 above, since this model does not allow negative prices, the minimum price is zero, and it is expressed as a fixed price of 300 EUR when the electricity demand cannot be provided by the available domestic resources.

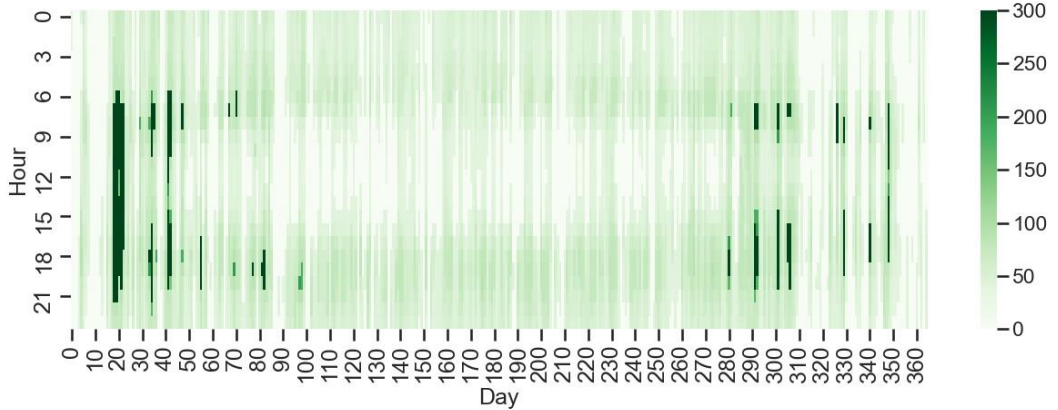


Figure 15. Simulated wholesale price for electricity in 2030 [EUR/MWh]

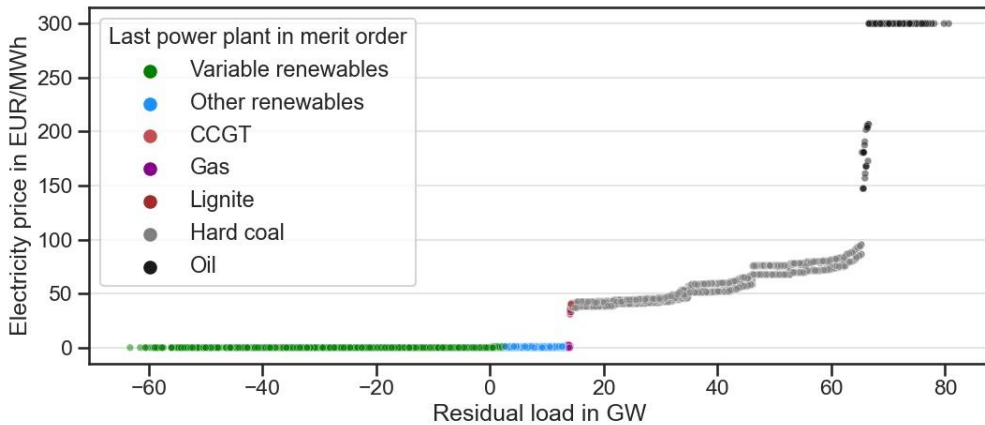


Figure 16. The electricity price and residual load. Each point represents the electricity price at the corresponding residual load. The color of the points represents the type of power plant that determines the price each time in the electricity market.

Electricity market status of the simulation period

The time series of the simulated residual load and price over the year 2030 have been examined. Among this one-year period, one week from day 4 to day 10 is selected for the simulation according to the following selection criteria.

- The contrast of residual load should be apparent during the simulation period.
- The power demand should be satisfied with the domestic available power supply during the simulation period. (Excluding the time step where the electricity price is 300)
- Seven consecutive days satisfying the above conditions.

The reason for the first point is that the effect of V2G interacting with the grid can be maximized when the contrast of the residual load is clear. Secondly, if the domestic available generation cannot meet the power demand, the price is set to a fixed price of 300. Therefore, the second point tries to avoid those assumed default price as much as possible.

The key elements of the electricity market during the simulation period are depicted in Figure 17 and Figure 18. As shown in Figure 17, over the simulation period, demand shows a distinct diurnal cycle: high demand during daytime and low demand during nighttime. Furthermore, the demand on weekdays is relatively larger than the one on weekends. During the selected simulation period, the PV generation is relatively low (< 20 GW), while the wind generation shows a large fluctuation. The wind generation shows almost 120 GW at some peak hours during the last half of the simulation week, which exceeds the demand. This causes the residual load to drop as shown in Figure 18.

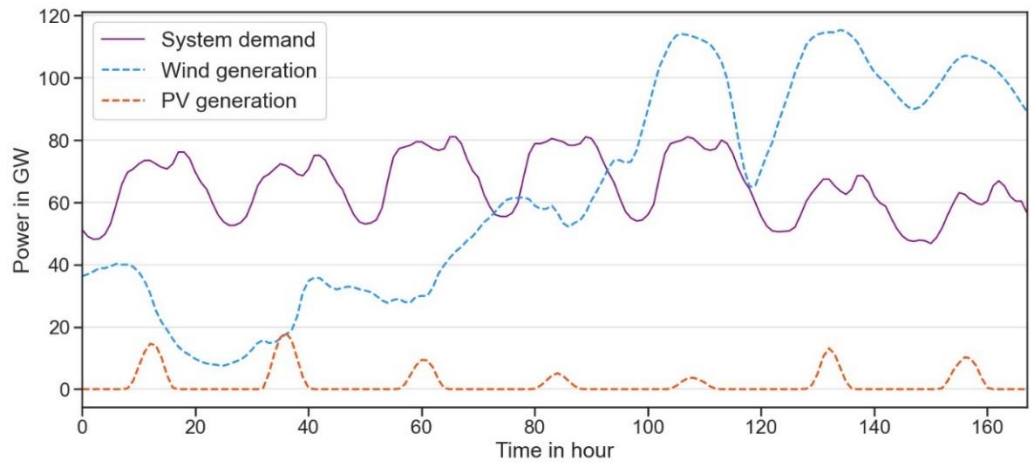


Figure 17. System demand and variable renewable energy source over the simulation week in 2030

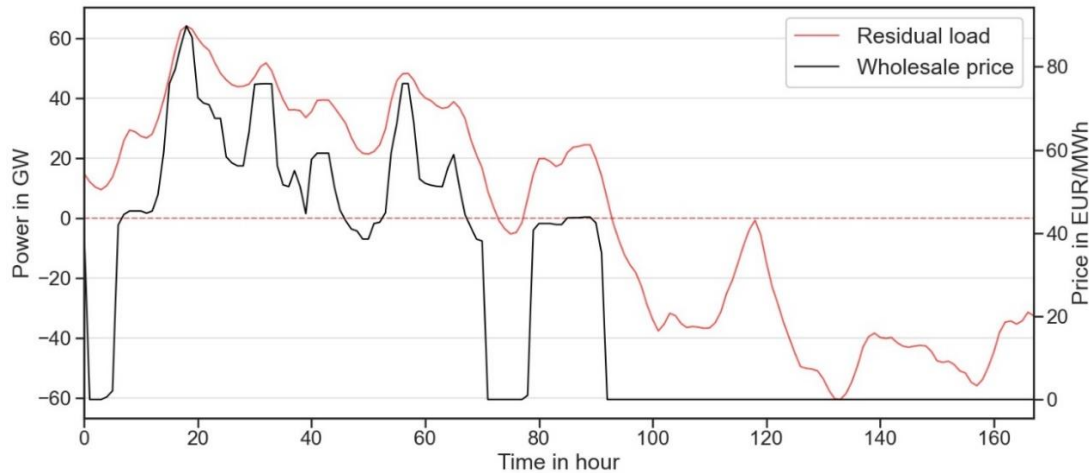


Figure 18. Residual load and electricity price over the simulation week in 2030

4. Results

4.1. Cost minimization based on pricing schemes (Part I)

In part I, the potential benefits of V2G according to several pricing schemes are examined to see the competitiveness of EV in the electricity market. For this purpose, an objective function that minimizes the cost for EV users was set and correspondingly the EV schedule was optimized. The applied pricing schemes are recited as follows.

- Pricing Scheme A: Retail price for charging; wholesale price for discharging
- Pricing Scheme B: Wholesale price for both charging and discharging
- Pricing Scheme C: Retail price for both charging and discharging

Charging and discharging schedule

The following Figure 19 shows the cost-optimized EV results according to each simulation case. In the case of UC on the top left of Figure 19 which does not apply any optimization, it is shown that the charging is scheduled based on a daily routine. This increases the existing system load even further, which causes higher final electricity prices during several peak times.

For DR cases, EV scheduling is almost identical for all three pricing schemes. This is caused by the limitation of one-directional charging. As the EV can only charge but not discharge into the grid, the scheduling is unaffected by price differences between purchase and selling prices for electricity. Furthermore, the constraints of the schedule optimization force the EV to fulfill its driving schedule. The optimized charging cycle is thereby solemnly based on the relative price fluctuations throughout the day and not the absolute price.

Likewise, In the case of V2G with Pricing Scheme A, there is no discharging back to the grid. In the case of Pricing Scheme A, the price of electricity purchase is including the surcharge fee, which makes it very high compared to the price of electricity sales, so there is no economic benefit to resell electricity at all. Although there is no discharging, the charging schedule of V2G is not identical with the DR charging schedule. The difference occurs in the last timesteps. This is because the wholesale prices in the last time steps are equal to zero, which would make no difference regarding charging time for cost optimization. It seems that the optimization solver in the optimization algorithm applies different initial points for DR and V2G cases.

On the other hand, in the case of V2G with Pricing Scheme B and C, there are discharging peaks, which means that there are active electricity sales back to the grid. All electricity sales occur during the peak time of the initial price to maximize the economic profit, and as a result of this, the final cost is also relatively leveled for the first half of the time steps.

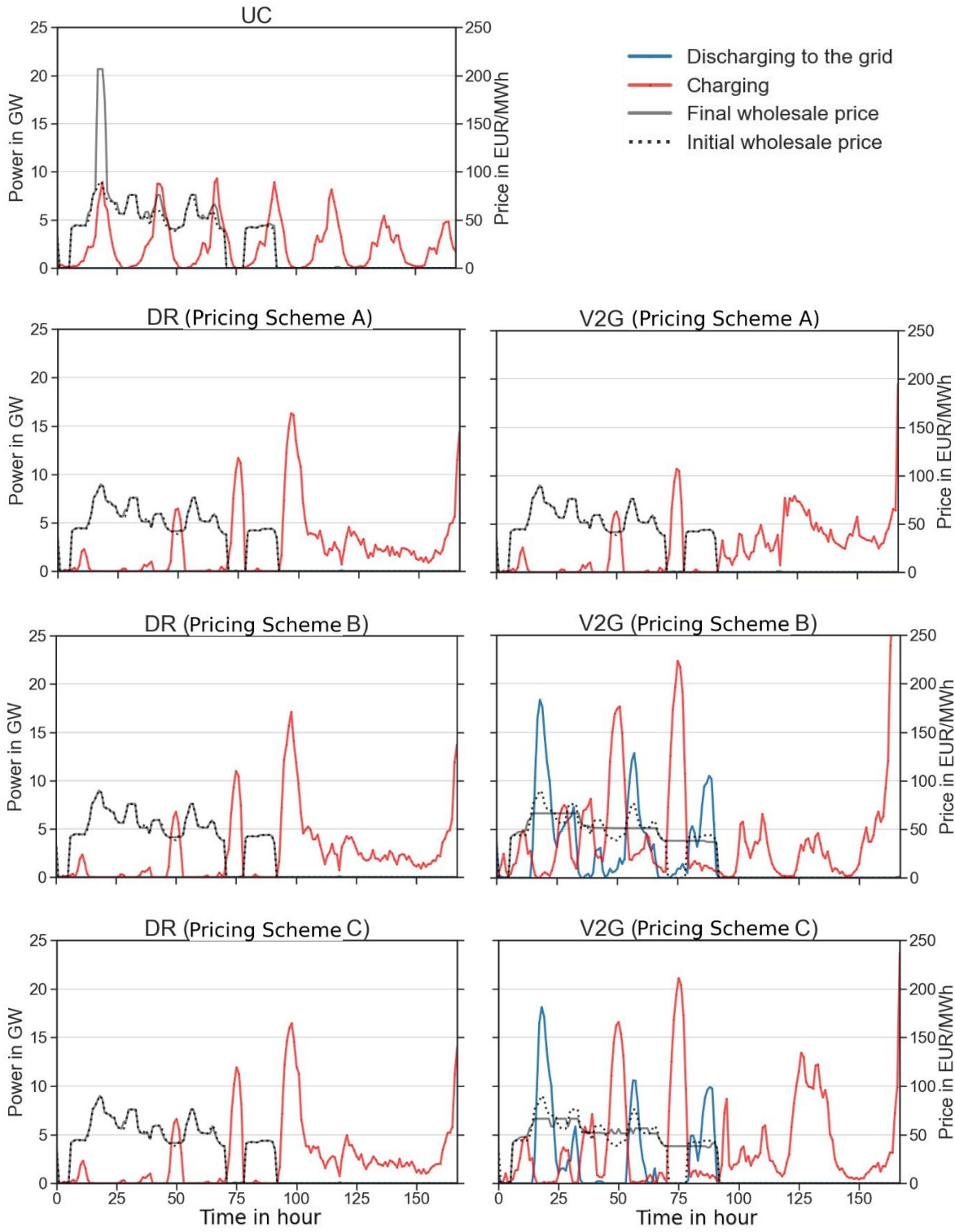


Figure 19. Comparison of charging and discharging schedule of EVs depending on charging strategies and pricing schemes. The charging and discharging of EVs are accumulated power of six million EVs.

Total cost comparison

The total cost for an individual EV is calculated by combining the electricity expenditures, the revenue of electricity sold, and the estimated battery degradation costs by the method suggested in Section 3.3. The weighted average and weighted standard deviation of the total cost for all EVs, are shown in Table 7 and the weighted distribution is depicted in Figure 20.



Figure 20. Total cost comparison depending on the cases with cost minimization. The dashed lines of each object represent the data distribution based on kernel density estimation scaled with width. UC uses double width for the scale of density estimation for the sake of visualization. The distribution does not follow the normal distribution because a different scale factor is applied for each EV.

Table 7. The weighted average and weighted standard deviation of the total cost according to the pricing scheme.

	UC	DR (A)	DR (B)	DR (C)	V2G (A)	V2G (B)	V2G (C)
Weighted average [EUR/week]	16.00	13.08	2.29	13.09	12.89	2.40	13.56
Weighted std. [EUR/week]	6.75	5.54	0.80	5.54	5.51	1.29	6.01

Overall, the total cost is reduced in all cases when a charging strategy is applied compared to UC. Even when Pricing Scheme A in which no incentive is given to EV users is applied, the total cost decreases. However, in the case of V2G with Pricing Scheme A, no actual bidirectional charging occurs. Therefore, the effect of V2G strategy with Pricing Scheme A can only be examined in the framework of the residual load minimization. This will be discussed in Part II.

The reason why Pricing Scheme B has a lower total cost is that the purchase price is substantially lower than the generation cost of electricity. For Pricing Scheme B and C, there is a larger benefit for V2G since the buying and selling prices are equal. Fluctuation in the electricity price could thereby easily be turned into a profit, unlike Pricing Scheme A.

In the case of DR, since EV scheduling came out very similar for all pricing schemes, the total cost of Pricing Schemes A and C, which have the same charging cost (retail price), are also almost the same. When comparing DR with Pricing Schemes A and B, even though the charging and discharging schedule is identical, the difference in total cost is significant. This means that the total cost is primarily affected by the electricity cost. From this, it can be inferred that the battery degradation cost is low. In the case of V2G with Pricing Scheme C, even though more charging is performed compared to the V2G with Pricing Scheme A or the DR cases, the total cost is shown to be more or less the same. This means that the remuneration profits balance well with the electricity purchase costs. When comparing DR and V2G with Pricing Scheme B and Pricing Scheme C where the bidirectional charging occurs, the total cost of V2G increased slightly to 4.8% and 3.6%, respectively. This is because, in V2G cost optimization, the price that is used for the optimization of each EV batch continues to change while the optimization is in progress. Therefore, the optimization for early batches is likely not perfectly ideal for the final price used for the evaluation. This can be explained for the time step 71 to 78, where the final price increased.

Looking at the individual plots in Figure 20, the distribution of the total cost is not following the normal distribution but has fluctuations. This is because a different scale factor is applied for each EV. For reference, the distribution of the total cost for each EV batch before the scale factor is applied follows the normal distribution.

In addition, the overall total cost distribution range is wide. The reason for this is not the influence of EV-specific optimization or competition between EVs according to the participation rate, but rather the driving profile of the individual EV. This means the largest contribution for the total cost variation between EV batches is the actual electricity purchases for the usage of driving. This can be explained through the correlation for each case shown in Figure 21. The figure on the left is arranged by EV batches with a large total cost based on UC, and the figure on the right gives the Pearson correlation factor between the different cases. The correlation is determined by comparing the final costs for each EV batch in the different cases. It shows high correlations between cases, that is, according to the trend of individual EV batches, the total cost changes proportionally for each pricing scheme. In the case of pricing scheme B, the correlation is relatively low because there are many time steps where the charging cost is zero.

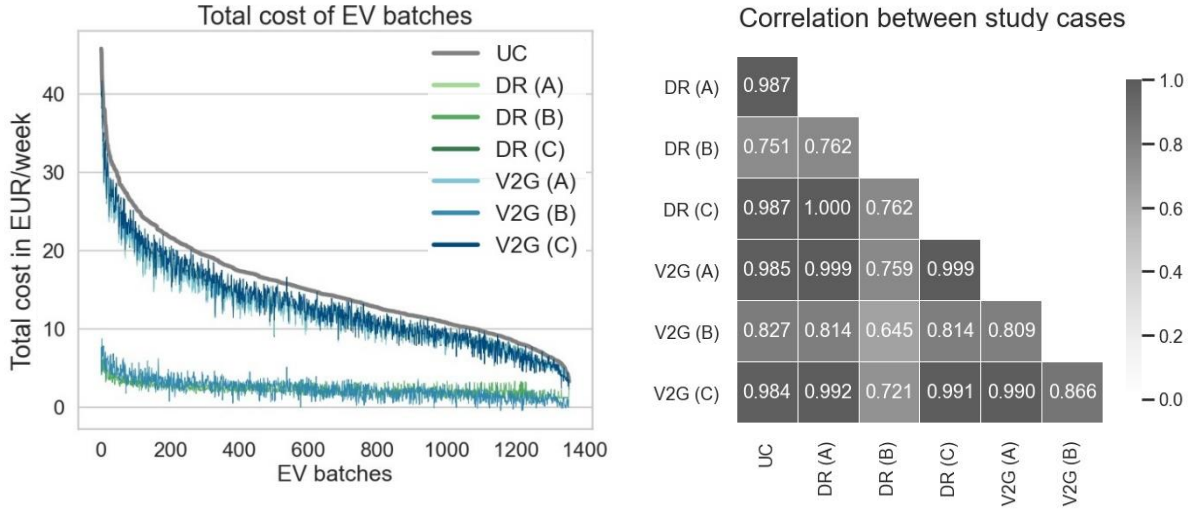


Figure 21. Total cost for each EV batch (left) and the correlation factors between cases (right). In the left plot, the EV batches are ordered by highest total cost of UC. Those two plots show that the trend of total cost for individual EV batch has high correlation for every cases.

In addition, the reason for the high variation of total cost between EV batches is also well depicted in Figure 22. It shows the EV schedule and battery status of EV batches with the lowest total cost (left plot, total cost: 2.26 EUR) and EV batch with the highest total cost (right plot, total cost: 47.70 EUR) in V2G Pricing Scheme C. Even though the EV batch on the left has more discharging back to the grid than the right one, the total cost is much lower. This means that the primary cost factor is the electricity consumed for driving.

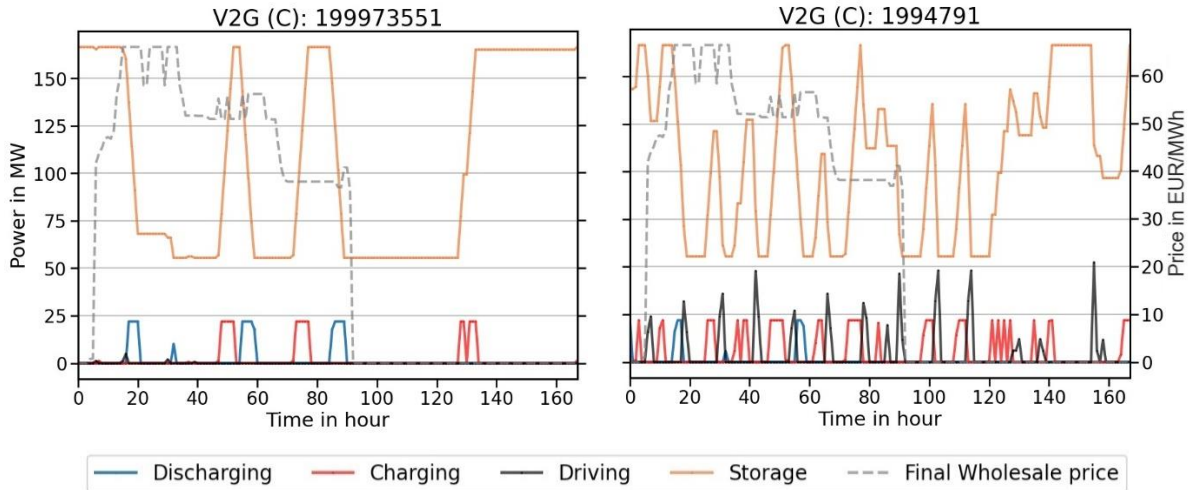


Figure 22. Battery status of EV batches that have the lowest (EV 199973551) and the highest (EV 1994791) total cost. The orange line (Storage) refers to the stored electricity in the battery.

The cost component is shown in Figure 23. The most striking factor here is electricity cost, which has the highest contribution to the total cost for most of the cases. The tendency for the quartiles to extend relatively long, that is a large total cost difference between each EV, can be attributed to

the driving profile of each EV batch rather than the influence of V2G, as explained earlier together with Figure 22. The profit from electricity sales appears only in V2G with Pricing Schemes B and C, where the actual bi-directional charging takes place. Compared to Pricing Scheme B, overall revenues are much larger for Pricing Scheme C. This is because Pricing Scheme C is compensated with the price including the charging fee when discharging.

Overall, the battery degradation cost is low compared to the electricity price. Only in Pricing Scheme B, battery degradation cost accounts for a large proportion of the total cost, because the total price is low since the surcharge fee is not included in the electricity purchase. Therefore, in the case of DR with Pricing Scheme B, battery degradation cost has the highest contribution among the total cost factors. On the other hand, V2G has a higher battery degradation cost in Pricing Scheme B (7%) and C (10%) compared to DR due to more battery usages caused by additional charging and discharging. Further discussion regarding battery degradation cost is covered in detail in Chapter 5.

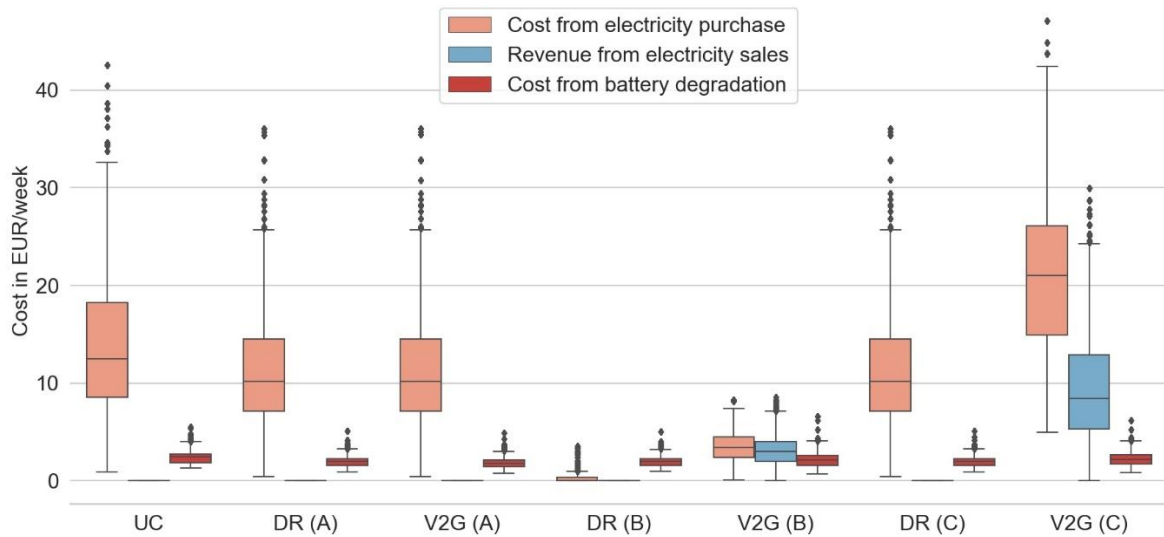


Figure 23. Comparison of the cost components for the cases with cost minimization. Each total cost consists of cost from electricity purchase (light red), revenue from electricity sales (blue), and cost from battery degradation (dark red).

Residual load comparison

Figure 24 shows the residual load time series that varies for each case. The corresponding quantified indicators are summarized in Figure 25 and Table 8.

The residual load in the case of UC is further increased since EV load overlaps with the peak of the residual load. As shown in Figure 24 and Figure 25, in the case of DR, the peak shaving is at a similar level regardless of the pricing schemes. V2G with Pricing Scheme A also shows similar peak shaving because only one-directional charging is applied like DR. In the case of V2G with Pricing Schemes B and C, the positive PLR is approximately 35%. This is more than three times

of the reduction compared to DR. These two schemes also show improvement in negative PLR and PSP compared to other strategies.

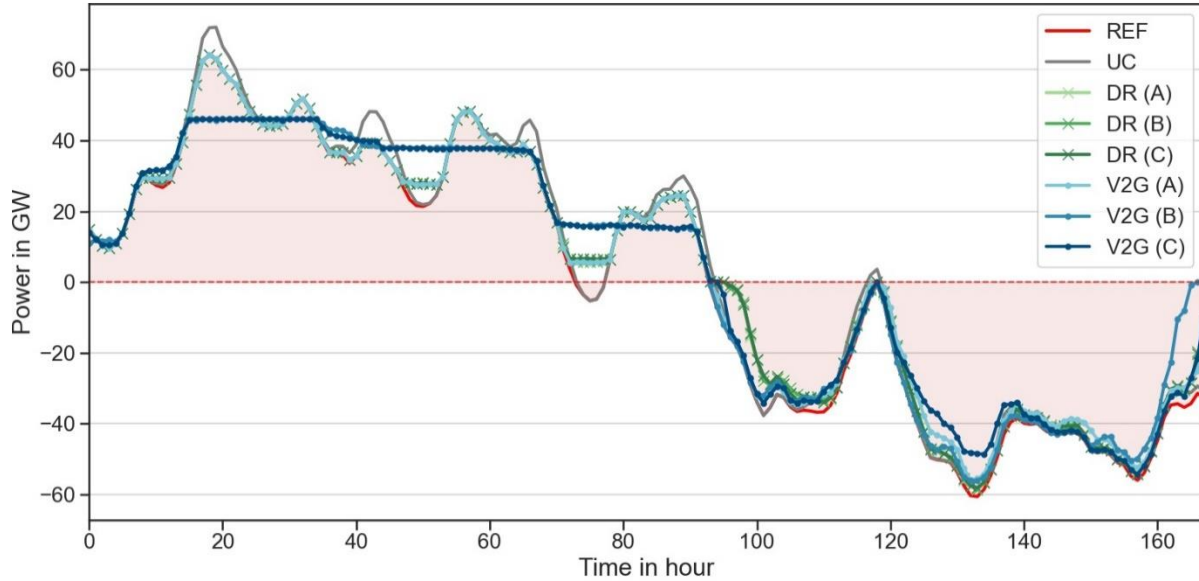


Figure 24. Residual load comparison on cases with different pricing schemes. REF is the reference case of the residual load without additional EV demand and supply, which is depicted in the red line and shaded area.

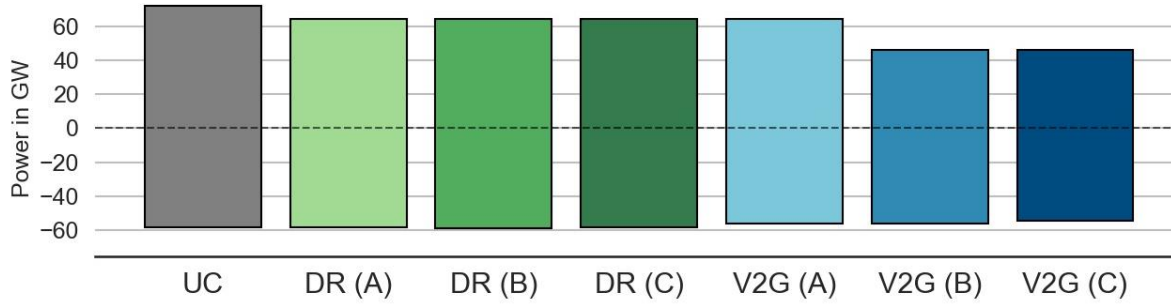


Figure 25. The comparison of positive and negative peak load

Table 8. Comparison of systemic impacts for the cases with cost minimization. PLR is the peak residual load reduction rate and PSP is the peak shaving percentages (see Equation (38)-(40) of Chapter 3.3 for calculation formula). The actual values for peak load max and min, and the accumulated absolute residual load for a week are written in gray.

	UC	DR (A)	DR (B)	DR (C)	V2G (A)	V2G (B)	V2G (C)
PLR pos. [%]	-	10.90	10.90	10.90	10.90	35.88	36.05
(Peak RL max [GW])	71.98	64.13	64.13	64.13	64.13	46.15	46.03
PLR neg. [%]	-	-0.55	-1.11	-0.19	3.63	3.40	6.44
(Peak RL min [GW])	-57.99	-58.31	-58.64	-58.10	-55.89	-56.02	-54.26
PSP [%]	-	5.59	5.70	5.60	5.81	6.40	6.47
(Abs. RL sum [GWh])	5745.90	5424.52	5418.16	5424.19	5411.78	5377.90	5374.10

Comparison of the ecological impact

Table 9 quantifies the ecological impacts in terms of CO₂ emissions reduction and surplus RES of each pricing scheme compared to UC. Similar to the previously estimated cost and residual load, the indicators were all similar to all DR cases and V2G with Pricing Scheme A. The CO₂ emission reduction of around 8.3% and the surplus RES reduction of around 6.2% are observed. On the other hand, the results of V2G Pricing Schemes B and C were similar. A CO₂ reduction of around 18% and a surplus RES reduction of around 7.4% are observed.

Table 9. Comparison of ecological benefits by cases with different pricing schemes. Reduction of CO₂ and RES surplus compared to UC are quantified in percentage.

	UC	DR (A)	DR (B)	DR (C)	V2G (A)	V2G (B)	V2G (C)
CO₂ reduction [%]	-	8.22	8.40	8.37	8.26	18.42	17.89
(CO ₂ emission [kton])	1533.21	1407.16	1404.49	1404.88	1406.63	1250.82	1258.90
Surplus RES reduction [%]	-	6.13	6.26	6.14	6.38	7.38	7.35
(Surplus RES [GWh])	2619.67	2458.98	2455.80	2458.81	2452.61	2426.46	2427.04

4.2. Residual load minimization (Part II)

In Part II, when EVs are scheduled to minimize the residual load, the expected benefits for the electricity system and the corresponding costs to compensate are examined.

Charging and discharging schedule

The following Figure 26 shows the total accumulated charging load and discharging supply of six million EVs to the grid. Compared with the cases for cost optimization (Figure 19) for both DR and V2G, a clear difference appears in the latter half of the simulation period. In the case of cost optimization, the price of the latter half of the simulation period is zero, so there is no benefit for the model. However, in the case of the residual load optimization, the residual load is negative for the same period. Therefore, active charging or discharging is carried out in the second half period to remedy this.

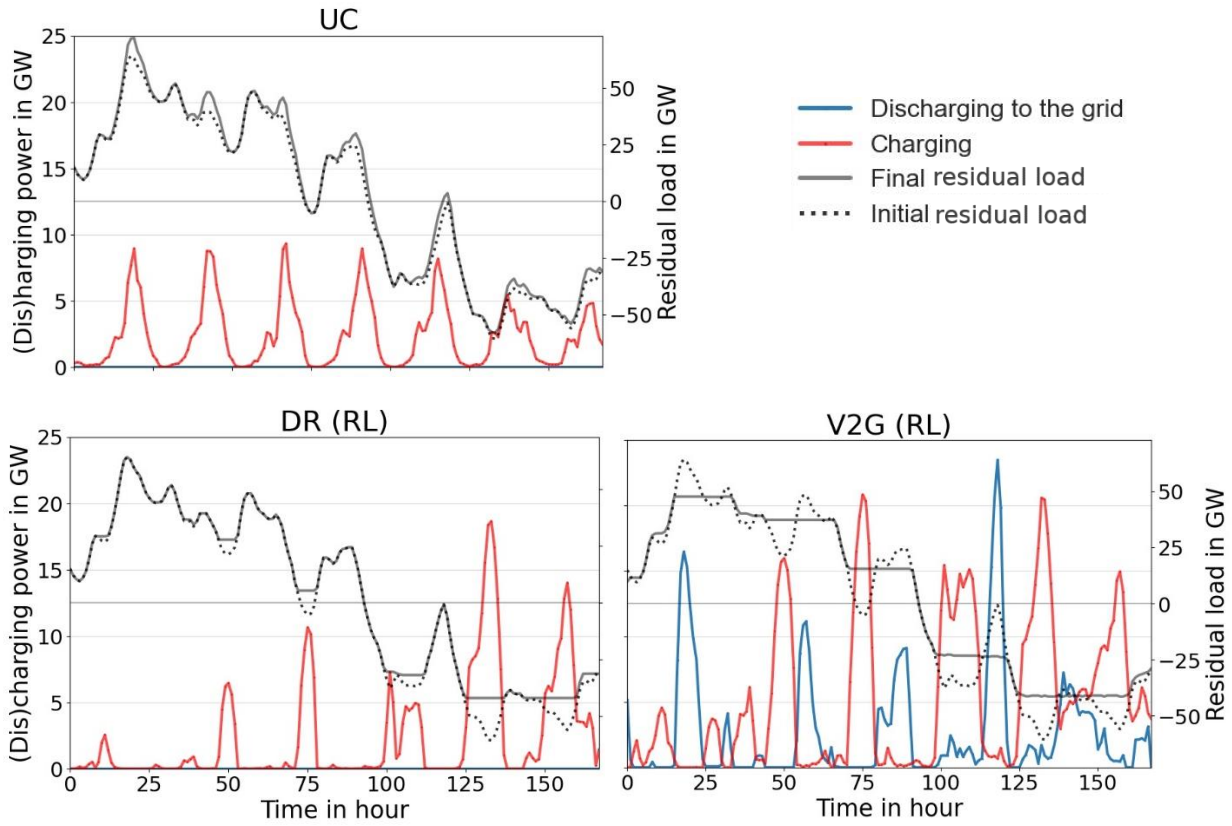


Figure 26. Comparison of charging and discharging schedule of EVs depending on EV charging strategies with residual load (RL) optimization. The charging and discharging of EVs are accumulated power of six million EVs.

Residual load comparison

For a comparison of the residual load variation according to the EV charging strategy, the final residual loads are visualized in Figure 27 and Figure 28. Further indicators are given in Table 10.

As explained in Part I, in the case of UC, the residual load overall increases because the charging time overlaps with the peak load time of the system load. In the case of DR, most of the additional load of EV is transferred to the time step when the negative peak is seen. On the other hand, in the case of V2G, it is shown that positive peaks have disappeared, and the overall residual load is flattened. Unlike DR, V2G can not only fill the negative peaks but also shave the positive peaks. As illustrated in Table 10, regarding the positive PLR, V2G shows a higher peak reduction rate (by a factor of 3) than DR. For the negative PLR and the PSP, improvements of around 28% and 6% respectively are observed for both DR and V2G compared to UC.

When compared to the cost optimization of Part I (Table 8), for DR cases, the positive PLR remained almost the same, but the negative PLR, which was slightly declined compared to UC in cost optimization, increases significantly (27.71%) with the residual load optimization. For V2G,

when compared with the cost optimization with Pricing Scheme C, the reduction rate for the positive PLR is rather slightly smaller, but negative PLR reduction is much higher by 20%.

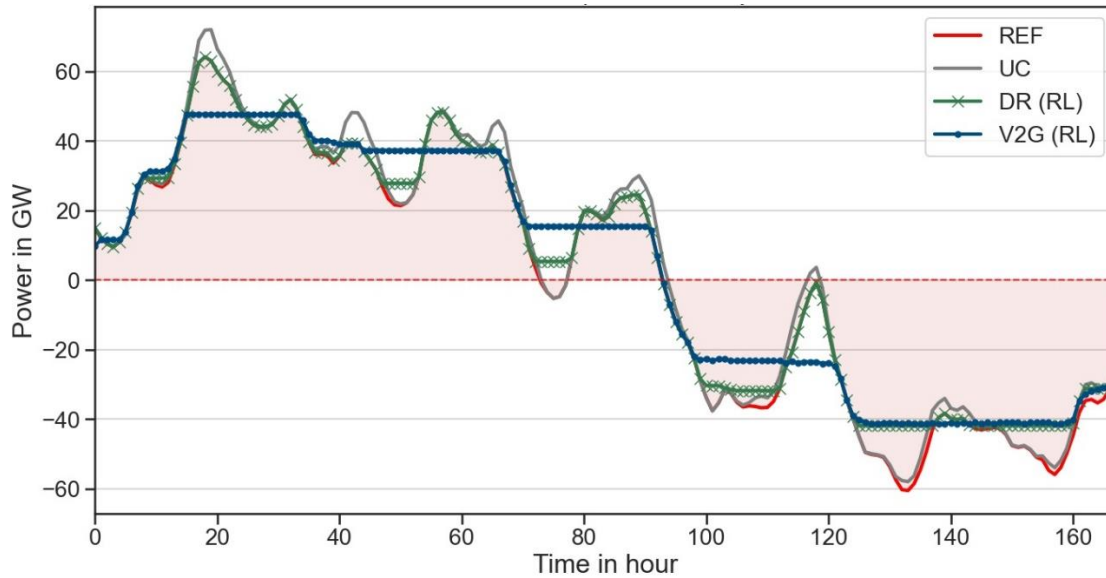


Figure 27. Residual load comparison based on cases with minimizing residual load. The system residual load excluding the EV demand and supply is depicted as the red line and the shaded area.

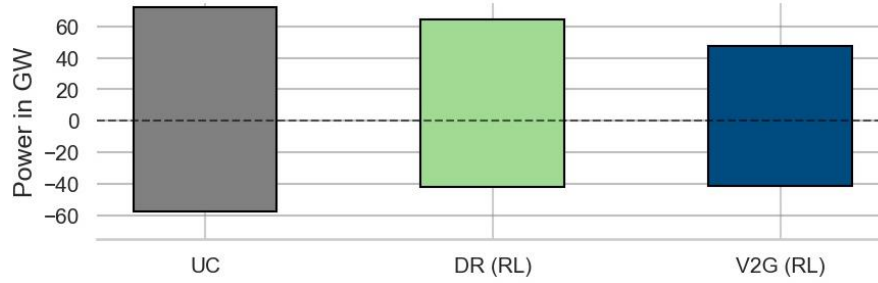


Figure 28. The residual load range between peak maximum and peak minimum of the cases with residual load minimization.

Table 10. Comparison of systemic impacts for the cases with residual load minimization. PLR is the peak residual load reduction rate and PSP is the peak shaving percentages (see Equation (38)-(40) of Chapter 3.3 for calculation formula). The actual values for peak load max and min, and the accumulated absolute residual load for a week are written in gray.

	UC	DR	V2G
PLR pos. [%]	-	10.90	33.76
Peak RL max [GW]	71.98	64.13	47.68
PLR neg. [%]	-	27.71	28.54
Peak RL min [GW]	-57.99	-41.92	-41.44
PSP [%]	-	5.90	6.67
Abs. RL sum [GWh]	5745.90	5406.65	5362.89

Comparison on ecological aspect

Regarding the ecological implications of the residual load optimization,

Table 11 shows the reduction rate of CO₂ emission and surplus RES for each EV charging strategy compared to UC.

Compared to UC, both DR and V2G show positive effects. DR shows a CO₂ reduction of 8.26%, while V2G shows a CO₂ reduction of 17.17% which is more than twice that of DR. This is mainly due to the higher positive peak load reduction of V2G since the CO₂ emission is generated from the operated conventional power plants in the model. surplus RES decreased by 6.48% with the DR strategy and 7.76% with utilizing V2G, compared with the UC strategy. Both cases show slightly larger reductions compared to the case of cost optimization, but there is no substantial difference. This seems to be due to the fact that the residual load optimization evened the fluctuation much more in the timestep of the negative residual load when compared to the cost optimization, but the charging demand itself during the timestep of the negative residual load is similar in cost optimization.

Table 11. Comparison of ecological impacts depending on the cases with residual load optimization.

	UC	DR	V2G
CO₂ emission reduction [%]	-	8.26	17.17
CO ₂ emission [kton]	1533.21	1406.54	1269.94
Surplus RES reduction [%]	-	6.48	7.76
Surplus RES [GWh]	2619.67	2450.04	2416.44

Total cost comparison

In the next step, the associated costs for the above benefits derived from minimizing residual load are examined. The resulting costs are seen by the EV users. The following assumption is that the EV users provide a service to society and the resulting costs for them have to be compensated. This compensation cost is calculated from the additional cost for EV users when they chose DR or V2G charging strategy instead of UC.

The cost for each charging strategy is shown in Figure 29 and Table 12. The weighted average total cost of DR came out as 12.85 EUR/week, which decreased by about 20% compared to UC, while V2G increased the cost by 65% to 26.36 EUR. The weighted standard deviation also decreased slightly in DR and increased by almost 2 times in V2G. In other words, the distribution is very wide in V2G, which means that the difference in total cost between EV batches is very large. Specifically, the EV batch with the lowest cost pays 4.29 EUR/week, while the EV batch with the highest cost pays 61.18 EUR/week.

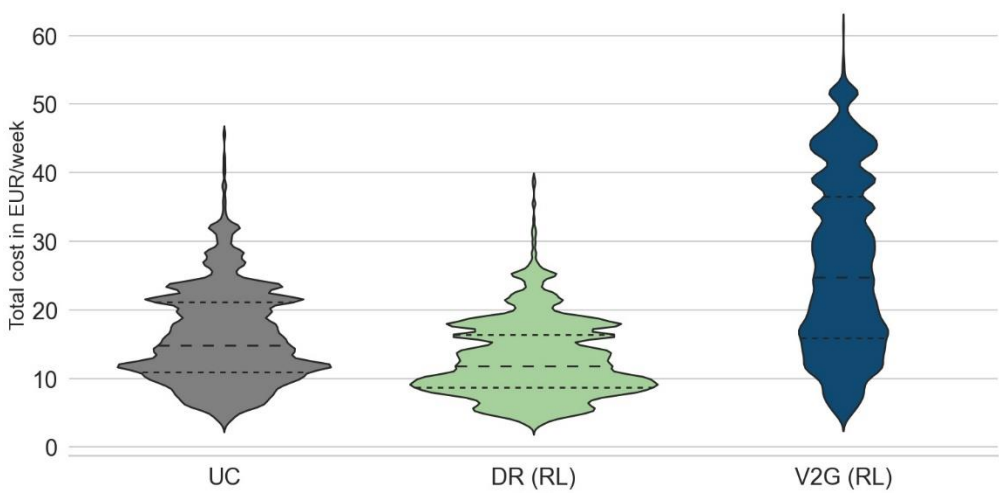


Figure 29. Total cost comparison by EV scheduling strategies. The dashed lines of each object in the figure represent quartiles while the width represents the data distribution based on kernel density estimation scaled with the area. As explained in Part I, the distributions differ from the normal distribution because of the applied scale factor.

Table 12. The weighted average and weighted standard deviation of the total cost. The difference rate compared to UC is in the bracket.

	UC	DR	V2G
Weighted average [EUR/week]	16.00	12.85 (-19.69%)	26.36 (64.75%)
Weighted standard deviation [EUR/week]	6.75	5.50	12.51

Figure 30 provides an explanation for the wide distribution of V2G. The graph on the left shows the total cost of each EV batch listed in the order of highest value based on UC, and the right shows the Pearson correlation factor calculated based on this. The correlation is determined by comparing the final costs for each individual EV in the different simulation cases. Unlike the cost optimization of Part I, the correlation between V2G and other strategies is not high. In other words, regarding the V2G case, it can be inferred that there is another primary factor to the total costs besides electricity costs derived from its own driving consumption.

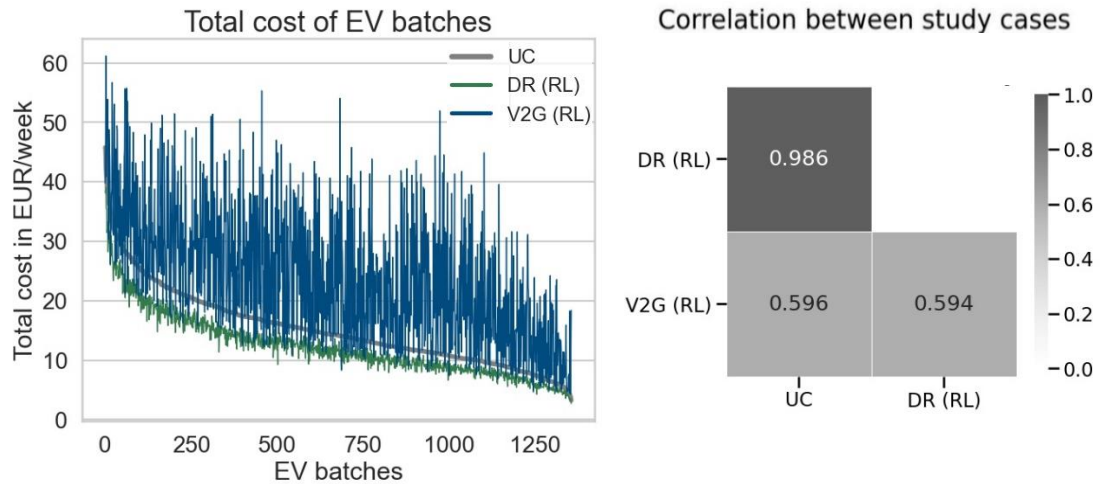


Figure 30. Total cost ordered by highest values based on UC (left) and the correlation factor between EV charging strategies (right). Those show how the total cost for individual EV batches differ depending on EV charging strategies.

Another factor for this wide distribution of total cost in V2G can be found in Figure 31. This figure delivers a cost total comparison between V2G (Pricing Scheme C, the case with incentive that rewards remuneration with retail price) applying cost minimization and V2G (RL) applying residual load minimization. Here, each EV batch on the x-axis is arranged in the order in which the optimization proceeded in the model. For reference, the overall total cost is lower in the case of V2G with Pricing Scheme C, because incentives are given to the electricity sales so that greater revenues can be obtained. The point to note here is the trend line (red) of the two cases. Regarding V2G (Pricing Scheme C) case, where the main effect of the total cost was mainly the driving pattern of individual EV batches, it has an almost flat trend line from the EV batches that were optimized first to the EV batches that were optimized last. On the other hand, regarding V2G (RL) case, it has a decreasing trend according to the optimization order of each EV batch.

This is because each EV is optimized to pursue an individual benefit in cost minimization, whereas, all EVs are optimized to pursue the same purpose in residual load minimization. Thus, in the former case, additional charging and discharging are not performed as long as the EV personal benefit is not expected, that is the minimizing cost. However, in the latter case, it is optimized to reduce residual load regardless of individual gain. Therefore, the first batches of the optimization order especially contribute a lot to stabilize the residual load through charging and discharging as much as possible. Therefore, it is inevitable to spend a high charging cost under Pricing Scheme A, where the charging cost is very high compared to the discharging cost. Meanwhile, for the last batches of the optimization order, the number of charging and discharging times that will contribute to the overall purpose is relatively small since the previous EV batches sufficiently stabilized the residual load.

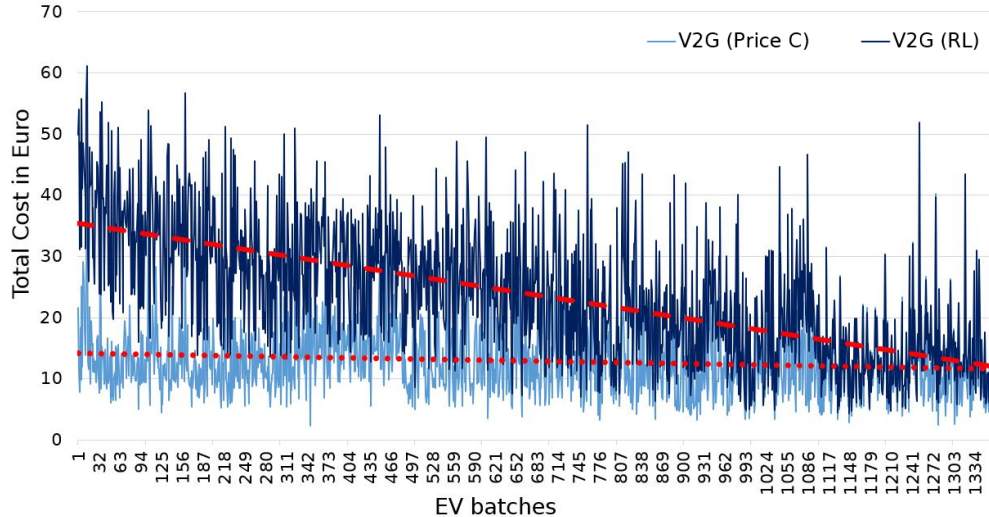


Figure 31. Comparison of the total cost of each EV batch according to the different objective functions. The EV batches are listed in the order of the optimization process in the model. The red lines represent the trend for each corresponding data.

The cost element for the total cost is shown in Figure 32. As expected, the cost of electricity charging shows the highest contribution to the total cost. On the other hand, the battery degradation cost is very low at 18.3% (UC), 16.0% (DR), and 9.8% (V2G) of the electricity cost. Further discussion regarding battery degradation cost is again covered in detail in Chapter 5. In addition, in the case of V2G, the revenue from electricity sales is very small because the selling price is too low even though discharging occurs frequently.

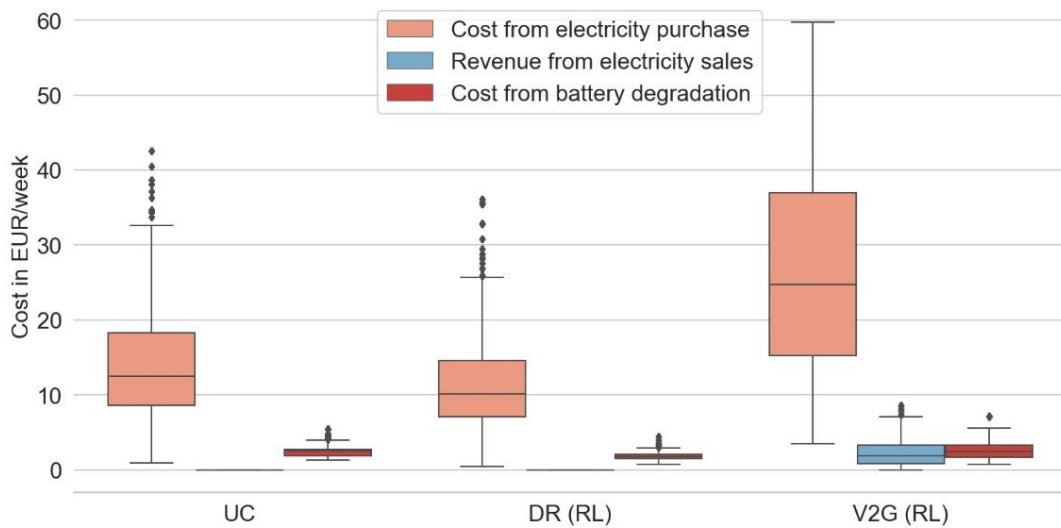


Figure 32. Cost comparison by cost elements for residual load minimization cases.

The specific compensation cost per benefit

Table 13 shows the specific cost that is calculated based on the systemic and ecologic benefits from V2G and the cost incurred for EV users by it. Therefore, it represents the compensation costs to be paid for EV users per benefit. For the DR case, the total cost for EV users is reduced compared to UC, so it becomes the economic benefit earned per benefit (negative value presented in the Table). In V2G, the cost per 1 MW of peak residual load reduction is 2558 EUR, meanwhile, DR would have an economic benefit of 2406 EUR per MW. For the CO₂ emissions, it costs 236 EUR per 1 ton of reduction in V2G, meanwhile, DR profits 149 EUR per 1 ton of reduction.

Table 13. Overall compensation cost to be paid for the benefits of DR and V2G. The detailed equation is written in Chapter 3.3.

	UC	DR	V2G
Total cost for all EVs [million EUR]	95.99	77.12	158.14
Cost per reduced peak load [EUR/MW]	-	-2405.68	2558.04
Residual load peak max [GW]	71.98	64.13	47.68
Cost per reduced CO₂ emission [EUR/ton]	-	-148.98	236.09
CO ₂ emission [kton]	1533.21	1406.54	1269.94

4.3. Sensitivity analyses (Part III)

To analyze the sensitivity of the model, the participation rate of the V2G or DR program and the battery SOC allowance range are varied. In both sensitivity analyses, the optimization minimizes the residual load, and Pricing Scheme A is applied for evaluation. As evaluation indicators, the benefits and the compensation costs that V2G or DR will ultimately bring are used.

4.3.1. Participation rate

The estimation of the number of EVs participating in DR or V2G in the year 2030 varies and is subject to policies and public perception. Therefore, a sensitivity analysis is carried out to validate the impact of the different participation rates: 10%, 50%, and 100% of all EVs.

Figure 33 shows the changes of the final residual load according to the participation rate of the DR or V2G program. As illustrated in the figure, in both the DR and the V2G cases, the higher the participation rate, the flatter the residual load.

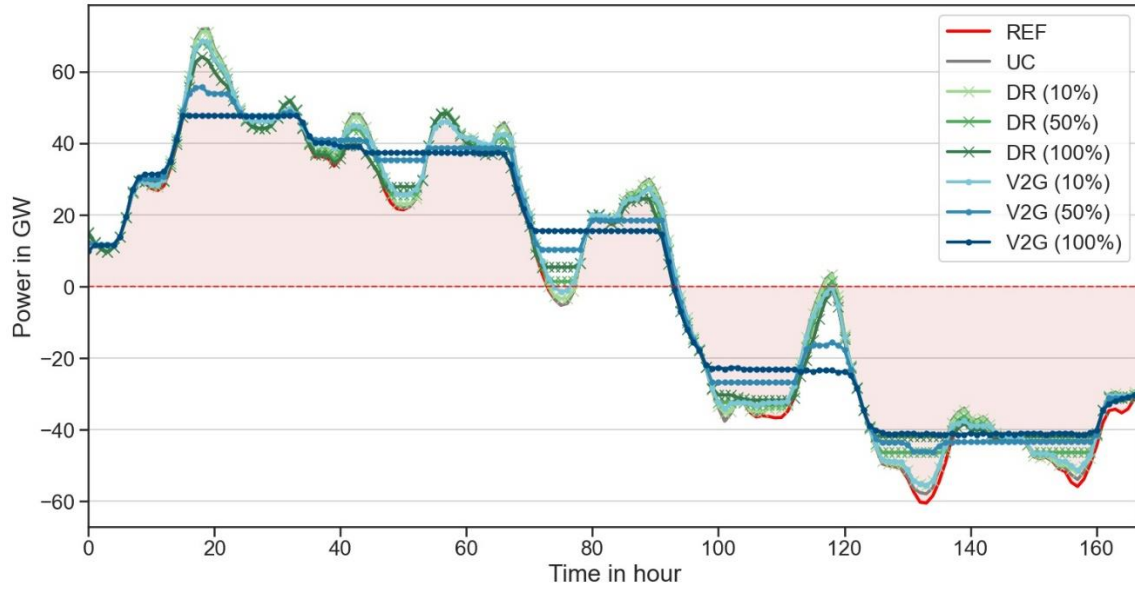


Figure 33. Final residual load variations depending on the participation rate of DR or V2G program.

Figure 34 shows the total cost for each EV batch according to the program participation rate. EV batches are listed in the order in which optimization proceeds in the model. Note that for DR, only 100% of the total cost is displayed, as almost the identical total costs are shown at all participation rates for DR. As previously mentioned, for V2G optimization with residual load, the total cost of each EV batch is affected by the processing order of the optimization of EV batch. The total cost is higher for the earlier EV batches in the optimization process.

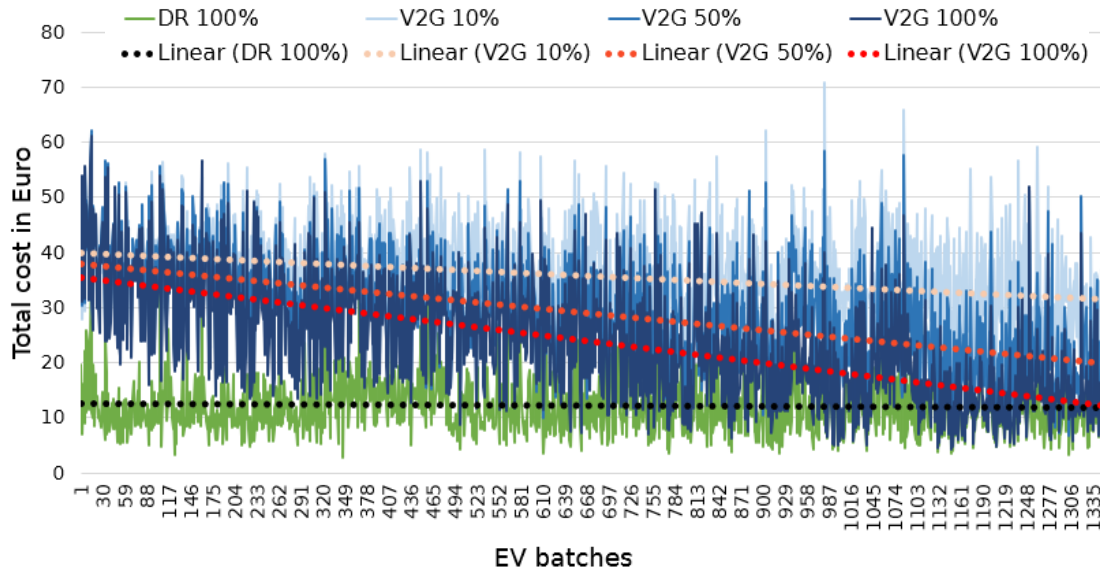


Figure 34. Total cost variation depending on the participation rate of DR or V2G program

Comparing the total cost trend depending on the participation rate, it is shown that the total cost gets lower as the participation rate gets higher. Furthermore, the difference in total cost between EV batches is also high when the participation rate is high.

Finally, Table 14 shows the specific compensation costs per benefit by participating in DR or V2G programs compared to UC. The detailed element values used to obtain these indicators are included in Appendix B. The total cost results in negative values for all participation rates of DR and the 10% participation rate of V2G. This means the economic benefit is also generated while the systemic and ecologic benefit occur. The specific economic benefits are higher at the lower participation rate. On the other hand, the 50% and 100% participation rates of V2G show that the specific compensation costs become higher as the participation rate increases. Therefore, for the larger reduction, larger compensation costs are required.

Table 14. The compensation costs per benefit depending on the participation rate of DR or V2G program. The values refer to the compensation costs incurred per benefit earned by participating in the program. In the case of negative numbers, the cost rather reduced by participating in the program, which means the revenue earned per benefit earned. The detailed values can be found in Appendix B. The detailed equation is written in Chapter 3.3.

	UC	DR			V2G		
		10%	50%	100%	10%	50%	100%
Cost per reduced peak load [EUR/MW]	-	-17231.61	-4383.76	-2405.68	-803.95	2037.75	2558.04
Cost per reduced CO ₂ emission [EUR/ton]	-	-1288.38	-300.35	-148.98	-55.96	186.24	236.09

4.3.2. SOC allowance range

The second sensitivity analysis examines the influence of the SOC allowance range. The default value for SOC allowance range in Part I and Part II is defined as 25-75% (SOC50). As mentioned in Section 2.2, the SOC has a strong influence on battery degradation. In this sensitivity analysis, additional SOC allowance ranges of 10-90% (SOC80, battery usage range is restricted to 80%) and 0-100% (SOC100, there is no restriction in battery usage) are examined.

Within the SOC allowance range, each EV batch establishes an optimized schedule for a given objective function. Figure 35 below is an example of an EV batch (ID: 1994791); the left is for the SOC50, and the right for the SOC100. For SOC100, the entire area of battery status is continuously utilized for charging and discharging.

Accordingly, there is a difference in the final residual load in the electricity system, which can be seen in Figure 36. Unlike in the previous sensitivity analysis, there is no big difference between the parameters, only small variance in the V2G cases in the earlier time steps.

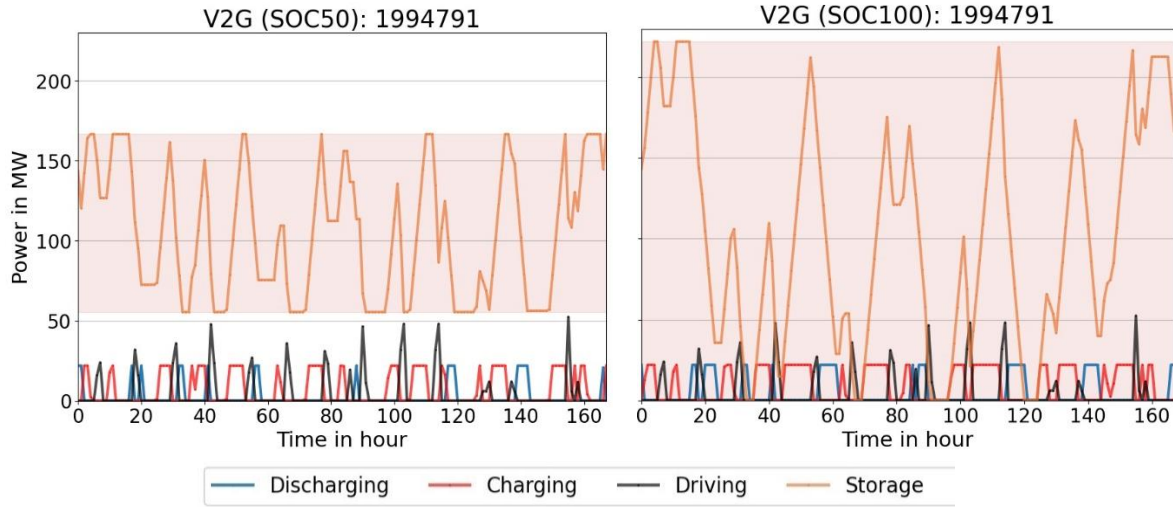


Figure 35. The charging scheme of an example EV batch with the different SOC allowance range. The left is when the SOC allowance range is between 25% to 75% while the right is between 0% to 100%. The orange line (Storage) refers to the stored electricity in the battery. The shaded area represents the SOC range that is allowed to use.

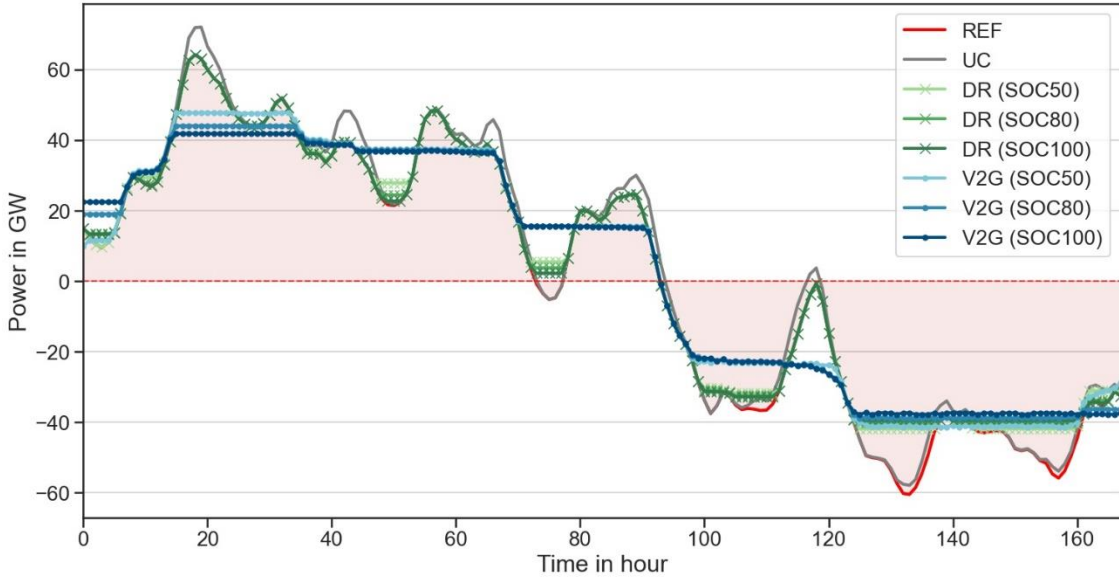


Figure 36. Comparison in the final residual load by different SOC allowance range

Even though the residual load does not change a lot according to the SOC allowance range, additional costs for EV users show a notable increase. This is shown in Table 15. When participating in DR, all the costs are reduced compared to UC, but no big difference between SOC allowance ranges. On the other hand, there are remarkable cost increases in V2G, e.g., more than 100% increases in the electricity cost for SOC80 and SOC100 compared to UC. This implies that high additional charging occurs for shaving the residual load. The cost differences between the

SOC allowance range are also significant. Especially, battery degradation cost gets higher as SOC allowance increases, e.g., 2.82% increase for half battery usage (SOC50) and 73.24% increase for the full battery usage (SOC100) for V2G. This means that the battery degradation is highly related to the SOC allowance range that the battery can utilize. These results are further discussed in Section 5.3.

Table 15. Cost comparison according to the SOC allowance ranges. The values in the bracket mean the ratio compared to UC. The detailed equation is written in Chapter 3.3.

	UC	DR			V2G		
		25-75%	10-90%	0-100%	25-75%	10-90%	0-100%
Electricity cost [million EUR]	81.15	66.48 (-18.07%)	65.18 (-19.67%)	64.90 (-20.03%)	155.93 (92.16%)	176.39 (117.37%)	187.02 (130.48%)
Revenue from sales [million EUR]	-	-	-	-	13.05	16.73	18.66
Battery degradation cost [million EUR]	14.84	10.64 (-28.34%)	10.46 (-29.55%)	10.45 (-29.61%)	15.26 (2.83%)	21.49 (44.75%)	25.71 (73.24%)
Total cost [million EUR]	95.99	77.12 (-19.66%)	75.64 (-21.20%)	75.34 (-21.51%)	158.14 (64.75%)	181.14 (88.71%)	194.08 (102.19%)

Finally, Table 16 shows the compensation costs incurred per benefit. The detailed costs and benefits for each element are shown in Appendix B. In DR cases, these values are the revenue per benefit unit because the total cost is reduced compared to UC. Meanwhile, In V2G cases, these values are the compensation cost that needs to be paid for EV users compared to UC. In V2G cases, the cost per unit increases as the SOC allowance range increases. This means that the compensation cost increases as the absolute value of the benefit increases.

Table 16. The specific compensation cost per benefit depending on the SOC allowance ranges. The values refer to the compensation costs incurred per benefit earned by participating in the program. In the case of negative numbers, the cost rather reduced by participating in the program, which means the revenue earned per benefit earned. The detailed values can be found in Appendix B.

	UC	DR			V2G		
		25-75%	10-90%	0-100%	25-75%	10-90%	0-100%
Cost per reduced peak load [EUR/MW]	-	-2405.68	-2594.29	-2631.79	2558.04	3039.95	3249.53
Cost per reduced CO ₂ emission [EUR/ton]	-	-148.98	-152.74	-148.98	236.09	277.37	302.93

5. Summary and discussion

Throughout the study, the potential impacts of V2G have been analyzed from the perspective of EV users, the electricity system, and the ecological domain. These impacts for each stakeholder can vary in a wide range depending on various factors, such as objective functions or pricing schemes. For this, an optimization model is developed, and different study cases are examined.

5.1. Impacts on the cost for EV users based on pricing schemes

The impact of V2G on the cost for EV users is determined when EVs are scheduled to minimize the operating cost. Other accompanying systemic and ecological benefits are presented as well. The study determines the voluntary participation of EV users and its impacts depending on electricity pricing schemes giving an insight into the necessity of an incentive program. As an essential parameter for cost optimization, three different pricing schemes are defined with or without incentives.

The analysis shows that DR and V2G provide an economic advantage for all pricing schemes compared with the conventional UC. However, in V2G with the current German pricing scheme, which does not have any incentives, no discharging electricity back to the grid occurs at all. This is caused by the added surcharge fees to the charging price. The charging price is nearly three times higher than the discharging price, and consequently, does not induce electricity back to the grid. On the other hand, pricing schemes with incentives, actual V2G implementation is observed. Due to the equal price of electricity charging and discharging, the EVs can easily profit from the electricity price fluctuation throughout the simulation period.

The largest portion of the total cost for EV users is observed as electricity purchasing. Battery degradation cost, which is one of the main barriers for EV users participating in DR or V2G programs, accounts for a relatively small portion (15%) of the total cost in most cases. Exceptionally, the battery degradation cost accounts for the largest portion (88%) of the total cost in the pricing scheme that applied wholesales prices for both charging and discharging. This is because of the very low charging costs due to the incentives. Considering the incentives given to the EV users, the resulting battery degradation cost will also be minor in the net cost of EV users.

In pricing schemes with incentives, in which the actual discharging back to the grid occurs in V2G cases, the average cost of the DR and the V2G cases are similar. V2G is slightly more expensive (average 4.2%). This is because the price used for each EV batch evolves until the last EV batch's optimization. Therefore, the price that was zero for the EV batches optimized earlier can sometimes increase due to the EV batches optimized later. This effect is restricted the most by

applying the appropriate batch size of EV batches, for which a batch size decision loop is implemented in this study. In addition, this issue can be further improved with a market model allowing negative prices. The larger negative price indicates the higher chance that there is a large amount of surplus in the market and vice-versa. This will provide an insight for EV to avoid the time which has the high potential of a price increase.

V2G has a much higher impact on the additional systemic and ecological benefits than DR, e.g., V2G shows a positive peak load reduction of 36% and CO₂ emission reduction of 18%; DR shows only 11% and 8.4%, respectively. These results are mainly related to the discharging schedule of EVs. In the DR cases, even though it shifts its load to where the residual load is low, the amount of load shifting is already fixed to its driving demand. Meanwhile, EVs with V2G have a larger capacity to contribute to the residual load by continuously interacting with the grid by charging and discharging. Even though the EV schedule is optimized for cost minimization, it balances the residual load since the electricity price is highly correlated with the residual load. As residual load is stable, more RES utilization results in higher systemic and ecologic benefits. However, these larger benefits can only be achieved when the incentives are given to the EV users as there is no actual discharging schedule under the current pricing scheme.

5.2. Impacts on the residual load of German electricity systems

EV charging schedules are optimized to reduce the residual load of the power system. With this object, EVs are scheduled to actively discharge electricity back to the grid regardless of the pricing scheme applied at the evaluation step. This is the main difference from the cases with cost minimization, in which there is no discharging schedule when there are no individual benefits.

For the positive peak residual load reduction, the results show high similarity with the cases of cost minimization (Section 5.1) (10.9% in DR and 33.8% in V2G). Meanwhile, there is a significant increase in negative peak reduction (27.7% in DR and 28.5% in V2G) comparing to cost minimization (-0.2% in DR and 6.4% in V2G at most). These benefits are due to the active load shifting encouraged by the apparent contrast of residual load during the simulation period. Compared with the cost minimization cases, both V2G and DR actively fill the valley of the residual load, but the results on ecological aspects are similar. Even though there are load shiftings between timesteps of the negative residual load, the charging demand itself during the corresponding timesteps is similar. This leads to not high impacts on the reduction of RES surplus or CO₂ emission. In addition, for residual load minimization, the fluctuation of the residual load is evened much more compared to the cost optimization. This is due to the setting of the objective function as a square of residual load. The load shifting is prioritized around the timestep where the peak loads are.

Even with the object of minimizing residual load, the total cost for EV users participating in DR is reduced by around 20% compared to UC. This is due to the limitation on one-directional charging for DR, which can only shift the demand to the timestep where the residual load is low. This implies that EVs shift their load to the low price timesteps, considering the residual load is highly correlated with price. On the other hand, the total cost for V2G is increased by 65% compared to UC. This is because V2G purchases much more electricity than its driving demand to reduce the residual load. This causes a high increase in the total costs.

Another finding is the high variation of total cost between EV batches when applying a V2G strategy. The weighted standard deviation of the total cost is observed to be around double that of UC. The total cost for the first EV batches optimized earlier is substantially higher than that of the latter EV batches. The first EV batches have much more charging and discharging schedules and contribute substantially to flatten the residual load, leading to higher charging costs under the current pricing scheme. Meanwhile, for the latter EV batches, there is a smaller degree of freedom to schedule discharge to contribute to the residual load stabilization while fulfilling their driving schedule.

Based on the above results, the specific compensation cost per social benefit is normalized. For V2G, it costs 2,558 EUR/MW and 236 EUR/ton for the reduction of the positive peak residual load and the CO₂ emission. Meanwhile, DR gets economic profits while still having these reductions. When simply comparing the specific cost between DR and V2G options, DR seems promising as it is the cheaper option. However, when there is a specific target to achieve in CO₂ emission or peak residual load reduction and if the amount of target reduction is higher than what the DR can provide, V2G should be considered. Moreover, considering that the potential to utilize V2G as a multipurpose such as frequency regulation, V2G will be a more competitive option. However, this should be investigated further together with other additional costs that are not covered in this study scope, e.g., higher hardware installation for two-way chargers of V2G and additional electrical standards.

5.3. Impacts of the participation rate and battery control

Sensitivity analyses on the participation rate of V2G and SOC allowance range of EV batteries are carried out under residual load minimization.

The larger the participation rate, the higher residual load reduction is observed. This is due to the increased capacity as distributed ESS available for the electricity system. The larger the participation rate, the lower the total cost for the EVs. This is because the higher the participation rate, the more residual load is stabilized and the lower the overall electricity price. Furthermore, the variation in total cost between EV batches participating in the program increases as the

participation rate increases. As described in Section 5.2, the total cost is proportional to the number of charging and discharging, and the total cost of the latter EV batches in the optimization process is lower than the first batches. Therefore, the more EV participating in V2G results in the further lower the total cost of latter EV batches.

This effect can be reversed when more attractive incentives are included in the pricing scheme, such as the higher the number of charging and discharging cycles, the greater the revenue. In such a case, certainly, competition between EV batches will exist to conduct as much charging and discharging as possible. If EVs participate in V2G at a national scale, competition between EVs must increase. Therefore, it is required to have an intermediate medium or program that can solve any competition issues smoothly. The role of these medium or program will become essential when more EVs emerge as governmental goals for EV market share get more ambitious [78].

Overall, even though the differences in the systemic and ecologic benefits between different SOC allowance ranges are small, the difference in total cost is significant, e.g., 64.8% increase in half SOC usage and 102.2% increase in full SOC usage. This is caused not only by the charging cost of the electricity for higher capacity but also by the battery degradation cost. There are significant differences in the degradation cost between the cases, e.g., 2.8% increase in half SOC usage and 73.2% in full SOC usage. This shows that the constraint-based approach chosen to reduce the battery degradation effect in this study is working in an intended way. In other words, the result suggests that restricting the SOC range would cause a big range of total cost saving at a small reduction in the systemic and ecological benefits. Therefore, the proper management system that can control the SOC allowance range will be beneficial and highly recommended for V2G implementation.

The specific costs to be paid per unit benefit becomes high for both the higher participation rate and the higher battery usage range. The reason is related to the electricity price for peak residual loads. As a higher sum of electricity storage is involved, a larger reduction of CO₂ emission or surplus RES is observed. This means not only the high peak residual load needs to be shaved, but also the additional relatively low peak residual load needs to be shaved. As residual load and electricity price have a high correlation, the remuneration profit is low when the relatively low peak residual load is shaved. Eventually, the specific cost is higher when the goal of residual load reduction is high. In other words, the larger the target reduction, the greater the additional cost.

5.4. Limitation and outlooks

Looking at the results of cost optimization and residual load optimization, substantial differences in EVs schedule are observed, particularly when the residual load is negative. In this period, the electricity is set to zero from the applied market model in this study, which leads to no arbitrage for EV users during this time. Therefore, in this study frame, implementing a model that is able to

produce negative prices could yield different results, e.g., there might exist discharging schedules that send the electricity back to the grid in V2G with the current pricing scheme when the negative price is high enough to cover the surcharge fees, or, the total cost for V2G could reduce due to the higher remuneration. However, from a long-term perspective, where the higher penetration of RES and the portion of conventional power plants decrease, this effect would get more negligible. Because the negative price is derived from the bids between conventional power plants having high ramp-up costs.

For all simulation cases, the battery degradation cost is observed to have a low contribution to the total cost. This result contains quite a number of assumptions. First, it is assumed that the battery price of all EVs used in this study equates to 62.05 EUR/kWh [70], which corresponds to the projected price for 2030. Varying this parameter could result in different impacts since the battery degradation cost is derived from the battery cost and capacity fade percentage. In addition, capacity fade is simulated by applying a semi-empirical battery degradation model based on NMC battery cells. In addition, the SOH of all EV batteries is assumed to be 95%. In other words, it means that the starting capacity fade is set to 5% in the battery degradation evaluation stage. This is derived from an assumption for calendric degradation of 1.5% and cyclic degradation of 3.5%. Without these assumptions, all EV batteries would be in an ideal state without any degradation, which would lead to a very high battery degradation cost. This is because battery degradation occurs at a rapid rate in the initial state [79]. For this reason, it is necessary to make an appropriate assumption to all EVs. However, to the best knowledge of the author, there are no such references presented. Therefore, the SOH is selected based on the value at which the degradation rate of the battery becomes linear in a battery simulation result under similar conditions (temperature 25°C, medium SOC) [79]. With this parameter, the battery degradation cost over a week, which is a relatively short period in battery lifetime, can be reasonably estimated. However, considering a longer period of study in the future, it would be required to applying different parameters reflecting the SOH of each EV for more realistic estimation.

In addition, throughout the study, the EV driving profiles used for the basic input of the model are simulated based on the driving profile of conventional vehicles. This is a state-of-art at the current stage where a transition from conventional vehicles to EVs is taking place. However, as the integration of EVs with the electricity system increases, the driving patterns could change. This could affect the results of the study. Likewise, there are more assumptions, such as renewable scenarios or constant surcharge fees. These assumptions are inevitable as the simulation is set up a decade in the future. However, the main contribution of this study can be found in the development of an optimization model applying battery degradation and the assessment method of the potential impacts of V2G at the national scale. Therefore, further studies can easily be implemented by substituting more accurate driving profile data or sub-models.

6. Conclusion

To encourage the voluntary participation of vehicle-to-grid (V2G) from electric vehicle (EV) users, the economic benefits for EV users and systemic and ecologic impacts are relevant. Therefore, in this study, an optimization model is created for optimal EV dispatch. In a holistic perspective, assorted variations are integrated and examined: objective functions, pricing schemes, charging strategies, participation rates, and battery control setting.

When cost minimization is applied for the optimal EV schedule, the cost for EV users is always reduced in all pricing schemes compared to uncontrolled charging. However, it is difficult to encourage the active implementation of V2G with the current pricing scheme in Germany due to the high electricity cost for charging. Instead, with the presence of incentives, the participation of EV users in V2G increases, and the cost gets lower. However, from a broad perspective, incentives given to EV users are expenses for third parties to bear.

In this regard, residual load minimization is carried out to determine the potential systemic benefits via V2G and the compensation cost to be delivered to EV users. With this object of residual load minimization, the EVs are more actively engaged in balancing the residual load via V2G, having much more charging and discharging schedules compared to cost minimization. This is due to the entire EVs are aiming at the public goal instead of pursuing individual economic benefits. Still, due to the high charging cost in the current pricing scheme, the average cost for EV users is increasing. Therefore, this cost should be considered as an expenditure for the social benefits that V2G brings and be compensated via a proper incentive program.

In all cases, V2G is compared with other charging strategies: demand response (DR) and uncontrolled charging. It seems that DR is preferable, considering that the cost is lowered while still having systemic and ecological benefits. However, in DR, the possible benefits are limited due to its one-way charging feature. Therefore, V2G can offer more options to result in higher reductions of CO₂ emission and peak residual load. For this, the proposed compensation cost per unit benefit should be further examined comparing with other flexibility options. In addition, as briefly introduced in the related works, if V2G is used together for the purpose of frequency regulation, even greater benefits can be expected for all stakeholders [20] and the potential of V2G will be further increased. V2G seems to be a competitive candidate for the flexibility option in the electricity system, but further studies considering other incidental expenses would be needed.

The constraint-based SOC restriction approach shows a high effect in reducing battery degradation cost even though the contribution of battery degradation to the total cost is small (approx. 10% of the total cost) under the conditions applied in the study. Rather the contribution of electricity price dominates the total cost. Therefore, the electricity prices with the surcharge fees seem to be the highest obstacle to apply V2G in the free market. The introduction of a fair and appropriate policy for all stakeholders is the primary priority in encouraging the participation of V2G.

Bibliography

- [1] IEA. Global EV Outlook 2020 – Analysis - IEA. [January 16, 2021.158Z]; Available from: <https://www.iea.org/reports/global-ev-outlook-2020>.
- [2] Statista. Electric vehicle market share in Germany 2014-2020 | Statista. [January 15, 2021.592Z]; Available from: <https://www.statista.com/statistics/1166826/electric-vehicles-market-share-germany/#statisticContainer>.
- [3] Hertzke P, Müller N, Schenk S, Wu T. The global electric-vehicle market is amped up and on the rise. McKinsey & Company 2018. 5. 4, 2018. 5. 4; Available from: <https://www.mckinsey.com/industries/automotive-and-assembly/our-insights/the-global-electric-vehicle-market-is-amped-up-and-on-the-rise>. [January 15, 2021.953Z].
- [4] Germany Trade and Invest. Future Mobility in Germany; 2019. 3. 12.
- [5] Federal Ministry for Economics Affairs and Energy. Regierungsprogramm Elektromobilität. [January 16, 2021.549Z]; Available from: https://www.bmwi.de/Redaktion/DE/Downloads/P-R/regierungsprogramm-elektromobilitaet-mai-2011.pdf?__blob=publicationFile&v=6.
- [6] Electric Mobility Act (in German). [January 16, 2021.021Z]; Available from: <http://www.gesetze-im-internet.de/emog/index.html>.
- [7] Lopes JAP, Soares FJ, Almeida PMR. Integration of Electric Vehicles in the Electric Power System. Proc. IEEE 2011;99(1):168–83. <https://doi.org/10.1109/JPROC.2010.2066250>.
- [8] Smith WJ. Can EV (electric vehicles) address Ireland’s CO₂ emissions from transport? Energy 2010;35(12):4514–21. <https://doi.org/10.1016/j.energy.2010.07.029>.
- [9] Yong JY, Ramachandaramurthy VK, Tan KM, Mithulananthan N. A review on the state-of-the-art technologies of electric vehicle, its impacts and prospects. Renewable and Sustainable Energy Reviews 2015;49:365–85. <https://doi.org/10.1016/j.rser.2015.04.130>.
- [10] Teixeira ACR, Sodré JR. Impacts of replacement of engine powered vehicles by electric vehicles on energy consumption and CO₂ emissions. Transportation Research Part D: Transport and Environment 2018;59:375–84. <https://doi.org/10.1016/j.trd.2018.01.004>.
- [11] IEA. World Energy Outlook 2020 – Analysis - IEA. [5-Apr-21]; Available from: <https://www.iea.org/reports/world-energy-outlook-2020#>.
- [12] Renewable Shares | Energy-Charts. [22-Apr-21]; Available from: https://energy-charts.info/charts/renewable_share/chart.htm?l=en&c=DE&interval=year.
- [13] Bundesministerium für Wirtschaft und Energie. Electricity 2030 - Long-term trends; 2016.
- [14] Kern T, Dossow P, Roon S von. Integrating Bidirectionally Chargeable Electric Vehicles into the Electricity Markets. Energies 2020;13(21):5812. <https://doi.org/10.3390/en13215812>.
- [15] Delucchi MA, Yang C, Burke AF, Ogden JM, Kurani K, Kessler J et al. An assessment of electric vehicles: technology, infrastructure requirements, greenhouse-gas emissions, petroleum use, material use, lifetime cost, consumer acceptance and policy initiatives.

- Philos Trans A Math Phys Eng Sci 2014;372(2006):20120325.
<https://doi.org/10.1098/rsta.2012.0325>.
- [16] Chen T, Zhang X-P, Wang J, Li J, Wu C, Hu M et al. A Review on Electric Vehicle Charging Infrastructure Development in the UK. *Journal of Modern Power Systems and Clean Energy* 2020;8(2):193–205. <https://doi.org/10.35833/MPCE.2018.000374>.
- [17] Hartmann N, Özdemir ED. Impact of different utilization scenarios of electric vehicles on the German grid in 2030. *Journal of Power Sources* 2011;196(4):2311–8.
<https://doi.org/10.1016/j.jpowsour.2010.09.117>.
- [18] Pillai JR, Bak-Jensen B. Integration of Vehicle-to-Grid in the Western Danish Power System. *IEEE Trans. Sustain. Energy* 2010. <https://doi.org/10.1109/TSTE.2010.2072938>.
- [19] Loisel R, Pasaoglu G, Thiel C. Large-scale deployment of electric vehicles in Germany by 2030: An analysis of grid-to-vehicle and vehicle-to-grid concepts. *Energy Policy* 2014;65:432–43. <https://doi.org/10.1016/j.enpol.2013.10.029>.
- [20] White CD, Zhang KM. Using vehicle-to-grid technology for frequency regulation and peak-load reduction. *Journal of Power Sources* 2011;196(8):3972–80.
<https://doi.org/10.1016/j.jpowsour.2010.11.010>.
- [21] A. Zahedi. Electric Vehicle as distributed energy storage resource for future smart grid. In: 2012 22nd Australasian Universities Power Engineering Conference (AUPEC); 2012, p. 1–4.
- [22] Kempton W, Tomić J. Vehicle-to-grid power implementation: From stabilizing the grid to supporting large-scale renewable energy. *Journal of Power Sources* 2005;144(1):280–94.
<https://doi.org/10.1016/j.jpowsour.2004.12.022>.
- [23] Jeon W, Cho S, Lee S. Estimating the Impact of Electric Vehicle Demand Response Programs in a Grid with Varying Levels of Renewable Energy Sources: Time-of-Use Tariff versus Smart Charging. *Energies* 2020;13(17):4365. <https://doi.org/10.3390/en13174365>.
- [24] Kim H, Myeong H, Park I, Choi JH, Kim K. Vehicle-to-Grid Charging Optimization of Electric Vehicle. In: 2020 IEEE Conference on Control Technology and Applications (CCTA). IEEE; 82020, p. 1–6.
- [25] Hutson C, Venayagamoorthy GK, Corzine KA. Intelligent Scheduling of Hybrid and Electric Vehicle Storage Capacity in a Parking Lot for Profit Maximization in Grid Power Transactions. In: 2008 IEEE Energy 2030 Conference. IEEE; 112008, p. 1–8.
- [26] Saber AY, Venayagamoorthy GK. Optimization of Vehicle-to-Grid Scheduling in Constrained Parking Lots. IEEE; 2009.
- [27] Jin C, Tang J, Ghosh P. Optimizing Electric Vehicle Charging With Energy Storage in the Electricity Market. *IEEE Trans. Smart Grid* 2013;4(1):311–20.
<https://doi.org/10.1109/TSG.2012.2218834>.
- [28] Zhang A, Sun B, Liu T, Tan X, Wang S, Tsang DHK. Joint voltage and frequency regulation by EV charging scheduling in the distribution network. In: 2018 IEEE Power &

- Energy Society Innovative Smart Grid Technologies Conference (ISGT). IEEE; 2018, p. 1–5.
- [29] Mohamed A, Salehi V, Ma T, Mohammed O. Real-Time Energy Management Algorithm for Plug-In Hybrid Electric Vehicle Charging Parks Involving Sustainable Energy. *IEEE Trans. Sustain. Energy* 2014;5(2):577–86. <https://doi.org/10.1109/TSTE.2013.2278544>.
- [30] Tushar W, Yuen C, Huang S, Smith DB, Poor HV. Cost Minimization of Charging Stations With Photovoltaics: An Approach With EV Classification. *IEEE Trans. Intell. Transport. Syst.* 2016;17(1):156–69. <https://doi.org/10.1109/TITS.2015.2462824>.
- [31] He Y, Venkatesh B, Guan L. Optimal Scheduling for Charging and Discharging of Electric Vehicles. *IEEE Trans. Smart Grid* 2012;3(3):1095–105. <https://doi.org/10.1109/TSG.2011.2173507>.
- [32] Huang Z, Fang B, Deng J. Multi-objective optimization strategy for distribution network considering V2G-enabled electric vehicles in building integrated energy system. *Prot Control Mod Power Syst* 2020;5(1). <https://doi.org/10.1186/s41601-020-0154-0>.
- [33] Jian L, Zhu X, Shao Z, Niu S, Chan CC. A scenario of vehicle-to-grid implementation and its double-layer optimal charging strategy for minimizing load variance within regional smart grids. *Energy Conversion and Management* 2014;78:508–17. <https://doi.org/10.1016/j.enconman.2013.11.007>.
- [34] Saber AY, Venayagamoorthy GK. Plug-in Vehicles and Renewable Energy Sources for Cost and Emission Reductions. *IEEE Trans. Ind. Electron.* 2011;58(4):1229–38. <https://doi.org/10.1109/TIE.2010.2047828>.
- [35] Yao L, Damiran Z, Lim WH. Optimal Charging and Discharging Scheduling for Electric Vehicles in a Parking Station with Photovoltaic System and Energy Storage System. *Energies* 2017;10(4):550. <https://doi.org/10.3390/en10040550>.
- [36] Moeini-Aghaie M, Abbaspour A, Fotuhi-Firuzabad M. Online Multicriteria Framework for Charging Management of PHEVs. *IEEE Trans. Veh. Technol.* 2014;63(7):3028–37. <https://doi.org/10.1109/TVT.2014.2320963>.
- [37] Kühnbach M, Stute J, Klingler A-L. Impacts of avalanche effects of price-optimized electric vehicle charging - Does demand response make it worse? *Energy Strategy Reviews* 2021;34:100608. <https://doi.org/10.1016/j.esr.2020.100608>.
- [38] Honarmand M, Zakariazadeh A, Jadid S. Optimal scheduling of electric vehicles in an intelligent parking lot considering vehicle-to-grid concept and battery condition. *Energy* 2014;65:572–9. <https://doi.org/10.1016/j.energy.2013.11.045>.
- [39] Kühnbach M, Stute J, Gnann T, Wietschel M, Marwitz S, Klobasa M. Impact of electric vehicles: Will German households pay less for electricity? *Energy Strategy Reviews* 2020;32:100568. <https://doi.org/10.1016/j.esr.2020.100568>.
- [40] Bdew - Energies, Wasser, Leben. Strompreis für Haushalte. [6-Apr-21]; Available from: <https://www.bdew.de/service/daten-und-grafiken/strompreis-fuer-haushalte/>.

- [41] Guille C, Gross G. Design of a Conceptual Framework for the V2G Implementation. In: 2008 IEEE Energy 2030 Conference. IEEE; 112008, p. 1–3.
- [42] Kempton W, Letendre SE. Electric vehicles as a new power source for electric utilities. *Transportation Research Part D: Transport and Environment* 1997;2(3):157–75. [https://doi.org/10.1016/S1361-9209\(97\)00001-1](https://doi.org/10.1016/S1361-9209(97)00001-1).
- [43] Sujitha N, Krithiga S. RES based EV battery charging system: A review. *Renewable and Sustainable Energy Reviews* 2017;75:978–88. <https://doi.org/10.1016/j.rser.2016.11.078>.
- [44] Dominik Pelzer, David Ciechanowicz, Alois Knoll. 2016 IEEE Innovative Smart Grid Technologies - Asia (ISGT-Asia): Melbourne, Australia, Nov 28-Dec 1, 2016. Piscataway, NJ: IEEE; 2016.
- [45] Englberger S, Hesse H, Kucevic D, Jossen A. A Techno-Economic Analysis of Vehicle-to-Building: Battery Degradation and Efficiency Analysis in the Context of Coordinated Electric Vehicle Charging. *Energies* 2019;12(5):955. <https://doi.org/10.3390/en12050955>.
- [46] Mukherjee JC, Gupta A. A Review of Charge Scheduling of Electric Vehicles in Smart Grid. *IEEE Systems Journal* 2015;9(4):1541–53. <https://doi.org/10.1109/JSYST.2014.2356559>.
- [47] Miao Y, Hynan P, Jouanne A von, Yokochi A. Current Li-Ion Battery Technologies in Electric Vehicles and Opportunities for Advancements. *Energies* 2019;12(6):1074. <https://doi.org/10.3390/en12061074>.
- [48] Xu B, Oudalov A, Ulbig A, Andersson G, Kirschen DS. Modeling of Lithium-Ion Battery Degradation for Cell Life Assessment. *IEEE Trans. Smart Grid* 2016;9(2):1131–40. <https://doi.org/10.1109/TSG.2016.2578950>.
- [49] Li S, Li J, Su C, Yang Q. Optimization of Bi-Directional V2G Behavior With Active Battery Anti-Aging Scheduling. *IEEE Access* 2020;8:11186–96. <https://doi.org/10.1109/ACCESS.2020.2964699>.
- [50] Jingli Guo, Jin Yang, Zhengyu Lin, Clara Serrano, Ana Maria Cortes (eds.). Impact Analysis of V2G Services on EV Battery Degradation -A Review; 2019.
- [51] Peter Keil, Simon F. Schuster, Jörn Wilhelm, Julian Travi, Andreas Hauser, Ralph C. Karl et al. Calendar Aging of Lithium-Ion Batteries. *J. Electrochem. Soc.* 2016;163(9):A1872. <https://doi.org/10.1149/2.0411609jes>.
- [52] Cui Y, Du C, Yin G, Gao Y, Zhang L, Guan T et al. Multi-stress factor model for cycle lifetime prediction of lithium ion batteries with shallow-depth discharge. *Journal of Power Sources* 2015;279:123–32. <https://doi.org/10.1016/j.jpowsour.2015.01.003>.
- [53] Zhao R, Zhang S, Liu J, Gu J. A review of thermal performance improving methods of lithium ion battery: Electrode modification and thermal management system. *Journal of Power Sources* 2015;299:557–77. <https://doi.org/10.1016/j.jpowsour.2015.09.001>.
- [54] Zhao K, Pharr M, Cai S, Vlassak JJ, Suo Z. Large Plastic Deformation in High-Capacity Lithium-Ion Batteries Caused by Charge and Discharge. *J. Am. Ceram. Soc.* 2011;94([5]):s226-s235. <https://doi.org/10.1111/j.1551-2916.2011.04432.x>.

- [55] Sieg J, Bandlow J, Mitsch T, Dragicevic D, Materna T, Spier B et al. Fast charging of an electric vehicle lithium-ion battery at the limit of the lithium deposition process. *Journal of Power Sources* 2019;427(2):260–70. <https://doi.org/10.1016/j.jpowsour.2019.04.047>.
- [56] Jeffrey Jenkins. EV tech explained: Why do EVs restrict the amount of battery capacity that can be used for driving? - Charged EVs. [January 20, 2021.574Z]; Available from: <https://chargedevs.com/newswire/ev-tech-explained-why-do-evs-restrict-the-amount-of-battery-capacity-that-can-be-used-for-driving/>.
- [57] Mathews I, Xu B, He W, Barreto V, Buonassisi T, Peters IM. Technoeconomic model of second-life batteries for utility-scale solar considering calendar and cycle aging. *Applied Energy* 2020;269:115127. <https://doi.org/10.1016/j.apenergy.2020.115127>.
- [58] A. Millner. Modeling Lithium Ion battery degradation in electric vehicles. In: 2010 IEEE Conference on Innovative Technologies for an Efficient and Reliable Electricity Supply; 2010, p. 349–356.
- [59] Abdullah Al-karakchi AA, Lacey G, Putrus G. A method of electric vehicle charging to improve battery life. In: 2015 50th International Universities Power Engineering Conference (UPEC). IEEE; 92015, p. 1–3.
- [60] Administrator. WB-LYP100AHA. [January 20, 2021.554Z]; Available from: http://en.winston-battery.com/index.php/products/power-battery/item/wb-lyp100aha?category_id=176.
- [61] Chen Y, Alamin KSS, Jahier Pagliari D, Vinco S, Macii E, Poncino M. Electric Vehicles Plug-In Duration Forecasting Using Machine Learning for Battery Optimization. *Energies* 2020;13(16):4208. <https://doi.org/10.3390/en13164208>.
- [62] Pelletier S, Jabali O, Laporte G, Veneroni M. Battery degradation and behaviour for electric vehicles: Review and numerical analyses of several models. *Transportation Research Part B: Methodological* 2017;103(4):158–87. <https://doi.org/10.1016/j.trb.2017.01.020>.
- [63] Lunz B, Yan Z, Gerschler JB, Sauer DU. Influence of plug-in hybrid electric vehicle charging strategies on charging and battery degradation costs. *Energy Policy* 2012;46:511–9. <https://doi.org/10.1016/j.enpol.2012.04.017>.
- [64] Schmalstieg J, Käbitz S, Ecker M, Sauer DU. A holistic aging model for Li(NiMnCo)O₂ based 18650 lithium-ion batteries. *Journal of Power Sources* 2014;257(1):325–34. <https://doi.org/10.1016/j.jpowsour.2014.02.012>.
- [65] Birkl CR, Roberts MR, McTurk E, Bruce PG, Howey DA. Degradation diagnostics for lithium ion cells. *Journal of Power Sources* 2017;341:373–86. <https://doi.org/10.1016/j.jpowsour.2016.12.011>.
- [66] Pyomo. Pyomo. [March 11, 2021]; Available from: <http://www.pyomo.org/>.
- [67] Gurobi. Gurobi - The fastest solver - Gurobi. [March 11, 2021]; Available from: <https://www.gurobi.com/>.
- [68] Michaelis J. Modellgestützte Wirtschaftlichkeitsbewertung von Betriebskonzepten für Elektrolyseure in einem Energiesystem mit hohen Anteilen erneuerbarer Energien [Model-

- based economic evaluation of operating concepts for electrolyzers in an energy system with high shares of renewable energies]. Stuttgart: Fraunhofer Verlag (ISI-Schriftenreihe Innovationspotenziale); 2018.
- [69] Institute for Electrical Energy Storage Technology - Technical University Munich. SimSES - Software for techno-economic simulation of stationary energy storage systems. [April 03, 2021]; Available from: <https://www.ei.tum.de/ees/fp-ees/simses/>.
 - [70] Lutsey N, Nicholas M. Update on electric vehicle costs in the United States through 2030. International Council on Clean Transportation; 2019.
 - [71] ERDOGAN N, ERDEN F, KISACIKOGLU M. A fast and efficient coordinated vehicle-to-grid discharging control scheme for peak shaving in power distribution system. *J. Mod. Power Syst. Clean Energy* 2018;6(3):555–66. <https://doi.org/10.1007/s40565-017-0375-z>.
 - [72] Netz Entwicklungs Plan STROM. Grid Development Plan 2030 (2019) | Grid Development Plan. [5-Apr-21]; Available from: <https://www.netzentwicklungsplan.de/en/grid-development-plans/grid-development-plan-2030-2019>.
 - [73] IEA. World Energy Outlook 2017 (Report). [28-Apr-21]; Available from: <https://www.iea.org/reports/world-energy-outlook-2017>.
 - [74] International Energy Agency. Germany 2020 - Energy Policy Review 2020.
 - [75] T. Gnann, D. Speth. Electric vehicle profiles for the research project "MODEX EnSaVes - Model experiments - development paths for new electricity applications and their impact on critical supply situations", 2021.
 - [76] Institut für Verkehrswesen der Universität Karlsruhe. "Mobilitätspanel Deutschland" 1994-2010 - Projektbearbeitung durch das Institut für Verkehrswesen der Universität Karlsruhe (TH). Verteilt durch die Clearingstelle Verkehr des DLR- Instituts für Verkehrsorschung: www.clearingstelle-verkehr.de ["Mobility Panel Germany" 1994-2010 - Project management by the Institute for Transportation at the University of Karlsruhe (TH). Distributed by the Clearing House Transport of the DLR Institute of Trnasport Research: www.clearingstelle-verkehr.de], Karlsruhe, Germany.
 - [77] Open Power System Data. Data package time series (Version: 2020-10-06); 2020. https://doi.org/10.25832/time_series/2020-10-06; Available from: https://data.open-power-system-data.org/time_series/.
 - [78] Bundesministerium für Umwelt, Naturschutz und nukleare Sicherheit. Förderung der Elektromobilität. [March 10, 2021]; Available from: <https://www.bmu.de/themen/luftlaerm-verkehr/verkehr/elektromobilitaet/foerderung/>.
 - [79] Danzer MA, Liebau V, Maglia F. Aging of lithium-ion batteries for electric vehicles. In: Advances in Battery Technologies for Electric Vehicles. Cambridge: Elsevier Science & Technology; 2015.

Appendix

A. Electricity market status of 2030

Figure A-1 to Figure A-3 show the simulated initial electricity market status of 2030 without considering additional load and supply from EV. Hourly time series of simulated system load and variable renewable generation for 2030 are depicted in the heat maps. The x-axis represents days of the year and the y-axis represents hours of each day. The starting point is the 1st of January.

Figure A-1 shows the system load without additional demand and supply from EV. There is a relatively high demand in the winter, which is the beginning and the end of the time window. There is high demand during the daytime, especially during the rush hour and after work while there is low demand during the dawn and night times which is notably bright. There is a section where the demand decreases slightly around 3 pm. For the whole year, white vertical lines are shown every two days a week, which are the weekends.

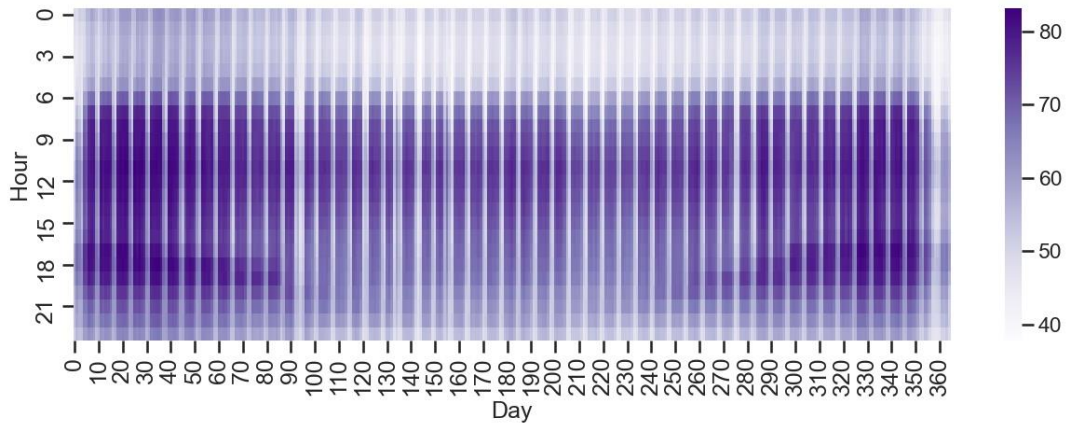


Figure A-1. Simulated system load as of 2030 without EV load [GW]

Figure A-2 shows the hourly PV generation over one year. The PV generation is distributed around noon where there is a lot of solar irradiation, and the highest power generation is shown at noon most of the time. Compared to winter, the power generation in summer is much higher and the power generation time is longer. Figure A-3 shows the hourly wind generation over one year. This is the sum of onshore wind power generation and offshore wind power generation. The Large power generations over 100 GWh are found several times in winter, and once in early spring which is around the end of March (around day 90), but not in summer. In the case of wind energy, since it is a continuous natural energy source, continuous vertical lines are observed in general, unlike solar energy.

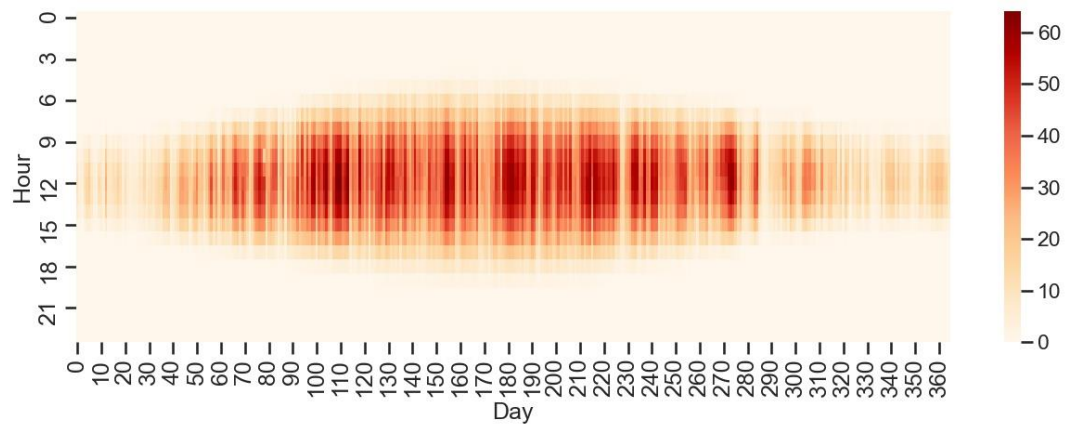


Figure A-2. Simulated PV generation of 2030 [GW]

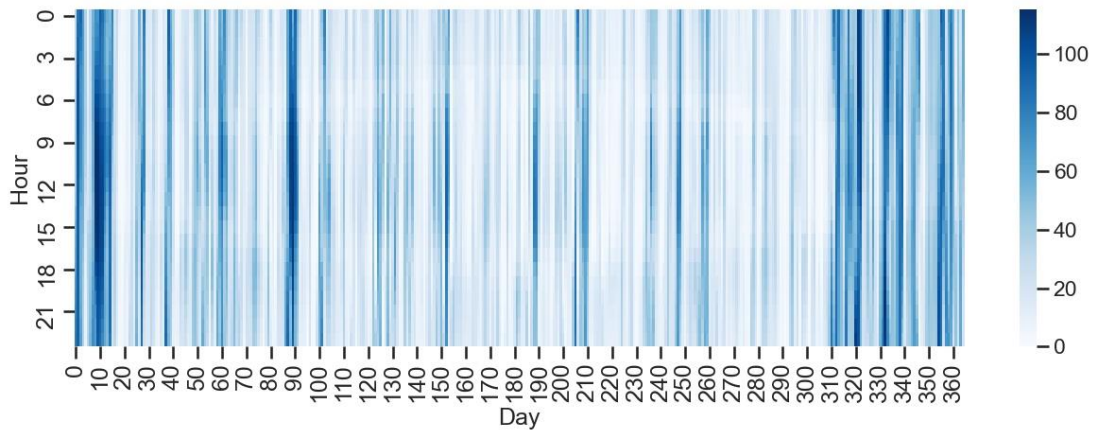


Figure A-3. Simulated wind generation as of 2030 [GW]

B. Detailed impact comparison of sensitivity analyses

Table B-1 and Table B-2 show benefits and costs depending on the cases of sensitivity analysis. The specific compensation cost per benefit refers to the compensation costs incurred per benefit compared to UC. For negative numbers, it refers to the cost reduced by participating in the program, which means the revenue earned per benefit. (See, Section 3.3 for calculation method)

Table B-1. Overview of benefits and cost depending on the participation rate of DR or V2G.

UC	DR			V2G		
	10%	50%	100%	10%	50%	100%
Specific compensation cost per benefit						
Cost per reduced peak load [EUR/MW]	-	-17231.61	-4383.76	-2405.68	-803.95	2037.75
Cost per reduced CO₂ emission [EUR/ton]	-	-1288.38	-300.35	-148.98	-55.96	186.24
Cost for EV user						
Total cost for all EVs [million EUR]	95.99	80.59	78.44	77.12	93.26	129.37
Total cost aver. for all EVs [EUR]	16.00	13.43	13.07	12.85	15.54	21.56
Total cost aver. for participated EV [EUR]	16.00	12.86	12.86	12.85	35.36	30.33
Benefits for electricity system: Residual load						
PLR pos. [%]	-	1.24	5.56	10.90	4.72	22.76
Peak RL max [GW]	71.98	71.08	67.97	64.13	68.58	55.59
PLR neg. [%]	-	4.14	19.95	27.71	4.14	20.25
Peak RL min [GW]	-57.99	-55.59	-46.42	-41.92	-55.59	-46.25
PSP [%]	0.00	0.71	3.28	5.90	1.20	3.70
Abs. RL sum [GWh]	5745.90	5705.21	5557.26	5406.65	5677.00	5533.39
Environmental benefits						
CO₂ reduction [%]	-	0.78	3.81	8.26	3.18	11.69
(CO ₂ emission [kton])	1,533.21	1,521.25	1,474.77	1,406.54	1,484.39	1,353.97
Surplus RES reduction [%]	-	0.78	3.60	6.48	1.40	4.36
(Surplus RES [GWh])	2,619.67	2,599.32	2,525.35	2,450.04	2,582.96	2,505.33

Table B-2. Overview of benefits and cost depending on the SOC allowance range.

UC	DR			V2G		
	25-75% (SOC50)	10-90% (SOC80)	0-100% (SOC100)	25-75% (SOC50)	10-90% (SOC80)	0-100% (SOC100)
Specific compensation cost per benefit						
Cost per reduced peak load [EUR/MW]	-	-2,405.68	-2,594.29	-2,631.79	2,558.04	3,039.95
Cost per reduced CO₂ emission [EUR/ton]	-	-148.98	-152.74	-148.98	236.09	277.37
Cost for EV user						
Total cost for all EVs [million EUR]	95.99	77.12	75.64	75.34	158.14	181.14
Total cost aver. for all EVs [EUR]	16.00	12.85	12.61	12.56	26.36	30.19
Benefits for electricity system: Residual load						
PLR pos. [%]	-	10.90	10.90	10.90	33.76	38.92
Peak RL max [GW]	71.98	64.13	64.13	64.13	47.68	43.96
PLR neg. [%]	-	27.71	30.63	31.83	28.54	32.63
Peak RL min [GW]	-57.99	-41.92	-40.23	-39.53	-41.44	-39.07
PSP [%]	0.00	5.90	6.90	7.44	6.67	8.20
Abs. RL sum [GWh]	5,745.90	5,406.65	5,349.42	5,318.20	5,362.89	5,274.49
Environmental benefits						
CO₂ reduction [%]	0.00	8.26	8.69	9.04	17.17	20.02
(CO ₂ emission [kton])	1,533.21	1,406.54	1,399.97	1,394.63	1,269.94	1,226.20
Surplus RES reduction [%]	0.00	6.48	7.57	8.16	7.76	9.56
(Surplus RES [GWh])	2,619.67	2,450.04	2,421.43	2,405.82	2,416.44	2,369.26